

PURIFICATION, CHARACTERIZATION AND RECONSTITUTION OF DRS2 PROTEIN,
A PHOSPHOLIPID FLIPPASE FROM BUDDING YEAST

By

Xiaoming Zhou

Dissertation

Submitted to the Faculty of the
Graduate School of Vanderbilt University

in partial fulfillment of the requirements

for the degree of

DOCTOR OF PHILOSOPHY

in

Biological Sciences

May, 2010

Nashville, Tennessee

Approved:

Professor Carl H. Johnson

Professor Todd R. Graham

Professor Katherine L. Friedman

Professor Charles R. Sanders

Professor Hassane S. Mchaourab

To my wife Ziyi, whose love keeps my dreams alive.

ACKNOWLEDGEMENTS

I would like to express my deepest and sincerest gratitude to my dissertation advisor Dr. Todd R. Graham for his insightful advice, direction, and continuous supportiveness. Dr. Graham's enthusiasm for science and broad knowledge has greatly inspired me. His positive attitude and scientific spirit has been enormous encouragement to me during my graduate studies. I would also like to thank my dissertation committee members, Dr. Carl H. Johnson, Dr. Katherine L. Friedman, Dr. Charles R. Sanders, and Dr. Hassane S. Mchaourab for their time, effort, and dedication in the development of my dissertation research. I am also grateful to Dr. David Daleke at Indiana University for his time and valuable input being an external reader of my dissertation.

I would also like to show my gratitude to my colleagues in the Graham lab for their friendship and assistance, both past and present, during my time at Vanderbilt, specifically Dr. Paramasivam Natarajan, Dr. Jing Xiao, Dr. Ke Liu, Dr. Baby-Periyanyaki Muthusamy, A'Drian Pineda, Maggie Ying, Kavitha Surendhran, Ryan Baldrige, Tessy Sebastian, Jake Randolph, and Sophie Chen. I also appreciate the help from the members of the Friedman lab, our yeast ally and neighbor. I am also grateful to Dr. Andrzej M. Krezel, Dr. Melanie D. Ohi, Melissa Chambers, and the staff at the Mass Spectrometry Research Center of Vanderbilt University for their technical assistance during this dissertation project. My thanks also go to my fellow graduate student friends for their companionship and being always supportive.

Lastly and most importantly, I want to thank my beloved wife, Ziyi Sun, for her undying love, support and encouragement from the first day I met her. I also want to express my utmost gratitude to my parents for their understanding and support during this arduous adventure of research and discovery.

TABLE OF CONTENTS

	Page
DEDICATION.....	ii
ACKNOWLEDGEMENTS.....	iii
LIST OF TABLES.....	vi
LIST OF FIGURES.....	vii
Chapter	
I. INTRODUCTION.....	1
Section 1.1: P4-ATPases in Budding Yeast.....	3
Section 1.1.1: The yeast P-type ATPases and nomenclature.....	3
Section 1.1.2: P4-ATPases in the yeast <i>S. cerevisiae</i>	3
Section 1.1.3: P4-ATPase chaperones.....	10
Section 1.2: Drs2p as a Potential Flippase.....	12
Section 1.2.1: Flip-flop of phospholipids.....	12
Section 1.2.2: Implication of Drs2p as a flippase.....	15
Section 1.2.3: Yeast plasma membrane flippase activities.....	17
Section 1.2.4: Drs2p-dependent flippase activity in Golgi membranes.....	20
Section 1.2.5: P4-ATPases in yeast membrane asymmetry.....	24
Section 1.3: Drs2p in Protein Transport and Vesicle Budding.....	27
Section 1.3.1: Vesicle-mediated protein transport.....	27
Section 1.3.2: Roles of Drs2p-Cdc50p in protein transport.....	29
Section 1.3.3: Influence of other P4-ATPases on protein transport.....	31
Section 1.3.4: Endocytosis of Drs2p.....	33
Section 1.3.5: The C-terminal tail of Drs2p.....	36
Section 1.3.6: Flippases and vesicle formation.....	37
Section 1.4: Objectives of the current project.....	41
II. RECONSTITUTION OF PHOSPHOLIPID TRANSLOCASE ACTIVITY WITH PURIFIED DRS2 PROTEIN, A TYPE-IV P-TYPE ATPASE FROM BUDDING YEAST.....	43
Section 2.1: Abstract.....	43
Section 2.2: Introduction.....	44
Section 2.3: Materials and Methods.....	47
Section 2.3.1: Reagents.....	47
Section 2.3.2: Yeast strains and protein purification.....	47
Section 2.3.3: Proteoliposome formation.....	49
Section 2.3.4: Flippase assay.....	50

Section 2.4: Results.....	51
Section 2.5: Discussion.....	71
Section 2.6: Chapter Acknowledgements.....	76
III. EXPLORING THE BASIS OF DRS2-TAP _C PROTEIN INACTIVITY: POTENTIAL AUTO-INHIBITION BY THE C-TERMINAL TAIL.....	77
Section 3.1: Abstract.....	77
Section 3.2: Introduction.....	78
Section 3.3: Materials and Methods.....	87
Section 3.3.1: Reagents.....	87
Section 3.3.2: Media and strains.....	87
Section 3.3.3: Protein purification.....	88
Section 3.3.4: ATPase assay.....	88
Section 3.3.5: Western blotting.....	89
Section 3.3.6: Mass spectrometry.....	89
Section 3.4: Results.....	90
Section 3.4.1: The content of the tag does not seem to cause the difference in ATPase activity between purified TAP _N -Drs2p and Drs2p-AP _C	90
Section 3.4.2: A cleaved form of Drs2p is present only in the TAP _N -Drs2p-TAP _C sample purified using the TAP _N tag, but not the TAP _C tag.....	92
Section 3.4.3: The ATPase activity is associated with the “NoC” form of TAP _N - Drs2p-TAP _C in purified samples.....	94
Section 3.4.4: A potential cleavage site that generates the “NoC” form of TAP _N - Drs2p-TAP _C is identified by mass spectrometry.....	95
Section 3.4.5: Cdc50p preferentially binds inactive Drs2p in purified samples...	96
Section 3.5: Discussion.....	98
Section 3.6: Chapter Acknowledgements.....	101
IV. FORMATION AND OBSERVATION OF GIANT UNILAMELLAR VESICLES.....	102
Section 4.1: Abstract.....	102
Section 4.2: Introduction.....	102
Section 4.3: Materials and Methods.....	105
Section 4.3.1: Reagents.....	105
Section 4.3.2: Formation of protein-free liposomes.....	105
Section 4.3.3: Formation of giant vesicles by uncontrolled swelling.....	106
Section 4.3.4: Formation of giant vesicles by electroformation.....	106
Section 4.4: Results and Discussion.....	107
V. SUMMARY AND FUTURE DIRECTIONS.....	112
REFERENCES.....	133

LIST OF TABLES

Table	Page
2-1. Proteins identified in purified Drs2p-TAP _C by MALDI-TOF mass spectrometry.....	55
2-2. Secondary structure prediction from circular dichroism spectra of Drs2p by the K2D and K2D2 web servers.....	63
2-3. Proteins identified in Drs2p proteoliposomes by MALDI-TOF mass spectrometry....	66

LIST OF FIGURES

Figure	Page
1-1. Asymmetrical distribution of phospholipids between the two leaflets of the erythrocyte plasma membrane.....	2
1-2. Phylogenetic tree of the yeast <i>S. cerevisiae</i> P-type ATPases.....	4
1-3. Sequence alignment between Drs2p and SERCA1.....	6
1-4. Homology model of Drs2p based on the crystal structure of the sarcoplasmic reticulum Ca ²⁺ ATPase 1 in the E2·P conformation.....	9
1-5. Yeast P4-ATPases and their noncatalytic subunits.....	11
1-6. Proteins proposed to mediate the transbilayer movement of phospholipids and regulate membrane asymmetry.....	13
1-7. Shape changes of human red blood cells by scanning electron microscopy.....	16
1-8. Vesicle-mediated protein transport and P4-ATPase requirements in various trafficking pathways in budding yeast.....	28
1-9. Proposed model for Drs2p regulation by its C-terminal tail.....	35
1-10. Proposed model for how Drs2p flippase activity could drive budding of AP-1/clathrin-coated vesicles.....	40
2-1. Expression and purification of Drs2p-TAP _C	52
2-2. Growth phenotype of yeast strains at 30 C and 20 C.....	53
2-3. Overexpression of <i>DRS2-TAP_C</i> and <i>TAP_N-DRS2</i> in yeast.....	54
2-4. Detection and disruption of mitochondrial F1-ATPase.....	57
2-5. Expression and purification of TAP _N -Drs2p.....	58
2-6. Characterization of purified Drs2p in 0.1% C ₁₂ E ₉	60
2-7. Size exclusion chromatography of purified Drs2p.....	61
2-8. Circular dichroism spectra of purified Drs2p.....	62
2-9. Flotation of TAP _N -Drs2p proteoliposomes in a glycerol gradient.....	65
2-10. Protease protection assay of TAP _N -Drs2p proteoliposomes using trypsin.....	67

2-11. Flippase assay with TAP _N -Drs2p proteoliposomes containing NBD-PS.....	69
2-12. Reconstitution of NBD-PS flippase activity with TAP _N -Drs2p proteoliposomes.....	70
2-13. Phospholipid stimulation of TAP _N -Drs2p ATPase activity.....	74
3-1. Structure and catalytic cycle of the sarcoplasmic reticulum Ca ²⁺ ATPase 1.....	79
3-2. Phylogenetic tree of the P-type ATPase family.....	82
3-3. Expression and purification of TAP _N -Drs2p-TAP _C	91
3-4. Partial separation of the “NoC” form from the intact form in purified TAP _N -Drs2p-TAP _C by calmodulin column.....	93
3-5. Partial separation of TAP _N -Drs2p/Cdc50p-TAP _C complex from TAP _N -Drs2p monomer in purified TAP _N -Drs2p by calmodulin column.....	97
4-1. Formation of giant vesicles by swelling methods.....	109
4-2. Shape change of giant vesicles induced by pH gradient.....	110
4-3. Shape change of giant unilamellar vesicles induced by osmolarity gradient.....	111

CHAPTER I*

INTRODUCTION

Membranes provide a physical boundary to separate a living organism from its environment and to divide eukaryotic cells into functionally distinct subcellular compartments. The plasma membrane of the cell has a unique protein and lipid composition that is optimized for establishing an interface between the intracellular and extracellular environments. An important aspect of this interface is the asymmetrical distribution of plasma membrane phospholipids between the two leaflets (Bretscher, 1973; Devaux, 1992) (**Figure 1-1**). For example, the cytosolic leaflet is enriched in phosphatidylserine (PS) and phosphatidylethanolamine (PE), whereas the extracellular leaflet contains primarily phosphatidylcholine (PC) and sphingolipids (Devaux, 1992; Zwaal and Schroit, 1997). This lipid organization appears to be conserved from yeast to man, but how is membrane asymmetry established and maintained? Research over the last two decades suggest that a P-type ATPase subfamily, called type-IV P-type ATPases or P4-ATPases, contributes significantly to this process by flipping specific phospholipid substrates from the extracellular or luminal leaflet to the cytosolic leaflet of the membrane bilayer (so-called “flippases”) (Daleke, 2003; Graham, 2004; Pomorski et al., 2004). Particularly, studies on the P4-ATPases from the yeast *Saccharomyces cerevisiae*, especially the founding member of the family, Drs2p, have greatly expanded our knowledge in this field. In addition to their potential flippase function and contribution to membrane asymmetry, the yeast P4-ATPases also play important roles in protein transport and vesicle budding (Graham, 2004; Muthusamy et al., 2009a; Zhou et al., 2010). These P4-ATPase activities create an intriguing link between phospholipid translocation and vesicle formation.

*This chapter was modified from: Zhou X, Liu K, Natarajan P, Muthusamy BP, and Graham TR (2010). "Coupling Drs2p to Phospholipid Translocation, Membrane Asymmetry and Vesicle Budding" In: *Membrane Asymmetry and Transmembrane Motion of Lipids*. (P. F. Devaux, ed.) John Wiley & Sons.

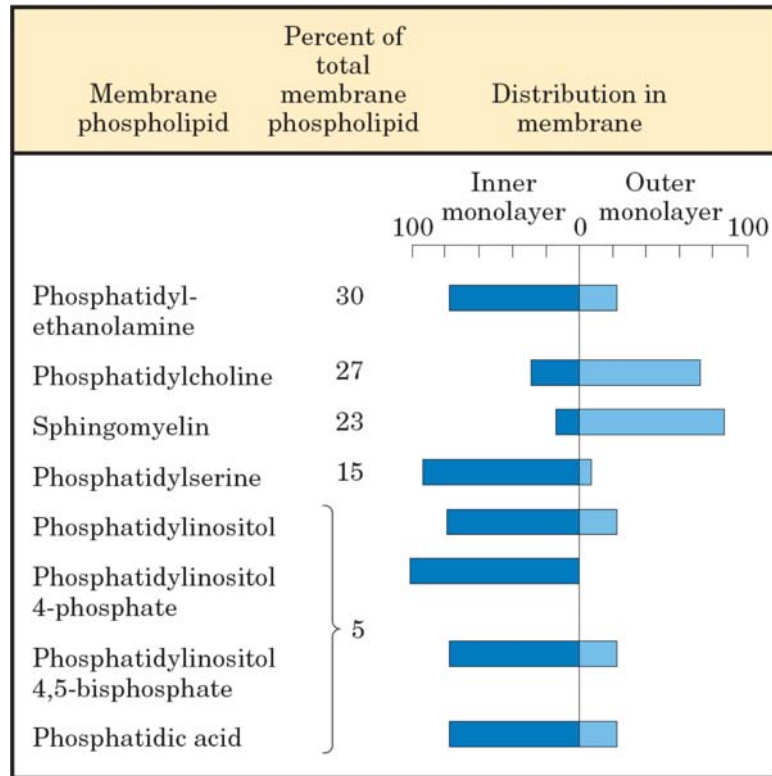


Figure 1-1. Asymmetrical distribution of phospholipids between the two leaflets of the erythrocyte plasma membrane (from: Principles of Biochemistry, 4th edition).

Section 1.1: P4-ATPases in Budding Yeast

Section 1.1.1: The yeast P-type ATPases and nomenclature

Sequencing of the *S. cerevisiae* genome identified a total of 16 P-type ATPases, which were initially categorized phylogenetically into three classes called P1-, P2- and P4-ATPases (Catty et al., 1997) (**Figure 1-2**).

The original P1 family consisted of two members of heavy metal ion pumps. The Drs2p family members, which are potential flippases, were originally placed in the P2 class together with H⁺, Na⁺ and Ca²⁺ pumps, whereas the term P4 was proposed for two new P-type ATPases whose substrates are still unknown.

In a more recent and detailed phylogenetic classification that included P-type ATPases from bacteria, fungi, plants and animals (Axelsen and Palmgren, 1998; Kuhlbrandt, 2004), yeast P-type ATPases, especially the original P2 family members, were reorganized into new categories and a new naming system was utilized. The heavy metal ion transporters remain in the first category, but were renamed type-I P-type ATPases (P1). Na⁺ and Ca²⁺ pumps were categorized as type-II (P2) and H⁺ ATPases type-III (P3). The Drs2p family was also placed into an independent new branch designated type-IV P-type ATPases (P4). The P-type ATPases with unknown substrates, i.e. the original P4-ATPases, were designated type-V P-type ATPases (P5). To promote a less cumbersome nomenclature, we and other groups have used the term P4-ATPases for the Drs2p family of potential phospholipid translocases.

Section 1.1.2: P4-ATPases in the yeast *S. cerevisiae*

The budding yeast *S. cerevisiae* contains five P4-ATPases: Drs2p, Neo1p, Dnf1p, Dnf2p and Dnf3p (Axelsen and Palmgren, 1998; Catty et al., 1997; Kuhlbrandt, 2004) (**Figure 1-2**). *NEO1* is the only essential gene of the P4-ATPase family and yeast

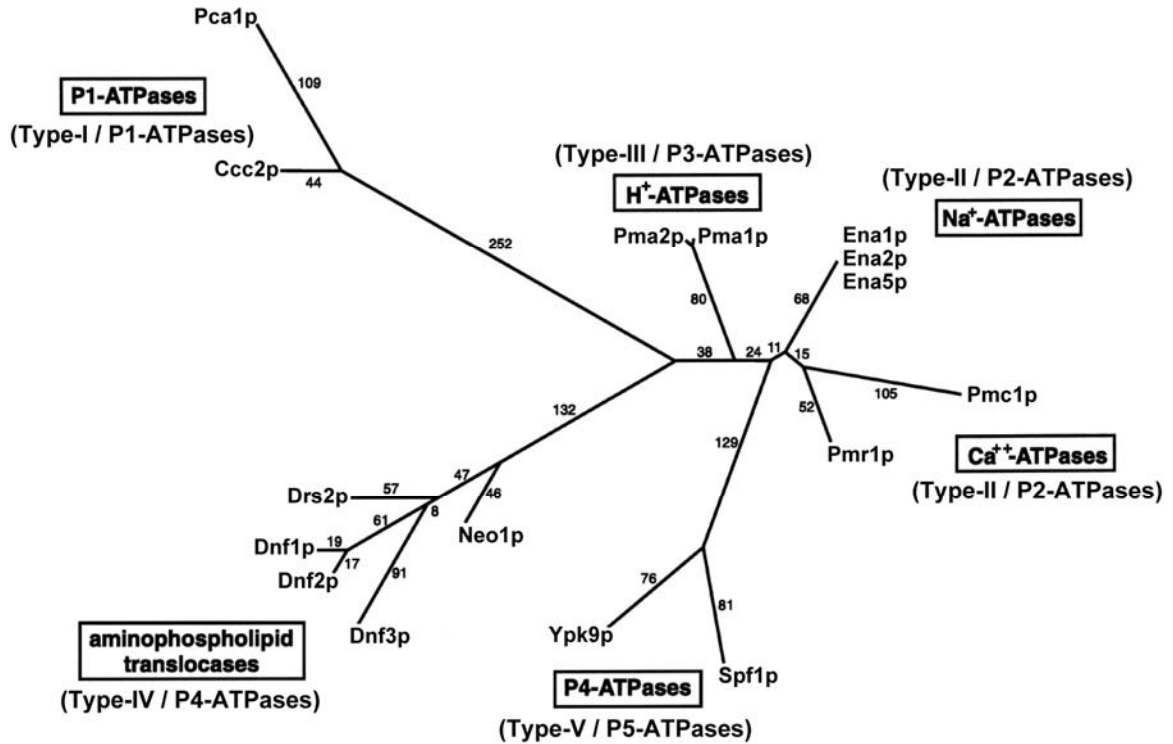


Figure 1-2. Phylogenetic tree of the yeast *S. cerevisiae* P-type ATPases (modified from Catty et al., 1997). Totally 16 P-type ATPases are divided into six subgroups. Numbers indicate the relative evolution distance between proteins. Boxed names are the terms used in the original classification. An updated classification for each subgroup is indicated in parentheses.

carrying a complete disruption of *NEO1* fail to grow at any temperature tested (Hua and Graham, 2003; Prezant et al., 1996). However, phenotypes associated with loss of *NEO1* function have been characterized in strains carrying temperature-conditional alleles of *NEO1* (*neo1-ts*) or by placing the *NEO1* gene under transcriptional control of a galactose-regulated promoter (Hua and Graham, 2003; Wicky et al., 2004). In the latter case, expression of *NEO1* can be shut off by growth of the strain in glucose.

The remaining members of the P4-ATPase family constitute an essential group (Hua et al., 2002). Disruption of *DRS2* yields a viable strain although these cells display an unusually strong cold-sensitive growth defect. Yeast normally grow over a range of temperatures, from approximately 10 C to 40 C, but *drs2Δ* cells fail to grow at temperatures below 23 C (Ripmaster et al., 1993). Individual knockout of *DNF* genes, or even the triple knockout (*dnf1,2,3Δ*), does not perturb growth of yeast. However, disruption of *DNF* genes in a *drs2Δ* background exacerbates the growth defect caused by *drs2Δ*, in decreasing order of severity: *drs2Δdnf1Δ*, *drs2Δdnf2Δ* and *drs2Δdnf3Δ*. Growth defects become more severe as more *DRS2-DNF* genes are deleted and the quadruple mutant (*drs2Δdnf1,2,3Δ*) is inviable. These observations indicate some degree of functional redundancy between the *DRS2* and *DNF* genes, with Drs2p primarily providing the essential activity of the group (Hua et al., 2002).

DRS2 was the first P4-ATPase gene cloned and was originally thought to be a Ca²⁺-ATPase based on homology searches with sequences available at the time (Ripmaster et al., 1993). Drs2p contains 1355 amino acids and is 14% identical and 41% similar to the sarcoplasmic/endoplasmic reticulum Ca²⁺-ATPase 1 (SERCA1, **Figure 1-3**). By comparison, Drs2p shares 20-30% identity and 40-50% similarity with other yeast P4-ATPases (Hua et al., 2002). Sequence analysis of Drs2p identified the key sequence “DKTGTLT”, containing the aspartyl phosphorylation site conserved in all P-type ATPases, as well as other signature motifs for P-type ATPases (Catty et al., 1997).

```

1      10      20      30      40      50      60      70      80
Drs2p  MNDDRETPPKRKPGEDDTLFDLDDTTS HSGSRKVTNSHANGYYIPPSHVLPEETIDL DADDDNIENLVHNLFMSN
SERCA1  .....MBA

90      100     110     120     130     140     150     160
Drs2p  NHDDQTSWNAANRFDS DAYQPQS LRAVKPPGLFARFNGLNKNAFTFKRKKGPESFEMNHYN AVTNNELDDNLYLDSRNKNFNIT
SERCA1  AHSKSTTEEC LAYFGVSET TGLTFDQVK.....R.HLEKRYGHNELP AEEGKSLWEVLVTEQFEDLLV

170     180     190     200     210     220     230     240
Drs2p  KILFNRYITL RKNVGD AEGNGEPRVTHITNDSLANS SFGYSDNHISTTKYNFATFLPKFLPQEF SKYANLFFLCTSAIQQVVP
SERCA1  RII LLAAC I SFV L AWF E EGE E TIT A F V E P ..... F . . V I L L I L I A N A I V G V W

250     260     270     280     290     300     310     320
Drs2p  HVSPINRYTTIG TLLVVLIVS AMKECEIEDIKRANS DKELNNSTAEIFSEAHDDFVEKRWI DIRVGDITR V KSEEP I PADT
SERCA1  QER.....I. N A E N A I E A L K . . . . . E Y E P . . E M G K V Y R A D R K S V Q R I K A R D I V E G D I V E V A V G D K K V P A D I

330     340     350     360     370     380     390     400
Drs2p  IILSSSEPEGLCY IETANLDGE TNLKIKOSR VETAKFIDV KTLKNMNGKVVSEQ PNSSLYTYEGTMTLND RQIPLSPDQOM
SERCA1  R I L S . . . . . I . K S . . . . . T T L R V D Q S I L T G E S V S V I R K H T E P V P . . . D . . . P R A V N Q . D . . . . . K K N M L F S G T N

410     420     430     440     450     460     470     480
Drs2p  IILRCATLRN T A W I F C L V I F T G H E T K L I R N A T A T P I K R T A V E K I I N R Q I I R L P T V L I V L I L I S S I C N V I M S T A D A K H L S Y L
SERCA1  I A A G K A L G . I V A T T G V S T E I G K I R D Q M A A T E Q D K T P L Q K L D E F G E Q L S K V I S L I C V A V W L I N I G . . . . .

490     500     510     520     530     540     550
Drs2p  YLEGTNKAC L F F K D F L T F W I L F S N L V P S L F V T V E L I K Y Q A F M I G S D L D L Y Y E K T D T P . T V V R T S S L V E L G Q I E Y I F S
SERCA1  H F N D P V H G C S W I R G A I Y F K . . . . . I A V A L A V A A I P E G L P A V I T C L A L G T R R M A K K N A I V R S L P S V E L G C T S V I C S

560     570     580     590     600     610     620     630
Drs2p  DKTCTLT R N I M E F K S C S I T A G H C Y I D K T I P E D K T A T V E D G I E V G . Y R K F D D L K K L N D P S D E D S P I I N D F L T L L A T C H T V I P
SERCA1  D K T C T L T . . . . . N Q M S V C K M F I I D K V D G D F C S L N E F S I T G S T Y A P E G E V L K N D K P I R S G Q F D G L V E L A T E C A L C N D S S L

640     650     660     670     680     690     700     710
Drs2p  E F Q S D G S I K Y Q A A S P D E G A L V Q G G A D L G Y K F I I R K G N S V T V L L E E T G E E K E Y Q L L N . . . I C E F N S I R K R M S A I F R P P D G S
SERCA1  D E N E T K G V Y E K V G E A T E T A L I T L V E K M . N . V F N T E V R N L S K V E R A N A C N S V I R Q L M K K E T L E F S R D R K S M S V Y C S P A K S S

720     730     740     750     760     770     780     790
Drs2p  . . . . I K L F K G A D T V I L E R L D D E A N Q Y V E A T M R H L E D Y A S E G L R I T C L A M R D I S E G E Y B E W N S T Y N E A A T L D N R A E K L
SERCA1  R A A V G N K M F K G A P E C V I D R C N . . . . . Y V R V G T T R V P M T G P V K E K I T S . V I K E W G T G R D T L R C L A L A T R D P P K R E M V L

800     810     820     830     840     850     860
Drs2p  D E A A N L I E K N . . L I L I G A T A T E D K L Q D S V P E T I H T L Q E A G I K I W V L T G D R Q E T A I N I G M S C R L L S E D M N L L I N E E T R D D
SERCA1  D D S S R F M E Y E T D L T F V G V V G M I T D P P R K F V M G S I Q L C R D A G I R V I M I T G D N K G T A I A I C R R I G I F G E N E . . . . .

870     880     890     900     910     920     930     940
Drs2p  T E R N L L E K I N A L N E H Q L S T H D M K S L A L V I D G K S L G F A L E P E L E D Y L L T V A K L C K A V I C G R V S P L O K A L V K M V K R K S S L
SERCA1  . . . . . E V A D R A Y T G R E F D D L P L A F Q R S . . . . . A C R R A C C F A R V E P S H K S K I V E Y L Q S . Y D E I

950     960     970     980     990     1000    1010    1020
Drs2p  L L A I A S G A N D V S M I Q A A H V G V G I S G M E C M Q A A R S A D I A L G Q F K F L K K L L L V H G S W S Y Q R I S V A I L S Y F Y K N T A L Y M T Q F W
SERCA1  T A M T G D G V N D A P A L K K A E I G I A M G . . S C T A V A K T A S . . . . . E M V L A D D N E S T I V A A V E B G R A I Y N N M K Q F I R . . Y

1030    1040    1050    1060    1070    1080    1090    1100
Drs2p  Y V F A N A F S G Q S I M E S W T M S F Y N L F F T V W P P F V I C V E D Q F V S R L L E R Y P O L Y K L G Q K G O F F S V Y I F W G W I N G F F H S A I V
SERCA1  L I S S N V G E V V C I F L N A A L G L P E A L I P V Q L L W V N I V T D G L P A T A L G F N P P D L D I M D R P P R S P K E P I T S G W L F . . F . . . . .

1110    1120    1130    1140    1150    1160    1170    1180
Drs2p  F I G T I L I Y R Y G F A L N M H G E L A D H W S W G V T Y T T S V I V I V L C H A A L V T N Q W T K F T I I A I P C S L L F W L I F F P I Y A S I F P H A N .
SERCA1  . . . . . R Y . . . . . M A L G G Y V G A A T V G A A A W W F M Y A E D G P C V T Y H Q L T H F M Q C T E D H P F E G

1190    1200    1210    1220    1230    1240    1250    1260
Drs2p  I S R E Y Y G V V K H T Y G S G V F W L T L V L P T P A L V R D F L W K Y Y K R M Y E P E T Y H V I T Q E M Q K Y N I S D S R P H V Q Q F Q N A I R K V R Q V Q
SERCA1  L D C E I F E A P E P . . . . . M T M A L S V L V T I E M C N A L N S L S E N Q S L M R M P P W V N I W L L G S I C L S M S L H P L L Y V D F L P

1270    1280    1290    1300    1310    1320    1330    1340
Drs2p  R M K R Q R G F A F S Q A E E G G Q E K I V R M Y D T T Q K R G Y G E L Q D A S A N P F N D N N G L G S N D F E S A E P F I E N F F A D G N Q N S N R F S S
SERCA1  M I F R I K A L D L T Q W . . . . . . . . . . . L M V L K I S L P V I G L D E L K F I A R N Y L E D P E D E R K . . .

1350
Drs2p  R D D I S F D I
SERCA1  . . . . .

```

Figure 1-3. Sequence alignment between Drs2p and SERCA1.

Figure 1-3. Sequence alignment between Drs2p and the sarcoplasmic/endoplasmic reticulum Ca²⁺ ATPase 1 (SERCA1). The alignment was performed using ClustalW on the PBIL server (Combet et al., 2000). Identical residues are shown in black blocks, and similar residues in grey. Numbers indicate residue positions in Drs2p.

Drs2p was also predicted to contain ten transmembrane segments as does SERCA1. SERCA1 can be considered an archetype of the entire P-type ATPase family because it was the first P-type ATPase whose atomic structure was determined by x-ray crystallography (Toyoshima et al., 2000). Moreover, the crystal structures of SERCA1 representing nine different states, which cover almost the entire reaction cycle, have been solved, providing the first structure-based mechanistic model for the pumping cycle of a P-type ATPase (Toyoshima, 2009).

An atomic structure of a P4-ATPase would be of great value to gain mechanistic insight into the function of these enzymes, but unfortunately this has not yet been achieved. However, we have built a homology model of Drs2p by threading its sequence on the atomic structure of SERCA1 (Zhou et al., 2010) (**Figure 1-4**). The premise of this method is a high degree of sequence similarity between the target and the template protein, which normally requires 60-70% similarity or above. However, using the predicted transmembrane segments as anchor points, the intervening loops of Drs2p could be successfully threaded onto the SERCA1 structure. In this homology model, Drs2p has a ten-transmembrane-segment membrane domain, with three well organized cytosolic domains easily recognized as the actuator domain (A), nucleotide binding domain (N), and phosphorylation domain (P). In the overlay mode, the majority of Drs2p can be superimposed well with the SERCA1 template, despite their relatively low homology. This homology model of Drs2p is not sufficient to substitute for an experimentally determined atomic model, but rather serves as complementary information that may facilitate mutational studies.

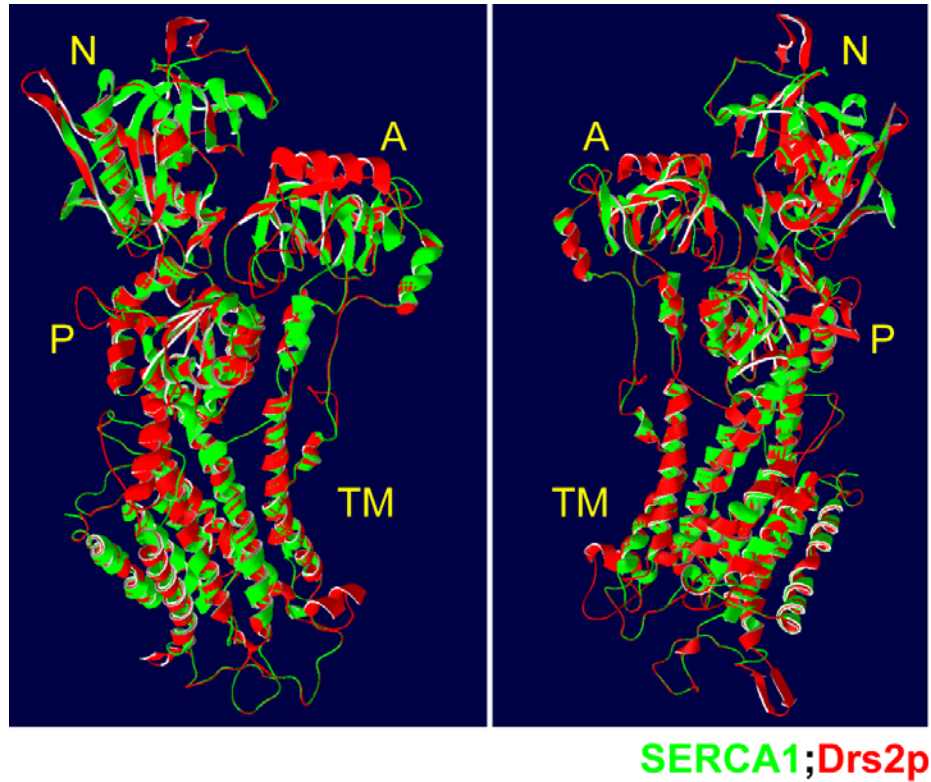


Figure 1-4. Homology model of Drs2p based on the crystal structure of the sarcoplasmic reticulum Ca^{2+} ATPase 1 (SERCA1) in the E2·P conformation (Toyoshima et al., 2004) (PDB ID: 1WPG). Green: SERCA1 template; red: Drs2p. A, actuator domain; N, nucleotide binding domain; P, phosphorylation domain; TM, transmembrane domain. The two panels display two different viewing angles. Homology modeling was performed using the SWISS-MODEL server (Guex and Peitsch, 1997; Kopp and Schwede, 2004; Schwede et al., 2003).

Section 1.1.3: P4-ATPase chaperones

Recent studies showed that most yeast P4-ATPases require Cdc50p family members (Cdc50p, Lem3p and Crf1p) for exit from the endoplasmic reticulum (ER) (Chen et al., 2006; Furuta et al., 2007; Saito et al., 2004) (**Figure 1-5**). In the absence of Lem3p, Dnf1p and Dnf2p show a characteristic ER pattern that is distinct from their normal localization. Similarly, the absence of Cdc50p causes ER localization of Drs2p, and absence of Crf1p causes ER retention of Dnf3p. A similar phenomenon was also observed with P4-ATPases in other organisms (Paulusma et al., 2008; Perez-Victoria et al., 2006; Poulsen et al., 2008). The chaperone function between the P4-ATPases and the Cdc50p family appears to be reciprocal. Cdc50p and Lem3p are also retained in the ER when their corresponding P4-ATPase partners are missing. In wild-type cells, Cdc50p co-localizes with Drs2p, and Lem3p with Dnf1p/Dnf2p. Co-immunoprecipitation between P4-ATPases and Cdc50p family members also supports the formation of physical complexes between Drs2p and Cdc50p, and Dnf1p (or Dnf2p) and Lem3p (Chen et al., 2006; Furuta et al., 2007; Saito et al., 2004).

The relationship between P4-ATPases and Cdc50p family members is reminiscent of Na^+/K^+ and H^+/K^+ ATPases, members of the type-IIc P-type ATPases (P2_c -ATPases), which are among a few oligomeric P-type ATPases possessing a β and even a γ subunit in addition to the catalytic α subunit (Geering, 2001; Kuhlbrandt, 2004). Cdc50p family members may be considered the β subunit for P4-ATPases (α subunit). An important unanswered question is whether the β subunits function solely as a chaperone or if they also contribute in a more direct manner to phospholipid translocation and in vivo function of the α subunits. Co-localization and co-immunoprecipitation data suggest that the α/β subunits remain associated after ER exit (Saito et al., 2004), but this does not necessarily reflect a requirement of β subunits for the α subunits beyond the ER \rightarrow Golgi transport step. Since it is not possible to directly evaluate the function of Drs2p in its

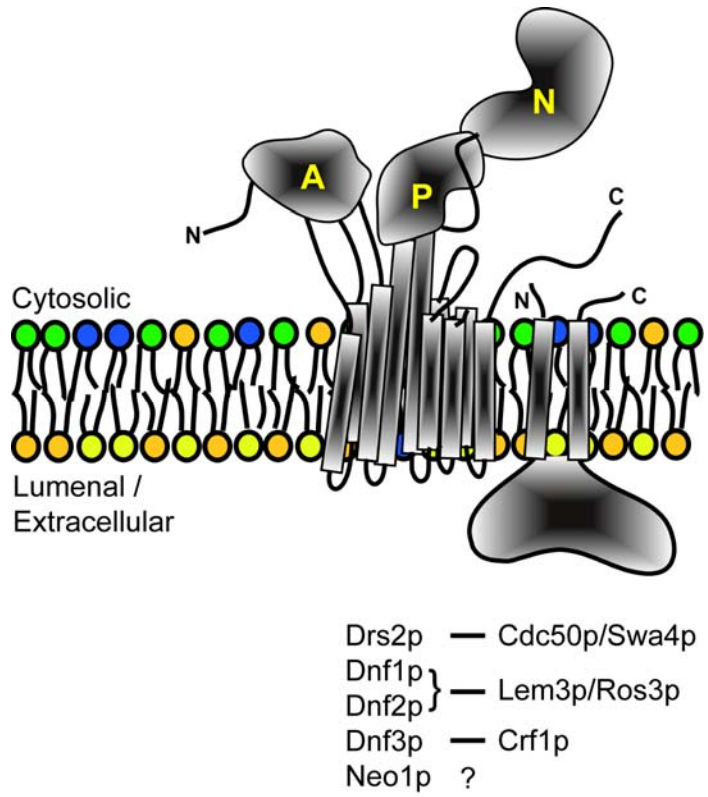


Figure 1-5. Yeast P4-ATPases and their noncatalytic subunits (modified from Zhou et al., 2010). The P4-ATPase (α subunit) is modeled on the crystal structure of SERCA1 in the $E1 \cdot 2Ca^{2+}$ conformation (Toyoshima et al., 2000). The connecting lines indicate the noncatalytic β subunit required to chaperone each P4-ATPase out of the ER. No β subunit for Neo1p has been identified.

native Golgi membrane environment in the absence of Cdc50p, alternative strategies are required. For example, a conditional allele of *CDC50* that disrupts its association with Drs2p could potentially be used to assess the requirement of the Drs2p-Cdc50p interaction for the flippase activity.

Section 1.2: Drs2p as a Potential Flippase

Section 1.2.1: Flip-flop of phospholipids

Phospholipids are amphiphilic molecules that can freely diffuse laterally in their own leaflet, but face a substantial barrier to transverse movement across the bilayer, known as flip-flop, due to their hydrophilic head groups. This barrier can be circumvented by involvement of lipid transporters, and several different types of lipid transporters are proposed to exist in eukaryotic cells (Daleke, 2003; Devaux, 1992; Graham, 2004; Menon, 1995; Pomorski et al., 2004) (**Figure 1-6**). The ER contains an ATP-independent flippase activity that moves phospholipids bidirectionally and without apparent headgroup specificity (Bishop and Bell, 1985; Menon et al., 2000). This ER flippase activity is presumably responsible for balanced growth of both leaflets of the ER during phospholipid synthesis, which appears to be catalyzed primarily on the cytosolic leaflet. Therefore, the ER membrane should be symmetric in lipid distribution. Membrane asymmetry appears to be generated in the post-ER compartments by ATP-consuming flippases and floppases that translocate specific lipid substrates unidirectionally across the membrane bilayer. Flippases mediate the inward movement of phospholipid from the extracellular or luminal leaflet to the cytosolic leaflet of the membrane, whereas floppases act in the reverse, outward direction. The scramblase, upon activation, collapses the lipid asymmetry of the plasma membrane and results in PS and PE exposure on the outer leaflet.

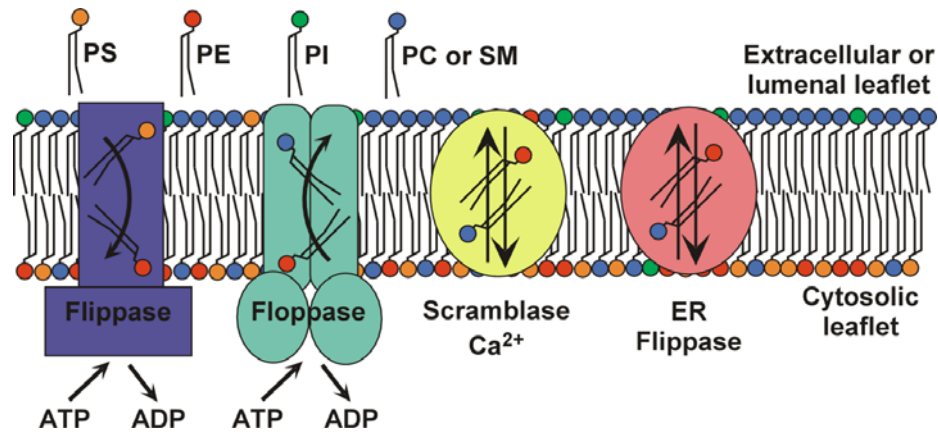


Figure 1-6. Proteins proposed to mediate the transbilayer movement of phospholipids and regulate membrane asymmetry (modified from Graham, 2004). ATP-dependent flippases mediate the inward movement of phospholipids from the extracellular or luminal leaflet to the cytosolic leaflet of membranes, whereas floppases catalyze the opposing outward movement of phospholipids. Scramblase at the plasma membrane is activated by Ca^{2+} influx and causes exposure of phosphatidylserine (PS) and phosphatidylethanolamine (PE) on the surface of the cell. The ER flippase allows phospholipids to diffuse across the ER membrane in an energy-independent manner without headgroup specificity. PI, phosphatidylinositol; PC, phosphatidylcholine; SM, sphingomyelin.

Despite decades of effort to uncover the identities of these lipid transporters, much uncertainty remains. The ER flippase has not been unambiguously identified (Sanyal et al., 2008), nor is the identity of the scramblase known even though several candidates have been suggested, including the ABC1/CED-7 ATP-binding cassette (ABC) transporters (Hamon et al., 2000; Venegas and Zhou, 2007; Wu and Horvitz, 1998), phospholipid scramblase (PLSCR) (Venegas and Zhou, 2007; Wang et al., 2007) and the TAT-1 P4-ATPase (Zullig et al., 2007). A class of ABC transporters involved in multidrug resistance (MDR) and bile secretion appears to be responsible for the floppase activity. For example, the human MDR3 and the mouse *mdr2* P-glycoproteins specifically flop a PC analogue, NBD-PC (Ruetz and Gros, 1994), whereas the human MDR1 and the mouse *mdr1a* flop lipids with a broader substrate specificity including NBD-PC, NBD-PE and NBD-sphingomyelin (NBD-SM) (Raggers et al., 1999; Romsicki and Sharom, 2001; van Helvoort et al., 1996). The floppase function of ABC transporters appears to be conserved even in prokaryotic cells. For instance, MsbA is a bacterial ABC transporter that is closely related to mammalian MDR proteins and is responsible for translocation of the lipid A moiety of lipopolysaccharide and probably PE from the cytoplasmic leaflet to the periplasmic leaflet of the inner membrane of Gram-negative bacteria (Doerrler et al., 2004; Dong et al., 2005). Specific phospholipids (such as PS and PE) are rapidly transported inwardly by flippases, whereas floppases move a much broader spectrum of lipids outwardly. These activities may establish the observed phospholipid asymmetry of the plasma membrane. The primary candidates for the inward-directed flippase activity are members of the ATPase II/Drs2p P4-ATPase family (Alder-Baerens et al., 2006; Gomes et al., 2000; Natarajan et al., 2004; Pomorski et al., 2003; Tang et al., 1996).

Section 1.2.2: Implication of Drs2p as a flippase

The first flippase activity observed was the aminophospholipid translocase activity in the plasma membrane of human red blood cells and was subsequently found to exist in the plasma membrane of many other cell types (Devaux et al., 2006; Seigneuret and Devaux, 1984). Spin-labeled PS and to a lesser extent PE, but not PC, were found to undergo rapid transverse movement across the bilayer resulting in their enrichment in the inner, cytosolic leaflet. Furthermore, shape changes of red blood cells induced by externally added phospholipids are indicative of and correlative of incorporation of these phospholipids in the outer leaflet and subsequent translocation of some lipid species to the inner leaflet. For example, incorporation of PS, PE and PC in the outer leaflet induced crenation of red blood cells (Daleke and Huestis, 1985; Daleke and Huestis, 1989; Seigneuret and Devaux, 1984) (**Figure 1-7**). PS-treated cells and to a lesser extent PE-treated cells reverted quickly from echinocytes back to discocytes and proceeded to stomatocytes, indicating movement of phospholipids to the cytosolic leaflet, whereas PC-treated cells remained echinocytes.

The aminophospholipid translocase activity is Mg^{2+} -ATP-dependent and sensitive to the ATPase inhibitors orthovanadate and N-ethylmaleimide, which are in good accordance with the properties of a novel ATPase, called ATPase II (now designated Atp8a1), purified from bovine chromaffin granules (Moriyama and Nelson, 1988). The connection between the aminophospholipid translocase activity and ATPase II/Atp8a1 was further enhanced by the observation of PS flippase activity in bovine chromaffin granules with a similar inhibitor spectrum as ATPase II/Atp8a1 (Zachowski et al., 1989). Tang et al. cloned a cDNA encoding bovine ATPase II/Atp8a1, and found that it shares 47% amino acid sequence identity and 67% similarity to the yeast protein Drs2p (Tang et al., 1996). There have been several reports describing purification of ATPase II/Atp8a1 (Ding et al., 2000; Paterson et al., 2006). Although this enzyme has not been

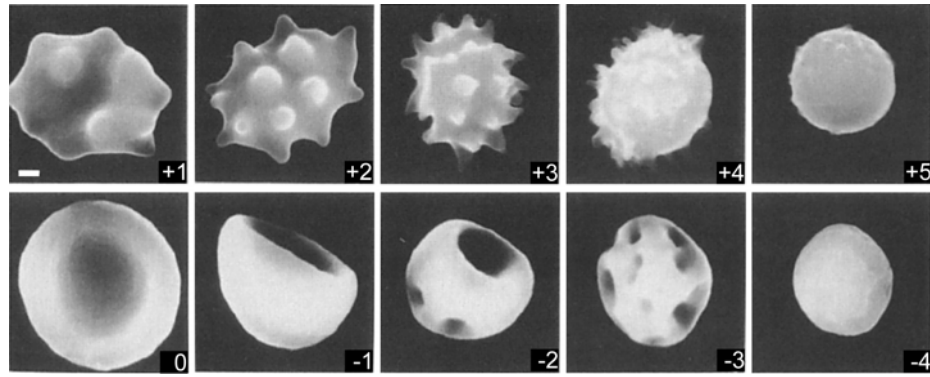


Figure 1-7. Shape changes of human red blood cells by scanning electron microscopy (modified from Daleke and Huestis, 1989). Echinocytes are assigned scores of +1 to +5 with increasing value denoting more severe crenation. Discocytes are scored 0, and stomatocytes are assigned scores of -1 to -4 with decreasing value denoting more severe invagination. Therefore, from the most crenate state to the most invaginated state, the cell morphology changes from +5 to -4. Human red blood cells treated with a relatively high concentration of dilauroylphosphatidylserine (DLPS) undergo shape changes from +5 to -4 within 1 h. Treatment of dilauroylphosphatidylethanolamine (DLPE) also causes shape changes of red blood cells from +3 to -1, although at a slower rate (2-3 h). In contrast, dilauroylphosphatidylcholine (DLPC) treatment only induces echinocytes ($\sim+4$), which revert to discocytes very slowly ($t_{1/2} \sim 8$ h). Scale bar, 1 μm .

reconstituted into liposomes to demonstrate that it can directly catalyze phospholipid flippase activity, its ATPase activity was showed to be maximally stimulated by PS and not stimulated by PC, suggesting that PS is a preferred substrate for ATPase II/Atp8a1.

Section 1.2.3: Yeast plasma membrane flippase activities

While we still do not know if a P4-ATPase in a purified form is sufficient to catalyze phospholipid flippase activity, a number of studies have tested whether P4-ATPases are necessary for flippase activity using genetic approaches in yeast. As with mammalian cells, yeast also sequester most PS and PE to the inner leaflet of the plasma membrane, and possess flippase activity there that mediates translocation of PS and PE fluorescent analogues (NBD-PS and NBD-PE) (Chen et al., 2006; Grant et al., 2001; Kato et al., 2002; Kean et al., 1997; Pomorski et al., 2003; Stevens et al., 2008; Tang et al., 1996). Distinct from the aminophospholipid translocase activity in the plasma membrane of human red blood cells, NBD-PC is also actively internalized by translocation (Grant et al., 2001; Kean et al., 1997; Pomorski et al., 2003), indicating that the yeast plasma membrane flippase(s) has a broader substrate spectrum than the mammalian red blood cell counterpart.

From the early studies after cloning of bovine ATPase II/Atp8a1, a major debate, that is still unresolved, has centered around the contribution of Drs2p to the yeast plasma membrane flippase activity that mediates NBD-PS uptake. Tang et al. exploited a back-exchange approach to monitor the translocation of NBD-PS across the yeast plasma membrane under conditions of partial energy depletion and low temperature (4 C) to block endocytic uptake of the probe (Tang et al., 1996). Wild-type yeast cells showed substantial uptake of PS analogue whereas *drs2Δ* cells were defective in doing so, suggesting a critical role for Drs2p in NBD-PS flip. However, Siegmund et al. found no significant difference between a *drs2Δ* strain and its isogenic wild-type parent for NBD-

PS uptake or distribution at low temperature using fluorescence microscopy or flow cytometry (Siegmund et al., 1998). The controversy continued as Marx et al. used an endocytosis mutant (*end4Δ*) to prevent endocytic uptake of the probe, rather than using low temperature and partial energy depletion, and found only a mild reduction of NBD-PS internalization in *drs2Δend4Δ* cells compared to the parental *end4Δ* strain (Marx et al., 1999). However, in another study on the *ALA1* gene product, a Drs2p homolog in the plant *Arabidopsis thaliana*, Gomes et al. repeated the original observation made by Tang et al., and showed that heterologous expression of *ALA1* in *drs2Δ* cells complemented the NBD-PS internalization defect (Gomes et al., 2000).

The reasons for these experimental discrepancies are still unclear. However, factors that could have contributed to these contradictory results were the presence of other lipid transporters that may also contribute to NBD-PS uptake, the pleiotropic phenotypes caused by deletion of the *DRS2* gene and lack of information on the subcellular localization of Drs2p. We know now that Drs2p is localized primarily to the *trans* Golgi network (TGN) rather than the plasma membrane (Chen et al., 1999; Hua et al., 2002). A relatively small percentage of Drs2p traffics to the plasma membrane, but the presence of multiple endocytosis signals in Drs2p ensures its rapid retrieval back to the TGN (Liu et al., 2007; Liu et al., 2008). The slow egress to the plasma membrane coupled with rapid removal leads to undetectable levels of Drs2p at the plasma membrane of wild-type cells grown under standard conditions. The influence of partial energy depletion and low temperature on Drs2p localization has not been tested. However, blocking endocytosis with an *end4Δ* mutant does cause a near complete redistribution of Drs2p to the plasma membrane (Liu et al., 2007). Therefore, the Marx et al. work suggests that Drs2p makes a relatively minor contribution to NBD-PS uptake across the plasma membrane under conditions where Drs2p is primarily localized to the plasma membrane. Overexpression of Drs2p and Cdc50p in an endocytosis mutant,

conditions that should dramatically increase the amount of Drs2p on the plasma membrane, only increased NBD-PS uptake across the plasma membrane by 2-3 fold relative to the control strains (Saito et al., 2004). As described below, Drs2p is required for robust NBD-PS flippase activity in Golgi membranes (Natarajan et al., 2004) and so it is surprising that redeployment of Drs2p to the plasma membrane leads to a relatively minor enhancement of NBD-PS flip in this location. We suggest that Drs2p is not fully active when it is at the plasma membrane.

Two other members of the P4-ATPase family, Dnf1p and Dnf2p, are easily detected on the plasma membrane and are therefore more likely candidates for the plasma membrane flippase activities (Hua et al., 2002). Consistently, the energy-dependent uptake of NBD-PC and NBD-PE across the yeast plasma membrane is virtually abolished in the *dnf1,2Δ* double deletion mutant (Pomorski et al., 2003). In addition, the *lem3Δ* mutant, which accumulates Dnf1p and Dnf2p in the ER, also exhibits a near complete defect in NBD-PC and NBD-PE uptake (Hanson et al., 2003; Kato et al., 2002; Saito et al., 2004). Importantly, the internalization of Lyso-PE across the yeast plasma membrane is also impaired in *dnf1,2Δ* or *lem3Δ* cells, suggesting that Dnf1p-Dnf2p/Lem3p can also pump a naturally occurring phospholipid across the plasma membrane (Riekhof and Voelker, 2006). Lyso-phospholipids are not transported at an appreciable rate by the aminophospholipid translocase in human red blood cells, again suggesting a unique mode of substrate recognition for the yeast plasma membrane flippases (Daleke and Huestis, 1985; Morrot et al., 1989). Other important potential substrates of Dnf1p-Dnf2p/Lem3p transport activity are edelfosine and miltefosine (Hanson et al., 2003). These drugs are phosphatidylcholine analogues that are toxic to leishmania and trypanosomes. The *lem3Δ* and *dnf1,2Δ* yeast strains are resistant to these drugs, as are leishmania harboring mutations in the analogous genes (Hanson et al., 2003; Perez-Victoria et al., 2006).

There remains some controversy on the influence of Dnf1p and Dnf2p on NBD-PS translocation across the yeast plasma membrane. The *dnf1,2Δ* cells were originally reported to be deficient in internalization of NBD-PS in addition to NBD-PC and NBD-PE (Pomorski et al., 2003). However, several groups found that in the *lem3Δ* strain, which should show the same phenotypes as *dnf1,2Δ* strains, only the NBD-PC and NBD-PE translocation uptake was impaired, leaving NBD-PS internalization unaffected or even increased (Hanson et al., 2003; Kato et al., 2002; Saito et al., 2004). A recent study also failed to detect any defect in NBD-PS uptake in *dnf1,2Δ* cells (Stevens et al., 2008). Moreover, this group tested a variety of strains carrying mutations in multiple P4-ATPases and found no deficit in NBD-PS uptake. These data suggest that NBD-PS uptake across the plasma membrane is likely not catalyzed by a P4-ATPase, with the caveat that *neo1* mutants were not tested. It seems that the protein(s) responsible for NBD-PS uptake across the yeast plasma membrane is still mysterious. Because the P4-ATPase mutants also perturb protein trafficking (Chen et al., 1999; Hua et al., 2002; Hua and Graham, 2003; Liu et al., 2008; Pomorski et al., 2003), these mutants have great potential for displaying pleiotropic phenotypes, for example by mislocalization of enzymes more directly involved in a transport process, perhaps contributing to the disparate data on the influence of *drs2* and *dnf* mutations on NBD-PS uptake across the yeast plasma membrane.

Section 1.2.4: Drs2p-dependent flippase activity in Golgi membranes

The most direct evidence supporting the potential flippase activity of Drs2p came from experiments designed to test if Drs2p is required for an NBD-PS flippase activity in yeast TGN membranes (Natarajan et al., 2004), where Drs2p is primarily localized. TGN membranes isolated from wild-type yeast cells contained an ATP-dependent activity that translocates NBD-PS, and to a lesser extent NBD-PE, from the inner (luminal) leaflet to

the outer (cytosolic) leaflet of the membrane. No NBD-PC flippase activity was observed with TGN membranes. This assay required the presence of NBD-phospholipid probes in the inner leaflet of the isolated TGN membranes, which was achieved by initial incorporation of probes in the outer leaflet and incubation of the membrane in the absence of ATP to allow passive diffusion of the probes to the inner leaflet. Flipping of NBD-phospholipid probes back to the outer leaflet, induced by ATP addition, was monitored by accessibility of the probe to BSA back-extraction (Natarajan and Graham, 2006; Natarajan et al., 2004).

Because of the controversies surrounding the influence of deleting *DRS2* on NBD-PS translocation across the plasma membrane, we sought a method to assess the contribution of Drs2p to the TGN flippase activity that could avoid the pleiotropic consequences of deleting *DRS2*. Ideally, one would like to compare the flippase activity in two TGN membrane preparations that are identical except for the presence or absence of one protein, in this case Drs2p. However, deletion of *DRS2* causes mislocalization of TGN resident proteins, and TGN membranes from *drs2Δ* cells were deficient in multiple proteins relative to the wild-type control membranes (Chen et al., 1999; Hua et al., 2002). To circumvent this problem, a temperature-conditional allele of *drs2* was isolated that could be used to assess the immediate consequences of inactivating Drs2p function (Gall et al., 2002). Strains carrying Drs2p-ts as the sole source of Drs2p were grown at permissive temperature, where Drs2p-ts is active, so a “normal” TGN membrane preparation could be harvested. This membrane preparation was split in half and assayed for flippase activity at permissive and nonpermissive temperatures (Natarajan et al., 2004). Thus, two membrane samples that are identical except for the presence or absence of the *activity* of a single enzyme could be compared. Robust ATP-dependent translocation activity for NBD-PS was detected at permissive temperature (27 C), but was lost when the membranes were assayed at nonpermissive

temperature (37 C). As a control, the TGN membrane isolated from an isogenic strain containing wild-type *DRS2* showed a similar NBD-PS flippase activity at both 27 C and 37 C. These results indicate that Drs2p activity is necessary for the NBD-PS flippase activity in the TGN membrane, and Drs2p most likely catalyzes this activity directly. No NBD-PE flippase activity was detected with the temperature-conditional mutant form of Drs2p, possibly due to insufficient sensitivity of this assay for detecting NBD-PE translocation.

Surprisingly, PS is not an obligatory substrate for Drs2p function in vivo even it appears to be the preferred substrate in vitro. Loss of Drs2p function (*drs2Δ*) perturbs various protein trafficking pathways (Chen et al., 1999; Hua et al., 2002; Liu et al., 2008). If translocation of PS by Drs2p is required to support the role of Drs2p in protein trafficking, we would expect cells deficient for PS to display a similar defect. However, *cho1Δ* yeast cells that lack the de novo PS synthesis and are devoid of PS do not phenocopy the trafficking defects of *drs2Δ* (Natarajan et al., 2004). The *cho1Δ* cells transport proteins normally via the secretory pathway, and still require Drs2p for protein transport as trafficking defects were observed in *drs2Δcho1Δ* cells. Therefore, Drs2p must have at least one additional substrate other than PS.

PE may be such a candidate substrate for Drs2p. Saito et al. showed that in addition to increased NBD-PS uptake, the accumulation of Drs2p-Cdc50p on the plasma membrane of endocytosis mutants also increased NBD-PE internalization (Saito et al., 2004). Consistently, Alder-Baerens et al. reported a Drs2p-dependent activity that was responsible for NBD-PS and NBD-PE translocation across yeast secretory vesicle membranes when Drs2p was overexpressed (Alder-Baerens et al., 2006). Importantly, this group also showed an ATP-dependent translocation of endogenous PE to the cytosolic leaflet of the vesicle membrane, and this activity was abolished in a *drs2Δdnf3Δ* strain. Thus, Drs2p may flip both PE and PS across the TGN membrane,

and it is possible that translocation of either substrate is sufficient to support Drs2p-dependent protein trafficking pathways. However, it is also possible that Drs2p has additional lipid or nonlipid substrates that contribute to vesicle budding.

Although a substantial amount of evidence supports the hypothesis that Drs2p and P4-ATPases in general are flippases, the possibility that they may not be direct phospholipid transporters cannot be ruled out. For example, in an alternative model, Drs2p family members may pump an undetermined ion to establish an ion gradient across the membrane, which can be used as an energy source by a second transporter (symporter) that is coupled to phospholipid translocation. This hypothesis has been partially tested in the isolated TGN membranes with a Drs2p-dependent NBD-PS flippase activity (Natarajan et al., 2004). Substitution of other ions for Na^+ and Cl^- , which were the major ions in the assay, did not affect NBD-PS translocation. Thus, if Drs2p pumps an ion (or heavy metal) across the membrane, it would have to do so with either a lack of ion specificity, or be able to drive the lipid translocation process using a very dilute external ion concentration (i.e. contaminating ions in the sample). Potentially supporting a secondary transport model, a proton gradient seems to be necessary for the translocation of NBD-PC, NBD-PE and NBD-PS across the yeast plasma membrane (Hanson and Nichols, 2001; Stevens et al., 2008; Stevens and Nichols, 2007). This gradient is generated by the plasma membrane H^+ ATPase (Pma1p) rather than the P4-ATPases Dnf1p/Dnf2p, so how a proton gradient contributes to the Dnf-dependent flippase activity is still unclear. The most definitive approach to determine if the P4-ATPase family members are flippases is to biochemically reconstitute a purified P4-ATPase into chemically defined proteoliposomes and assay for flippase activity. This has been a major goal in the flippase field for 25 years and has not yet been achieved.

Section 1.2.5: P4-ATPases in yeast membrane asymmetry

One major function proposed for Drs2p and other P4-ATPases is to generate and maintain membrane phospholipid asymmetry (Daleke, 2003; Devaux, 1992; Graham, 2004; Pomorski et al., 2004). The fact that the yeast plasma membrane is asymmetrical with PS and PE restricted to the cytosolic leaflet suggests that the membrane asymmetry must be established as membranes flow through the Golgi and/or upon arrival at the plasma membrane. The detection of energy- and P4-ATPase-dependent translocation activities for NBD-derivatives of PS, PE and/or PC analogues in the TGN (Natarajan et al., 2004), post-Golgi secretory vesicles (Alder-Baerens et al., 2006) and the plasma membrane (Pomorski et al., 2003; Riekhof and Voelker, 2006; Stevens et al., 2008) suggests that P4-ATPases may act at multiple sites to establish and maintain phospholipid asymmetry in yeast. While PS and PE are restricted to the cytosolic leaflet, the distribution of PC between the inner and outer leaflets of the yeast plasma membrane has not been characterized. The presence of an NBD-PC translocase activity suggests that PC might also be restricted to the inner leaflet. Intriguingly, the plasma membrane of yeast has nearly equal parts of glycosphingolipid and glycerophospholipid by mass (Hechtberger et al., 1994; Zinser et al., 1991), perhaps suggesting a partitioning of these two lipid classes on either side of the plasma membrane.

When the function of one or more P4-ATPases is disrupted, the asymmetrical distribution of PS and PE on the plasma membrane is perturbed. The detection of cells exposing PS and PE on the outer leaflet is greatly facilitated by reagents that specifically target, bind, or react with these lipid species, including the use of Ro09-0198 (Ro) peptide for PE detection (Chen et al., 2006; Kato et al., 2002; Pomorski et al., 2003), papuamide B (PapB) (Chen et al., 2006; Parsons et al., 2006) and annexin V for PS detection (Chen et al., 2006; Hamon et al., 2000; Zullig et al., 2007), and

trinitrobenzenesulfonic acid (TNBS) (Alder-Baerens et al., 2006; Pomorski et al., 2003) for aminophospholipid detection (PE and PS).

Ro is a tetracyclic peptide antibiotic that specifically binds PE exposed on the cell surface and causes cytolysis (Aoki et al., 1994). In a genetic approach to identify flippases in yeast that control phospholipid asymmetry of the plasma membrane, yeast cells were screened for mutants that exhibit hypersensitivity to Ro peptide (Kato et al., 2002). One of the most sensitive mutants isolated was *ros3* (for Ro-sensitivity), indicating more PE was exposed on the cell surface in this mutant. *ROS3* (also known as *LEM3*) encodes the chaperone and potential β subunit for Dnf1p and Dnf2p (Saito et al., 2004). Moreover, cells losing both Dnf1p and Dnf2p function (*dnf1,2 Δ*) exposed more endogenous PE to the outer leaflet of the plasma membrane compared to wild-type cells, as judged by increased availability to TNBS labeling and increased Ro sensitivity (Pomorski et al., 2003). Disruption of *DRS2* in *dnf1,2 Δ* cells caused even more PE exposure, supporting the role suggested for Drs2p in regulating the plasma membrane asymmetry by pumping PE to the cytosolic leaflet of the Golgi prior to export of membrane in vesicles targeted to the plasma membrane. Consistently, isolated post-Golgi secretory vesicles also exhibited less PE to the cytosolic leaflet when the function of Drs2p and/or Dnf3p was disrupted (Alder-Baerens et al., 2006).

In a recent study, PapB, a cyclic lipopeptide, was shown to specifically target PS exposed on the cell surface to induce cytolysis (Chen et al., 2006; Parsons et al., 2006). Hypersensitivity to PapB and the PS-binding protein annexin V were used to monitor the exposure of PS in the P4-ATPase and Cdc50p family mutants. *drs2 Δ* , *cdc50 Δ* and several P4-ATPase mutant combinations, such as *dnf1,2 Δ* , exposed significantly more endogenous PS on the cell surface than did wild-type cells. Particularly, the triple mutant *drs2 Δ dnf1,2 Δ* exposed much more PS than either *drs2 Δ* or *dnf1,2 Δ* mutants, supporting

the hypothesis that Drs2p at the TGN and Dnf1p/Dnf2p on the plasma membrane are working together to maintain PS asymmetry of the plasma membrane.

An important caveat of this interpretation is that *drs2Δ*, *cdc50Δ* and other mutants such as *dnf1,2Δ* also perturb the exocytic and endocytic protein transport pathways (Chen et al., 1999; Chen et al., 2006; Hua et al., 2002). Thus, it is possible that loss of PS asymmetry of the plasma membrane is an indirect consequence of protein and membrane trafficking perturbation in these mutants. In fact, clathrin and ARF mutants (*chc1Δ*, *clc1Δ* and *arf1Δ*), as well as endocytosis mutants (*end3Δ* and *end4Δ*), also exposed PS on the cell surface to a level that is comparable to *drs2Δ* (Chen et al., 2006). Surprisingly, a screen of the entire yeast knockout collection for PapB sensitivity identified several hundred mutants that displayed an increased sensitivity to PapB relative to wild-type cells (Parsons et al., 2006). Moreover, acute inactivation of Drs2p or clathrin function by shifting cells bearing *drs2-ts* or *chc1-ts* alleles to nonpermissive temperature failed to cause exposure of PS on the cell surface (Chen et al., 2006), suggesting that loss of PS asymmetry of the plasma membrane may be a secondary consequence of a chronic defect in protein transport. Because of a lack of specificity for this mutant phenotype, loss of plasma membrane phospholipid asymmetry in P4-ATPase mutants does not prove that these enzymes directly pump endogenous phospholipid across the membrane, nor can these phenotypes be used to infer substrate specificity for the P4-ATPases. Again, reconstitution of a P4-ATPase may provide a solution to this problem if sufficiently sensitive assays to measure natural phospholipid asymmetry in proteoliposomes can be established.

Section 1.3: Drs2p in Protein Transport and Vesicle Budding

Section 1.3.1: Vesicle-mediated protein transport

Protein transport in the exocytic and endocytic pathways is primarily mediated by small transport vesicles (Kirchhausen, 2000b) (**Figure 1-8**). For example, vesicles coated with coat protein complex II (COPII) bud from the ER and transport protein cargos to the Golgi, whereas COPI-coated vesicles mediate the retrograde transport from the Golgi back to the ER. Clathrin associates with pathway-specific adapter proteins (APs) and generates clathrin-coated vesicles from the TGN, endosomes and the plasma membrane. Vesicle budding involves a sequence of critical steps, including recruitment of coat components and accessory proteins to the proper membrane site, coat assembly, membrane deformation, incorporation of cargo, and finally scission to release the vesicle.

ADP-ribosylation factor (ARF) is a small GTP-binding protein that plays a key role in vesicle biogenesis by directly binding and recruiting coat proteins onto membranes (D'Souza-Schorey and Chavrier, 2006). ARF-dependent coats include the COPI coatomer complex, clathrin/AP-1, clathrin/GGA (Golgi-localized, γ-ear-containing, ARF-binding protein), AP-3 and AP-4 coat complexes. ARF acts as a molecular switch by cycling between active GTP-bound and inactive GDP-bound forms. The GDP-bound form is largely soluble, whereas the GTP-bound form exposes its myristoylated N-terminus and associates with membranes. The cycling of ARF between its two nucleotide bound states requires catalytic assistance from two classes of proteins. The guanine nucleotide exchange factors (GEFs) promote exchange of GDP for GTP, whereas the GTPase-activating proteins (GAPs) stimulate the hydrolysis of GTP by ARF to convert the GTP-bound to the GDP-bound form (Donaldson and Jackson, 2000).

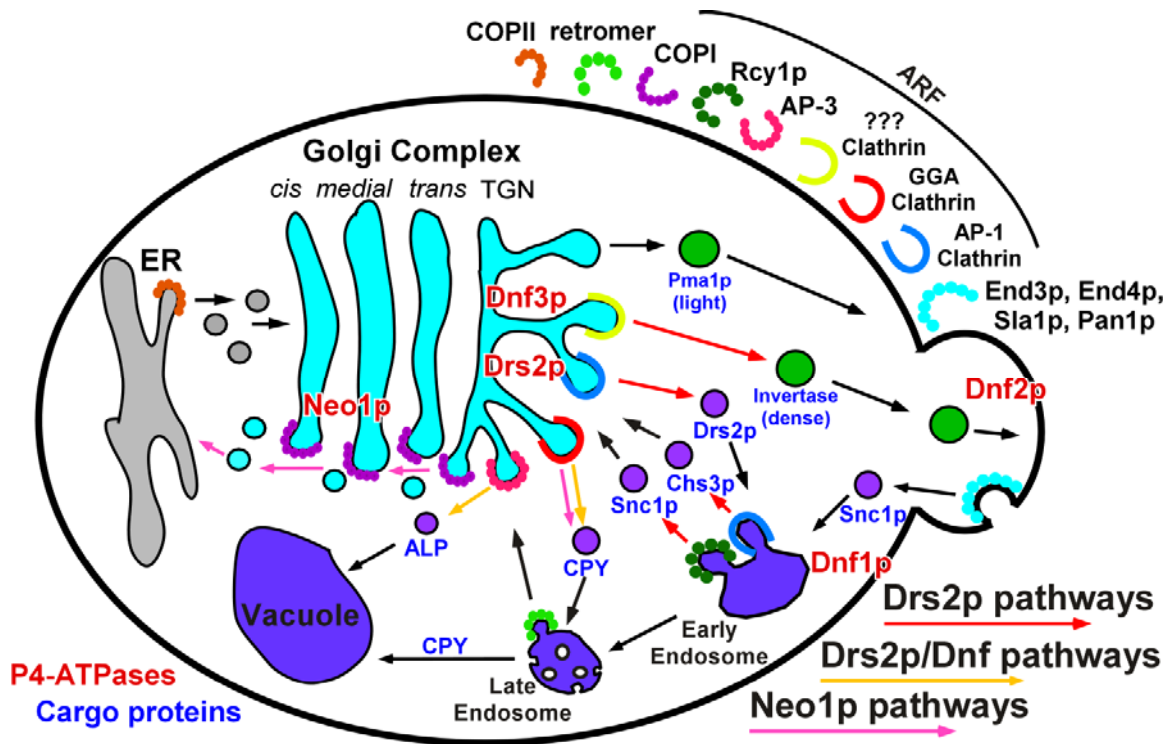


Figure 1-8. Vesicle-mediated protein transport and P4-ATPase requirements in various trafficking pathways in budding yeast (modified from Muthusamy et al., 2009a). Trafficking pathways are defined by cargo proteins (blue text) traveling the route and the vesicle coat proteins (labeled in the upper right quadrant) required for sorting and transport of the cargo. The three major transporting vesicles are coated by COPI (purple coat), COPII (orange coat), and clathrin (yellow, red and blue coats). The coat requirement for the early endosome to TGN recycling pathway traveled by Snc1p is indicated by Rcy1p, although it is not known if Rcy1p is a vesicle coat constituent. Pathways with known P4-ATPase requirements are indicated with colored arrows (see text for details).

In *S. cerevisiae*, ARF is encoded by an essential pair of genes, *ARF1* and *ARF2*, which are 96% identical in protein sequence and redundant in function (Stearns et al., 1990a; Stearns et al., 1990b). In wild-type cells, Arf2p is only expressed at 10% of the level of Arf1p and strains carrying *arf2Δ* show a wild-type phenotype (Stearns et al., 1990a). In contrast, *arf1Δ* cells exhibit partial defects in protein secretion and Golgi-specific glycosylation (Stearns et al., 1990b), as well as altered morphology of the Golgi and endosomes (Gaynor et al., 1998). To identify other factors involved in vesicle biogenesis with ARF, a genetic screen for mutants that are synthetically lethal with *arf1Δ* (the *swa* mutants) was performed (Chen and Graham, 1998). Seven complementation groups were isolated and among them were *DRS2* (*SWA3*) and *CDC50* (*SWA4*) (Chen et al., 1999; Chen et al., 2006). This screen also isolated mutant alleles of the clathrin heavy chain gene (*CHC1/SWA5*) and yeast auxilin (*SWA2*), a protein required for uncoating clathrin-coated vesicles (Chen and Graham, 1998; Gall et al., 2000).

Section 1.3.2: Roles of Drs2p-Cdc50p in protein transport

The genetic interaction between *DRS2* and *ARF1* first implied a role for Drs2p in vesicle-mediated protein transport (Chen and Graham, 1998) (**Figure 1-8**). Drs2p is localized primarily to the TGN, where clathrin-coated vesicles are actively formed. Consistently, *drs2Δ* is also synthetically lethal with a temperature-sensitive allele of clathrin, and exhibits several phenotypes in common with clathrin mutants, such as accumulation of swollen Golgi cisternae (Chen et al., 1999). This phenotype normally indicates a defect in vesicle biogenesis from the Golgi. Consistent with this possibility, disruption of *DRS2* resulted in a marked reduction of clathrin-coated vesicles that can be isolated from these cells (Chen et al., 1999). Another indication that Drs2p facilitates vesicle budding came from epistasis analyses in which *drs2* alleles were combined with mutations that cause an accumulation of transport vesicles (Gall et al., 2002). For

example, disrupting the actin cytoskeleton (with the *sla2Δ* mutation or the drug latrunculin A, LatA) causes accumulation of the dense, post-Golgi vesicles carrying the exocytic protein invertase. Both clathrin and Drs2p are required for the formation of these vesicles as *sla2Δ* cells harboring temperature-sensitive alleles of *DRS2* or clathrin rapidly lose these vesicles upon shift to nonpermissive temperature.

Another similarity to clathrin mutants is that *drs2Δ* mislocalizes the TGN resident protein Kex2p (Chen et al., 1999; Natarajan et al., 2004), which normally cycles between the TGN and endosomal compartments to maintain its steady-state TGN localization (Bryant and Stevens, 1997). Therefore, Drs2p seems to be involved in the clathrin-dependent protein trafficking between the TGN and early endosomes, a pathway associated with AP-1 and clathrin. Indeed, Drs2p was co-immunoprecipitated with AP-1 and genetic data argued that Drs2p is essential for AP-1 function in yeast (Liu et al., 2008). Drs2p itself appears to be a cargo of AP-1/clathrin-coated vesicles that bud from the TGN and are presumably targeted to the early endosome. This view is suggested by the observation that deletion of AP-1 subunits causes rerouting of Drs2p to the plasma membrane, where it can be trapped behind an endocytosis block (Liu et al., 2008). When the endocytosis block is lifted, Drs2p returns back to the TGN in the absence of AP-1. Thus, Drs2p likely uses an AP-1/clathrin pathway to move from the TGN to the early endosome, but does not use AP-1 for retrieval from the early endosome back to the TGN.

Strikingly, inactivation of Drs2p activity (using the temperature-sensitive form of Drs2p) also causes rerouting of Drs2p to the plasma membrane (Liu et al., 2008). These data strongly suggest that the Drs2p activity drives the formation of AP-1/clathrin-coated vesicles from the TGN, and that Drs2p is a cargo of these vesicles. As mentioned above, the most likely destination for these AP-1 vesicles is the early endosome; however, it is also possible that these vesicles carry Drs2p back to earlier Golgi cisternae. Drs2p is

also required for the AP-1-dependent retrograde transport of a cargo protein, Chs3p, from the early endosome to the TGN (Liu et al., 2008). In the absence of AP-1 or Drs2p, Chs3p is rerouted into the late endosome. Thus, Drs2p is needed at both the TGN and early endosome to support AP-1/clathrin function.

Drs2p and Cdc50p are also required for another early endosome to TGN pathway traveled by Snc1p, an exocytic v-SNARE (Hua et al., 2002; Sakane et al., 2006). Snc1p cycles in a TGN → plasma membrane → early endosome → TGN loop, but maintains steady-state localization at the plasma membrane of wild-type cells (Lewis et al., 2000). In contrast, *drs2Δ* or *cdc50Δ* cells accumulate Snc1p in punctate, cytosolic organelles, shown to be early endosomes in *cdc50Δ* (Furuta et al., 2007; Hua et al., 2002). The recycling of Snc1p also requires Rcy1p, an F-box protein involved in the early endosome to TGN transport (Wiederkehr et al., 2000). Cdc50p accumulates in the early endosome of *rcy1Δ* cells, suggesting that Drs2p also requires Rcy1p for retrieval back to the TGN. Furthermore, Drs2p-Cdc50p physically associates with Rcy1p, suggesting a direct role for Drs2p in budding the “Rcy1p” vesicles (Furuta et al., 2007). A subset of COPI mutations also perturb Snc1p recycling (Robinson et al., 2006) and so it is possible that Drs2p and Rcy1p facilitate budding of COPI vesicles. How Rcy1p contributes to protein transport is unknown. The Rab11 homologs Ypt31p and Ypt32p and the ARF-GAP Gcs1p are also implicated in the Snc1p recycling pathway and displayed genetic interactions with Drs2p and Cdc50p (Furuta et al., 2007; Sakane et al., 2006).

Section 1.3.3: Influence of other P4-ATPases on protein transport

Importantly, other members of P4-ATPase family are also involved in various protein trafficking pathways (**Figure 1-8**). Drs2p and Dnf ATPases constitute an essential group in yeast with functional redundancy, which also occurs at the level of protein transport (Hua et al., 2002). For example, Drs2p and Dnf1p show redundant functions for alkaline

phosphatase transport from the TGN to the vacuole in a pathway requiring AP-3, but not clathrin. Carboxypeptidase Y (CPY) transport from the TGN to the late endosome, a pathway that appears to use GGA adaptors and clathrin, is kinetically delayed in *drs2Δdnf1Δ* cells (Hua et al., 2002). A similar kinetic delay in CPY transport was observed when *drs2Δ* single mutant was shifted to a low, nonpermissive growth temperature (Chen et al., 1999). Disruption of *DNF1* and *DNF2* caused a cold-sensitive defect in the internalization step of endocytosis, which was exacerbated by additional disruption of *DRS2*, indicating these three proteins may contribute to endocytosis (Pomorski et al., 2003). Moreover, the *dnf1,2Δ* mutant accumulates Snc1p in internal membranes but has no effect on the trafficking of Ste2p, the α -factor receptor that travels the endocytic pathway to the vacuole for degradation, suggesting that Dnf1p and Dnf2p play overlapping roles with Drs2p in the early endosome to TGN pathway as well (Hua et al., 2002).

The essential Neo1p has also been implicated in vesicle-mediated protein transport (Hua and Graham, 2003; Singer-Kruger et al., 2008; Wicky et al., 2004). The *neo1-ts* mutants show several defects at nonpermissive temperature in common with COPI mutants (Hua and Graham, 2003), including the cargo-specific defects in secretion, aberrant glycosylation of cargos in the Golgi and the mislocalization of Rer1p, a protein that normally cycles between the ER and the Golgi, to vacuole. These observations suggest that Neo1p is required for a COPI-dependent retrograde transport pathway from the Golgi to the ER, a pathway essential for yeast viability. On the other hand, *neo1-ts* mutants were also reported to exhibit fragmented vacuoles and defects in endocytosis (Wicky et al., 2004), accumulation of adapter protein Gga2p on aberrant membranes (Singer-Kruger et al., 2008) and delayed CPY transport (Wicky et al., 2004). Deletion of *GGA2* or *ARL1*, which encodes an ARF-like protein that functions within the endosomal/Golgi system, suppressed the temperature-sensitive phenotype of *neo1-ts*

mutants (Singer-Kruger et al., 2008; Wicky et al., 2004). In addition, Neo1p showed both genetic and physical interactions with Ysl2p (Singer-Kruger et al., 2008; Wicky et al., 2004), a potential GEF for Arl1p. Thus, Neo1p seems also to play a role in protein trafficking within the endosomal/Golgi system.

Section 1.3.4: Endocytosis of Drs2p

Drs2p maintains steady-state localization to the TGN, and cannot be detected on the plasma membrane of wild-type cells (Chen et al., 1999; Hua et al., 2002; Liu et al., 2007; Liu et al., 2008; Saito et al., 2004). However, in several endocytosis-defective mutants such as *vrp1*, *end3* and *end4*, a substantial amount of Drs2p accumulates on the plasma membrane concomitant with a depletion of the TGN pool of Drs2p (Liu et al., 2007; Saito et al., 2004). This observation suggests that Drs2p transits the plasma membrane as part of its normal trafficking itinerary. Consistently, Drs2p is also found in post-Golgi secretory vesicles that are targeted to the plasma membrane (Alder-Baerens et al., 2006). To determine the kinetics of Drs2p transport to the plasma membrane, cells expressing GFP-Drs2p were monitored over time after acutely blocking endocytosis by treatment with LatA (Liu et al., 2007), an inhibitor of actin assembly. GFP-Drs2p was found to accumulate very slowly on the plasma membrane over the course of ~3 h. Based on quantitative western blots, we estimate that wild-type yeast cells have ~4,000 Drs2p molecules per cell distributed among 5-6 TGN cisternae. If the redistribution of Drs2p to the plasma membrane occurs linearly over the 3-h incubation with LatA, then only 20 Drs2p molecules per min (0.5% of the total) are transported from the TGN to the plasma membrane. Upon washout of LatA, Drs2p rapidly returns to the TGN, indicating that Drs2p must contain functional endocytosis signals (Liu et al., 2008).

In yeast, two types of endocytosis signals have been characterized that sort membrane proteins into a clathrin/actin-based endocytic pathway for internalization from

the plasma membrane: sequences that mediate phosphorylation and ubiquitination of the cargo (Hicke and Dunn, 2003), such as PEST-like sequences (Roth et al., 1998), and the NPF_{XD} motif (Howard et al., 2002). The NPF_{XD} signal is recognized by the Sla1p subunit of an endocytic coat complex consisting of clathrin, Pan1p, End3p, Sla2p/End4p and Sla1p (Howard et al., 2002; Kaksonen et al., 2006; Newpher et al., 2005). Pan1p is a member of the Eps15 family of modular scaffolding proteins and interacts with the clathrin binding proteins AP180 and epsin, as well as the Arp2/3 complex (Aguilar et al., 2003; Duncan et al., 2001; Wendland and Emr, 1998). Therefore, Pan1p may be capable of linking adaptor-bound cargo proteins to clathrin and actin assembly. Pan1p, End3p and actin assembly are required for both ubiquitin-dependent and NPF_{XD}-dependent endocytosis, while Sla1p is only required for endocytosis of cargos bearing the NPF_{XD} signal (Howard et al., 2002; Miliaras et al., 2004).

Drs2p contains two NPF_{XD} motifs in its C-terminal cytosolic tail (Liu et al., 2007) (**Figure 1-9A**). These two NPF_{XD} motifs interact with the Sla1p homology domain 1 in Sla1p. Surprisingly, disruption of Sla1p or the NPF_{XD} motifs did not cause accumulation of Drs2p on the plasma membrane, suggesting the presence of other endocytic signal(s) in Drs2p. Sequence analysis of Drs2p revealed three PEST-like sequences on its N-terminus, as well as several other weak PEST-like sequences throughout Drs2p. Deletion of all three N-terminal PEST-like sequences from Drs2p did not perturb its function, but caused accumulation of Drs2p on the plasma membrane in *sla1Δ* cells. These data indicate that Drs2p has multiple endocytosis signals that are functionally redundant.

Interestingly, Dnf1p possesses an NPF_{XD} motif near its N-terminus, which contributes significantly to its Sla1p-dependent endocytosis (Liu et al., 2007). However, the closely related Dnf2p does not contain such a motif. In addition, Dnf1p, but not Dnf2p, shows

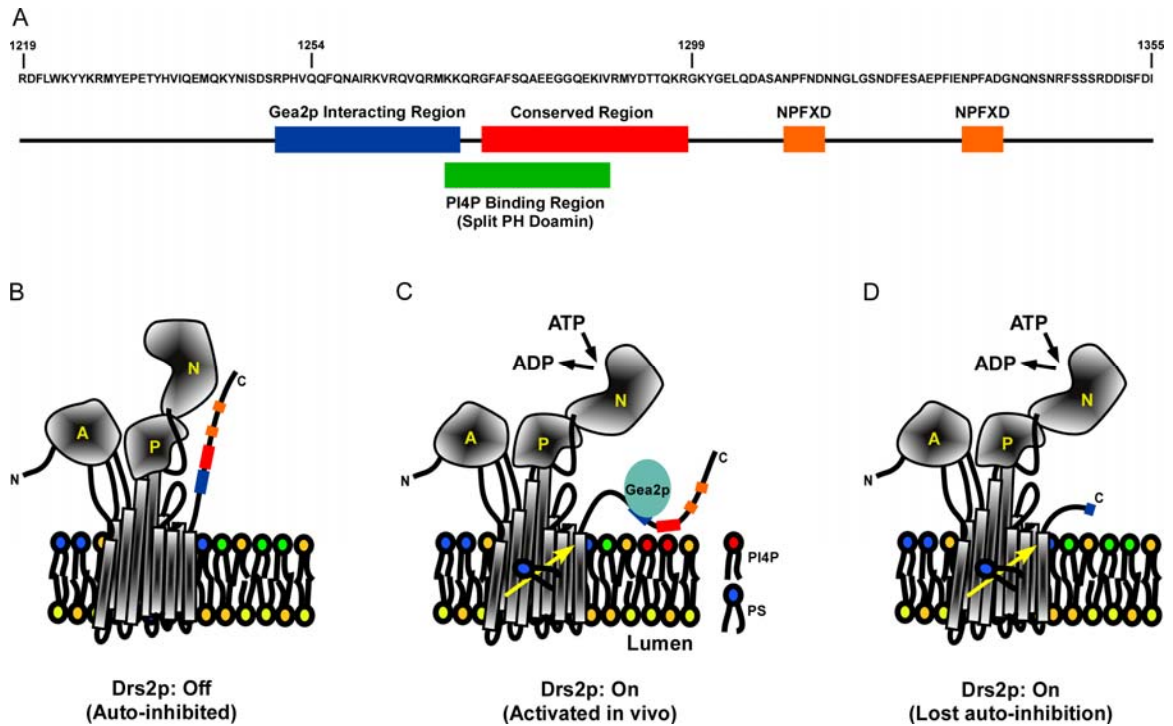


Figure 1-9. Proposed model for Drs2p regulation by its C-terminal tail (modified from Natarajan et al., 2009). (A) The Drs2p C-terminal tail is predicted to be 137-aa long (R1219-I1355) (Chantalat et al., 2004). Various motifs are indicated below the corresponding sequences and are color coded throughout Figure 1-9. The phosphatidylinositol 4-phosphate (PI4P) binding region is slightly overlapped with the Gea2p (ARF-GEF) interacting region. Residues Q1254 and G1299 are also indicated, which are discussed in chapter III (see text for details). (B)-(D) A model is proposed for Drs2p regulation. In vivo, Drs2p is localized primarily to the *trans* Golgi network (TGN) and is auto-inhibited by its C-terminal tail in the absence of regulators (B). Upon binding of regulators, such as Gea2p and PI4P, to its C-terminal tail, Drs2p is activated and catalyzes ATP-dependent flippase activity (C). During Drs2p purification, a C-terminally cleaved form of Drs2p, designated “NoC” form, is generated by unknown proteolytic events (see chapter III for details). When reconstituted into artificial membranes, the Drs2p “NoC” form is active even in the absence of regulators such as Gea2p and PI4P, and is capable of catalyzing phosphatidylserine (PS) flippase activity (D).

redundant protein transport function with Drs2p at the TGN (e.g. in the AP-3 pathway) (Hua et al., 2002), suggesting that the NPFXD/Sla1p-dependent endocytosis of Dnf1p may be important for its function at the Golgi. Supportively, when the NPFXD motif of Dnf1p was mutated to the sequence found in Dnf2p, the mutant Dnf1p was unable to support protein transport in the AP-3 pathway (Liu et al., 2007). Similarly, mutation of Drs2p NPFXD motifs is lethal in *pan1-20* cells (Liu et al., 2007). These data strongly imply that P4-ATPases cannot exert their essential function from the plasma membrane.

Section 1.3.5: The C-terminal tail of Drs2p

The C-terminal tail of Drs2p is essential to Drs2p function as a C-tail truncation allele of *DRS2* cannot complement the cold-sensitive growth and protein transport defects of *drs2Δ* (Liu et al., 2007). The precise function of the C-terminal tail is not known, although it may serve a regulatory function analogous to the C-terminal tail of the plasma membrane Ca^{2+} ATPase in animals (Carafoli, 1994; Enyedi et al., 1989), or the plant or yeast plasma membrane H^+ ATPase (Palmgren, 2001; Portillo, 2000). Three functionally important motifs have been mapped within the Drs2p C-terminal tail so far (from the N- to C-terminus): a Gea2p interacting region, a highly conserved region that follows right after the Gea2p interacting site, and the NPFXDs (Chantalat et al., 2004) (**Figure 1-9A**). The Gea2p interacting region binds directly to the SEC7 (GEF) domain of the ARF-GEF Gea2p, and mutations in the Gea2p interacting region only partially perturb Drs2p function in vivo. In addition, the Golgi localization of Gea2p was not perturbed in *drs2Δ* cells, so Drs2p is not required to recruit Gea2p to the Golgi. Adjacent to the Gea2p interacting region is a highly conserved region that is found in most close homologs of Drs2p, including mammalian ATPase II/Atp8a1. Deletion of this conserved region also partially disrupts Drs2p function in vivo. However, a deletion that impinges on both the Gea2p interacting region and the conserved region eliminates Drs2p function in vivo.

Recent work from our laboratory showed that the conserved region is part of a phosphatidylinositol 4-phosphate (PI4P) binding region that is homologous to a split PH domain (Natarajan et al., 2009). Furthermore, binding of Gea2p and PI4P to the C-terminal tail of Drs2p was found to be necessary to activate the Drs2p flippase activity in isolated TGN membranes. These data further support a regulatory function of the C-terminal tail to the Drs2p activity (**Figure 1-9B and C**).

Section 1.3.6: Flippases and vesicle formation

It has been proposed for many years that flippases may play a critical role in vesicle biogenesis and protein transport (Devaux, 1991; Graham, 2004; Pomorski et al., 2004). Translocation of phospholipids by flippases from the extracellular or luminal leaflet to the cytosolic leaflet of the membrane increases the surface area of the cytosolic leaflet at the expense of the extracellular leaflet. As suggested by the bilayer couple hypothesis (Sheetz and Singer, 1974), the imbalance of phospholipid number and surface area of the membrane bilayer would result in membrane deformation and induction of membrane bending toward the side with more phospholipids and a larger surface area. For instance, incorporation of exogenous aminophospholipids (PS and PE) to the outer leaflet of human red blood cells caused an initial echinocytic morphological change to the cells (Daleke and Huestis, 1985; Daleke and Huestis, 1989; Seigneuret and Devaux, 1984). Subsequent translocation of the added PS or PE to the inner leaflet, catalyzed by the aminophospholipid translocase, drove the cells back to discocytes or even stomatocytes. Therefore, changes in the shape of red blood cells (membrane curvature) correlate well with the imbalance of phospholipid number across the membrane bilayer (**Figure 1-7**).

Many observations support the concept that unbalanced changes in monolayer surface area can impinge on vesicular transport. For example, sphingomyelinase

treatment of cells, which cleaves the head group from SM thereby reducing the surface area of the outer leaflet of the plasma membrane, drives ATP-independent formation of functional endocytic vesicles (Zha et al., 1998). Similarly, incorporation of exogenous PS or PE in the outer leaflet of the plasma membrane and subsequent translocation to the inner leaflet significantly enhances endocytosis. In contrast, addition of Lyso-PS, which cannot be translocated across the plasma membrane and remains in the outer leaflet, inhibits endocytosis (Farge et al., 1999). These observations are in agreement with the role proposed for flippases in vesicle budding. However, the limitation of these approaches is that they make use of unusual perturbations to the cells. The studies on yeast P4-ATPases demonstrate that these enzymes are part of the normal machinery required for vesicle-mediated protein transport, providing the first line of evidence that cells use a bilayer-couple mechanism under normal physiological conditions to support vesicle biogenesis.

Generation of positive membrane curvature required for vesicle formation is a role that has traditionally been assigned to coat proteins such as clathrin (Kirchhausen, 2000a; Schmid, 1997). Structural studies have revealed an intrinsic curvature in the clathrin triskelion (Musacchio et al., 1999; Smith et al., 1998) and clathrin is capable of self-assembly into polyhedral baskets in the absence of lipids (Woodward and Roth, 1978). In an in vitro system, clathrin-coated buds can form from protein-free liposomes with a minimal requirement of clathrin and adaptor proteins (Takei et al., 1998). However, recent theoretical studies estimated that the rigidity of clathrin-AP complex is of the same order of magnitude as the resistance of lipid membranes to bending (Nossal, 2001), suggesting that the clathrin coat assembly is unlikely to provide sufficient energy to drive membrane deformation in vivo. Instead, it may serve to stabilize an already curved membrane and prevent the membrane from collapsing back into a planar form. In the “Brownian ratchet” model (Hinrichsen et al., 2006), membranes fluctuate

spontaneously, resulting in transient membrane invaginations, which could be captured by the clathrin lattice to form vesicles. Formation of the positive curvature may also be driven directly by accessory proteins such as the BAR-domain-containing proteins (Itoh and De Camilli, 2006; Ren et al., 2006) and epsins (Ford et al., 2002) with the capability of deforming membranes.

Flippases may facilitate vesicle formation by several means (**Figure 1-10**). First, flippases may help generate the positive curvature and prime the membrane deformation by pumping phospholipids across the membrane bilayer using the energy from ATP hydrolysis (Graham, 2004). Secondly, flippases (e.g. Drs2p) may interact directly with coat/accessory proteins (e.g. the AP-1 complex, the ARF-GEF Gea2p and Rcy1p) (Chantalat et al., 2004; Furuta et al., 2007; Liu et al., 2008), recruit and concentrate these proteins to vesicle budding sites. Interestingly, loss of Drs2p perturbs clathrin/AP-1 function and formation of clathrin-coated vesicles but not the association of clathrin/AP-1 to the membrane (Chen et al., 1999; Gall et al., 2002; Liu et al., 2008), suggesting that the recruitment role of Drs2p is less important. Rather, the ability of Drs2p to generate and/or stabilize positive curvature appears to be more critical to the process of vesicle formation. Another influence that flippases may have on vesicle biogenesis is that, in the process of translocation of specific phospholipids, flippases could concentrate certain lipid species and generate a unique local membrane environment (e.g. PE-rich) that is necessary and favorable for vesicle budding. A reconstitution system with purified flippases and chemically defined liposomes should be useful to assess these hypotheses.

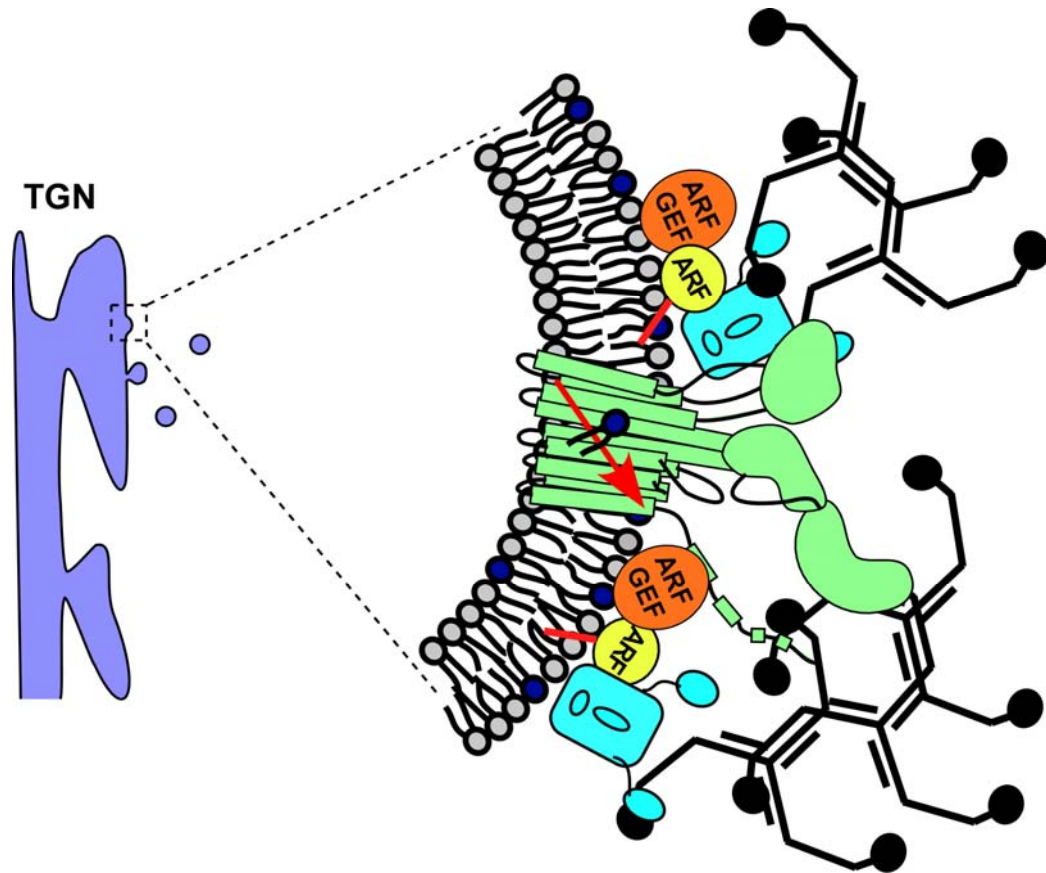


Figure 1-10. Proposed model for how Drs2p flippase activity could drive budding of AP-1/clathrin-coated vesicles (modified from Zhou et al., 2010). Interaction of Drs2p (green) with ARF-GEF (Gea2p) helps concentrate ARF (Arf1p), AP-1 (blue) and clathrin triskelia (black) at sites of phospholipid translocation. Flippase activity induces membrane curvature that is stabilized and localized by assembly of the clathrin lattice. Drs2p is not required for recruitment of ARF-GEF, AP-1 or clathrin to the TGN, but these coat components appear to be incapable of forming vesicles without Drs2p.

Section 1.4: Objectives of the current project

Research on Drs2p and other yeast P4-ATPases has supported their proposed flippase function, and greatly expanded our understanding of how membrane asymmetry is generated. From its position in the TGN and the early endosome, Drs2p controls the trafficking of proteins between the Golgi, plasma membrane and endocytic pathway, thereby influencing the protein composition of the plasma membrane as well as the lipid organization in this membrane. Furthermore, the requirement of Drs2p in protein trafficking pathways is tightly correlated with the proposed phospholipid flippase activity. Conditional mutations in Drs2p inactivate both flippase activity *in vitro* and vesicle budding *in vivo*. Thus, Drs2p appears to prime the membrane in the TGN-endosomal system for delivery to the cell surface by imparting curvature to the membrane to facilitate protein sorting into different vesicle-mediated transport pathways, and by establishing an asymmetric concentration of PS and PE in the cytosolic leaflet.

However, many uncertainties remain. For example, although Drs2p is necessary for NBD-PS flippase activity in the TGN membrane, is it sufficient to directly catalyze this activity when purified and reconstituted in proteoliposomes? What role does Cdc50p play in phospholipid translocation? Are there additional, unknown components of the phospholipid transport system, such as an ion-coupled phospholipid symporter? How is the activity of Drs2p regulated? Does Drs2p induce curvature in the membrane to facilitate vesicle formation or is it coupled to vesicle biogenesis by another mechanism? The current project was carried out to seek answers to these questions.

In chapter II, I describe the purification of Drs2p, its reconstitution into chemically defined artificial membranes, and the development of an assay for testing if the purified Drs2p catalyzes flippase activity directly. The biochemical reconstitution of flippase activity has been deemed as a most direct test on the hypothesis that Drs2p and P4-

ATPases are flippases and has been pursued for years. In a reconstitution system, the requirement of Cdc50p and other components for flippase activity can also be assessed.

In chapter III, I describe a potential regulation of Drs2p activity by its C-terminal tail. This study was inspired by an interesting observation that Drs2p purified using a C-terminal tag seems to be always inactive. The C-terminal tail of Drs2p has been suggested to be auto-inhibitory *in vivo*. Therefore, a mechanistic dissection of the inactive, C-terminally purified Drs2p will help to understand the regulation of Drs2p activity *in vivo*.

In chapter IV, I describe several techniques to generate giant unilamellar vesicles (GUVs). The ultimate goal of this study is to reconstitute Drs2p into GUVs and test if Drs2p can induce membrane curvature and potentially vesicle budding by phospholipid translocation. The preliminary study in this chapter should provide useful information for future biochemical reconstitution and morphological studies of Drs2p-containing GUVs.

Completion of the current project will provide answers to some key questions in the flippase field, as well as establishing new techniques and tools to address remaining questions in the future.

CHAPTER II*

RECONSTITUTION OF PHOSPHOLIPID TRANSLOCASE ACTIVITY WITH PURIFIED DRS2 PROTEIN, A TYPE-IV P-TYPE ATPASE FROM BUDDING YEAST

Section 2.1: Abstract

Type-IV P-type ATPases (P4-ATPases) are putative phospholipid translocases, or flippases, that translocate specific phospholipid substrates from the exofacial to the cytosolic leaflet of membranes to generate phospholipid asymmetry. In addition, the activity of Drs2p, a P4-ATPase from *Saccharomyces cerevisiae*, is required for vesicle-mediated protein transport from the Golgi and endosomes, suggesting a role for phospholipid translocation in vesicle budding. Drs2p is necessary for translocation of a fluorescent phosphatidylserine (PS) analogue across purified Golgi membranes. However, flippase activity has not been reconstituted with purified Drs2p, or any other P4-ATPase, and so whether these ATPases directly pump phospholipid across the membrane bilayer is unknown. Here, we show that Drs2p can directly catalyze phospholipid translocation through purification and reconstitution of this P4-ATPase into proteoliposomes. The noncatalytic subunit, Cdc50p, was also reconstituted in the proteoliposome although at a substoichiometric concentration relative to Drs2p. In proteoliposomes containing Drs2p, a PS analogue is actively flipped across the liposome bilayer to the outer leaflet in the presence of Mg^{2+} -ATP, while no activity toward the phosphatidylcholine (PC) or sphingomyelin (SM) analogues was observed. This flippase activity is mediated by Drs2p, since protein-free liposomes or proteoliposomes reconstituted with a catalytically inactive form of Drs2p show no translocation activity. These data demonstrate for the first time the reconstitution of flippase activity with a purified P4-ATPase.

*This chapter was modified from: Zhou X and Graham TR (2009) Reconstitution of phospholipid translocase activity with purified Drs2p, a type-IV P-type ATPase from budding yeast. *Proc Natl Acad Sci U S A* 106:16586-16591.

Section 2.2: Introduction

Phospholipids are asymmetrically distributed across the plasma membrane of eukaryotic cells and the control of this membrane asymmetry plays important roles in many cellular processes (Bretscher, 1973; Devaux, 1992). For example, in resting human red blood cells, phosphatidylserine (PS) and phosphatidylethanolamine (PE) are primarily restricted to the inner leaflet of the plasma membrane, while phosphatidylcholine (PC) and sphingomyelin (SM) are exposed on the cell surface (Devaux, 1992; Zwaal and Schroit, 1997). Regulated exposure of PS in the outer leaflet of red blood cells and platelets provides an interface for stimulating coagulation reactions (Zwaal and Schroit, 1997). Apoptotic cells also expose PS as a signal for removal by macrophages or other cells (Williamson and Schlegel, 2002). In addition, phospholipid asymmetry of the bile canalicular membrane is critical to the integrity of membrane and normal bile secretion by hepatocytes (Cai et al., 2009; Paulusma et al., 2006). Loss of phospholipid asymmetry caused by mutations in the human FIC1/ATP8B1 gene may be the fundamental cause of the liver disease progressive familial intrahepatic cholestasis (PFIC), and its milder form, benign recurrent intrahepatic cholestasis (BRIC) (Bull et al., 1998; Folmer et al., 2009). The altered membrane structure appears to make the bile canalicular membrane susceptible to damage by secreted bile (Cai et al., 2009; Paulusma et al., 2006).

Membrane asymmetry is thought to be generated by proteins that transport phospholipids unidirectionally across a membrane bilayer (Daleke, 2003; Devaux, 1992; Graham, 2004; Pomorski et al., 2004). ATP-dependent flippases are proposed to mediate the inward movement of phospholipid from the extracellular leaflet to the cytosolic leaflet, whereas the opposing outward transport is carried out by floppases. It has been suggested that a subset of ATP-binding cassette (ABC) transporters involved in multidrug resistance (MDR) and bile secretion, including human MDR1 P-

glycoprotein/ABCB1, MDR3/ABCB4, MRP1/ABCC1, and their homologs in other organisms, catalyzes floppase activity (Daleke, 2003; Pomorski et al., 2004). Several of these ABC transporters have been purified and reconstituted into liposomes. For example, proteoliposomes formed with MDR1 P-glycoprotein purified from Chinese hamster ovary cells were shown to transport a variety of lipid analogues, including PS, PE, PC, SM and glucosylceramide analogues bearing a fluorescent 7-nitro-2-1,3-benzoxadiazol-4-yl (NBD) group, across the liposome bilayer (Eckford and Sharom, 2005; Romsicki and Sharom, 2001). Another class of active transporters, the P4-ATPases, is proposed to catalyze the flippase activity that restricts PS and PE to the cytosolic leaflet of the plasma membrane (Daleke, 2003; Graham, 2004; Pomorski et al., 2004). Slow flop of phospholipids without headgroup specificity, combined with rapid flip of PS and PE, is thought to establish the observed membrane asymmetry.

The first ATP-dependent flippase activity described was the aminophospholipid translocase in human red blood cells, which rapidly translocates spin-labeled or unmodified PS and PE in the outer leaflet of the plasma membrane to the inner leaflet (Daleke and Huestis, 1985; Seigneuret and Devaux, 1984). Since the discovery of the aminophospholipid translocase, a major goal has been to define the enzyme responsible for this activity through purification and reconstitution. Flippase activity toward spin-labeled PS and PE analogues has been reconstituted with a partially purified, but unidentified, Mg^{2+} -ATPase from human red blood cells (Auland et al., 1994). ATPase II/Atp8a1, a Mg^{2+} -ATPase that potentially catalyzes aminophospholipid translocase activity in bovine chromaffin granules (Zachowski et al., 1989), has been purified to homogeneity (Ding et al., 2000; Paterson et al., 2006). Phylogenetic analysis of the ATPase II/Atp8a1 sequence indicates that it is a member of the P4-ATPase family (Tang et al., 1996), which includes Fic1/Atp8b1 and Drs2p from yeast (Axelsen and Palmgren,

1998; Kuhlbrandt, 2004). However, flippase activity has not been reconstituted with any purified P4-ATPase, including mammalian ATPase II/Atp8a1.

Although it is not known if a P4-ATPase in a purified form is sufficient to catalyze flippase activity, yeast P4-ATPases are necessary for flippase activities detected in the plasma membrane (Pomorski et al., 2003; Riekhof and Voelker, 2006; Stevens et al., 2008), secretory vesicles (Alder-Baerens et al., 2006) and the *trans*-Golgi network (TGN) (Natarajan et al., 2004). Drs2p is localized primarily to the TGN (Chen et al., 1999; Hua et al., 2002), and requires a chaperone protein Cdc50p for its proper localization (Chen et al., 2006; Saito et al., 2004). Isolated TGN membranes containing a temperature-sensitive mutant form of Drs2p translocate NBD-PS, but not NBD-PC, to the cytosolic leaflet at permissive temperature (Natarajan et al., 2004). However, inactivation of this mutant Drs2p at higher temperature ablates the NBD-PS flippase activity (Natarajan et al., 2004). One possible interpretation of these data is that Drs2p directly pumps phospholipid substrates across membrane bilayer. Alternatively, Drs2p may pump an unidentified ion into the TGN to generate an ion gradient, which is then coupled by another transporter (an unidentified symporter) to phospholipid translocation. To gain further insight into the mechanism of phospholipid translocation, we sought to purify and reconstitute Drs2p to determine if it can directly pump phospholipid substrates across a lipid bilayer.

Towards the goal of reconstituting Drs2p, we have overexpressed Drs2p in yeast and purified it using affinity purification techniques. The ATPase activity of purified Drs2p is Mg^{2+} -ATP dependent and sensitive to orthovanadate. After reconstitution, the Drs2p-containing proteoliposomes actively translocate NBD-PS to the outer leaflet upon addition of Mg^{2+} -ATP, demonstrating that a purified P4-ATPase is sufficient to catalyze flippase activity.

Section 2.3: Materials and Methods

Section 2.3.1: Reagents

IgG Sepharose 6 Fast Flow, calmodulin Sepharose 4B and ATP (>99% purity) were from GE Healthcare (Uppsala, Sweden). Ni-NTA agarose was from Qiagen (Hilden, Germany). AcTEV protease and SimplyBlue SafeStain (Coomassie G-250) were from Invitrogen (Carlsbad, CA), and Bio-Beads SM-2 was from Bio-Rad (Hercules, CA). Phospholipids and fluorescent derivatives were from Avanti Polar Lipids (Alabaster, AL) and were egg PC (L- α -phosphatidylcholine from chicken egg), POPS (1-palmitoyl-2-oleoyl-*sn*-glycero-3-phospho-L-serine), POPC (1-palmitoyl-2-oleoyl-*sn*-glycero-3-phosphocholine), NBD-PS (1-palmitoyl-2-[6-[(7-nitro-2-1,3-benzoxadiazol-4-yl)amino]-hexanoyl]-*sn*-glycero-3-phospho-L-serine), NBD-PC (1-palmitoyl-2-[6-[(7-nitro-2-1,3-benzoxadiazol-4-yl)amino]-hexanoyl]-*sn*-glycero-3-phosphocholine) and NBD-SM (N-[6-[(7-nitro-2-1,3-benzoxadiazol-4-yl)amino]-hexanoyl]-sphingosine-1-phosphocholine). Lipids were dissolved in chloroform and stored at -20 C.

Section 2.3.2: Yeast strains and protein purification

Yeast strains used for protein purification were XZY10b (*MATa his3 leu2 ura3 met15 P_{GPD}::DRS2::TAP_C P_{GPD}::CDC50*), XZY38b (*MATa his3 leu2 ura3 met15 P_{GPD}::DRS2::TAP_C P_{GPD}::CDC50 atp2 Δ ::URA3*), and XZY60m (*MATa his3 leu2 ura3 lys2 P_{GPD}::TAP_N::DRS2 P_{GPD}::CDC50 atp2 Δ ::URA3*), where *TAP_C* encodes the calmodulin binding peptide-TEV protease cleavage site-protein A tag, and *TAP_N* encodes the protein A-TEV protease cleavage site-decahistidine tag.

Yeast strains were grown in 1 liter of 2x YPD (2% yeast extract/4% peptone/4% dextrose) medium to saturation (usually 10-15 OD₆₀₀/mL) at 30 C before harvesting by centrifugation at 5,000 x g for 5 min. All steps following harvest were performed at 4 C

unless otherwise stated. Cells were washed with 10 mM NaN₃, resuspended in 20 mL of lysis buffer (40 mM Tris-HCl, pH 7.5/150 mM NaCl/10% glycerol), and lysed using an EmulsiFlex-C3 High Pressure Homogenizer (Avestin, Inc., Ottawa, Canada) at 25,000 psi for 6 complete passes in the presence of protease inhibitors (500 μM benzamidine hydrochloride, 10 μM phenanthroline, 250 nM aprotinin, 3 μM pepstatin A, 4 μM leupeptin, 2 mM EDTA, 1 mM PMSF). The cell lysate was centrifuged at 15,000 x g for 12 min and 10% polyoxyethylene 9-lauryl ether (C₁₂E₉) was added to the supernatant to a final concentration of 1%. Samples were mixed on an end-over-end rotator for 2 h to solubilize Drs2p. 400 μL of IgG Sepharose 6 Fast Flow beads (50% slurry in 50 mM potassium phosphate and 20% ethanol) pre-washed with 10 mL of wash buffer (40 mM Tris-HCl, pH 7.5/150 mM NaCl/10% glycerol/0.1% C₁₂E₉) was then added and rotated for 2 h, followed by a wash with 10 mL of wash buffer. The IgG beads were resuspended in 1 mL of TEV buffer (40 mM Tris-HCl, pH 7.5/150 mM NaCl/10% glycerol/0.1% C₁₂E₉/10 mM 2-mercaptoethanol/0.5 mM EDTA) with 100 units of AcTEV protease and Drs2p was released by rotating the mixture for 2 h at 16 C.

In the second affinity step, Drs2p-TAP_C was bound to 200 μL of calmodulin Sepharose 4B beads in 5 mL of calmodulin binding buffer (40 mM Tris-HCl, pH 7.5/150 mM NaCl/10% glycerol/0.1% C₁₂E₉/1 mM imidazole/10 mM 2-mercaptoethanol/2 mM CaCl₂) by rotating for 1 h, followed by a wash with 20 mL of calmodulin binding buffer, and was eluted with 1 mL of calmodulin elution buffer (40 mM Tris-HCl, pH 7.5/150 mM NaCl/10% glycerol/0.1% C₁₂E₉/6 mM EGTA). Similarly, TAP_N-Drs2p was incubated with 200 μL of Ni-NTA agarose beads in 5 mL of Ni²⁺ binding buffer (40 mM Tris-HCl, pH 7.5/300 mM NaCl/10% glycerol/0.1% C₁₂E₉/20 mM imidazole/10 mM 2-mercaptoethanol) by rotating for 1 h, followed by a wash with 20 mL of Ni²⁺ binding buffer, and was eluted with 1 mL of Ni²⁺ elution buffer (40 mM Tris-HCl, pH 7.5/150 mM NaCl/10% glycerol/0.1% C₁₂E₉/200 mM imidazole). Protein eluates were stored at -20 C in the

presence of 50% glycerol. Recovery of Drs2p was determined using Odyssey Infrared Imaging System (LI-COR, Inc., Lincoln, NE) to quantify SimplyBlue-stained bands relative to a BSA standard curve. Purified Drs2p was assayed for ATPase activity in ATPase buffer (50 mM Tris-HCl, pH 7.5/100 mM NaCl/50 mM KCl/0.1% C₁₂E₉/4 mM Na⁺-ATP/10 mM MgCl₂) at 37 C for 2 h, and released phosphate was measured colorimetrically using protocols previously described (Carter and Karl, 1982; Paterson et al., 2006; Zimmerman and Daleke, 1993).

Section 2.3.3: Proteoliposome formation

Proteoliposomes were formed by detergent removal using Bio-Beads SM-2 adsorption (Gummadi et al., 2003; Levy et al., 1990a; Levy et al., 1990b). All steps were performed at 4 C unless otherwise stated. Normally, 4 mg of lipid mixture (99% egg PC and 1% NBD-phospholipid) was dried under N₂ stream and solubilized completely with 1 mL of 1% C₁₂E₉ in reconstitution buffer (40 mM Tris-HCl, pH 7.5/150 mM NaCl) at room temperature. 1 mL of TEV buffer containing 20 µg of Drs2p purified by single-affinity purification (IgG Sepharose 6 Fast Flow) was gently mixed with the lipid solution, and the protein-lipid-detergent solution was incubated by rotation for 1 h before SM-2 beads addition. After addition of 100 mg of extensively-washed SM-2 beads and 6 h of incubation on an end-over-end rotator, a second portion of 200 mg of SM-2 beads was added and incubated for another 12 h without removing the original SM-2 beads. The supernatant containing proteoliposomes was then carefully removed and mixed with 500 mg of fresh SM-2 beads for 3 h of incubation. The resulting proteoliposome was removed and stored at 4 C. 200 µL of proteoliposomes was mixed with 200 µL of 80% glycerol, and placed at the bottom of a glycerol step gradient consisting of 40% glycerol, 30% glycerol (300 µL), 10% glycerol (400 µL) and reconstitution buffer (100 µL, top). The samples were centrifuged in a TLS-55 rotor (Beckman Coulter, Inc., Fullerton, CA)

at 50,000 rpm for 6 h, and fractions (200 μ L each) were collected by piercing the bottom of the tube. The recovery of lipids for each fraction was calculated as (Fluorescence of NBD-phospholipid in each fraction) / (Initial fluorescence of total NBD-phospholipid used for reconstitution) x 100%, and Drs2p recovery was determined by (Drs2p quantified by SimplyBlue staining in each fraction) / (Initial Drs2p used for reconstitution) x 100%. For flippase assays, proteoliposome fractions containing both phospholipids and Drs2p were pre-treated with 10 mM dithionite for 3 min to quench most fluorescent NBD-phospholipid in the outer leaflet of proteoliposomes. Treated proteoliposomes were re-floated as described above to separate them from dithionite.

Section 2.3.4: Flippase assay

Flippase activity was defined by a change of interleaflet distribution of fluorescent lipid probes (NBD-phospholipids) in proteoliposomes measured using a dithionite-based quenching approach (McIntyre and Sleight, 1991). For each individual measurement, 10 μ L of proteoliposomes containing \sim 50 ng of Drs2p and \sim 10 nmol of phospholipids were incubated with either 5 mM Na⁺-ATP or Mg²⁺-ATP in 40 μ L of flippase buffer (40 mM Tris-HCl, pH 7.5/200 mM NaCl) at 37 C. At 0 and 30 min of incubation, each sample was assayed for probe distribution. Samples were diluted to 1 mL with flippase buffer in a quartz cuvette and mixed by inverting the cuvette 10 times, and the total fluorescence (F_T) was recorded for 30 s in an AB2 fluorometer (SLM Instruments, Inc.) (λ_{ex} = 460 nm, λ_{em} = 534 nm) to obtain a stable baseline. Then, 10 μ L of 1 M dithionite dissolved in 1 M Tris (pH 10) was added to the sample and mixed to quench the fluorescent probes in the outer leaflet of liposomes, and fluorescence was recorded until a stable line was obtained (120 s, F_D). The sample was then solubilized by addition of 100 μ L of 10% Triton X-100, and the background fluorescence (F_0) was recorded for another 30 s. The percentage of NBD-phospholipid in the outer leaflet of proteoliposomes that is

accessible to dithionite quenching was calculated as $(F_T - F_D) / (F_T - F_0) \times 100\%$ (defined as P_O), and the percentage of NBD-phospholipid flipped to the outer leaflet over a 30-min period was calculated as $P_O^{30\text{min}} - P_O^{0\text{min}}$.

Section 2.4: Results

Drs2p under its endogenous promoter is expressed in a low abundance estimated to be ~4,000 molecules per cell in our wild-type strain (10 ng Drs2p/10⁷ cells, data not shown). To increase the yield of Drs2p, *DRS2* was overexpressed in its native host *S. cerevisiae* by substituting the strong glyceraldehyde-3-phosphate dehydrogenase (GPD) promoter for its endogenous promoter (**Figure 2-1A**) (Janke et al., 2004). To facilitate purification, a tandem affinity purification (TAP) tag was integrated into the 3' end of the *DRS2* gene to express C-terminally TAP-tagged Drs2p (Drs2p-TAP_C, **Figure 2-1A and B**) (Rigaut et al., 1999). Drs2p-TAP_C was functional in vivo, since strains expressing *DRS2-TAP_C* as the sole source of Drs2p grew at 20 C (**Figure 2-2**). Strains carrying loss of function *drs2* alleles cannot grow at 20 C or below (Chen et al., 1999; Hua et al., 2002; Ripmaster et al., 1993). Drs2p requires Cdc50p, a noncatalytic subunit and chaperone protein, for its export from the endoplasmic reticulum (ER) (Chen et al., 2006; Saito et al., 2004), so we also overexpressed *CDC50* using the GPD promoter (**Figure 2-1A**). These modifications led to a 10-fold increase in Drs2p expression relative to wild-type cells (**Figure 2-3**).

For purification of Drs2p-TAP_C, a cell lysate prepared without detergent was centrifuged at 15,000 x g for 12 min to pellet ER membranes, along with any misfolded Drs2p-TAP_C retained there by the quality control machinery. 1% C₁₂E₉ was used to solubilize Drs2p-TAP_C from TGN membranes that remained in the supernatant (see Materials and Methods). As seen in **Figure 2-1C**, Drs2p-TAP_C was successfully purified by the TAP procedure, and composed greater than 90% of protein in the final eluate (lane 4). Cdc50p was not detected in this preparation by SimplyBlue staining, but was

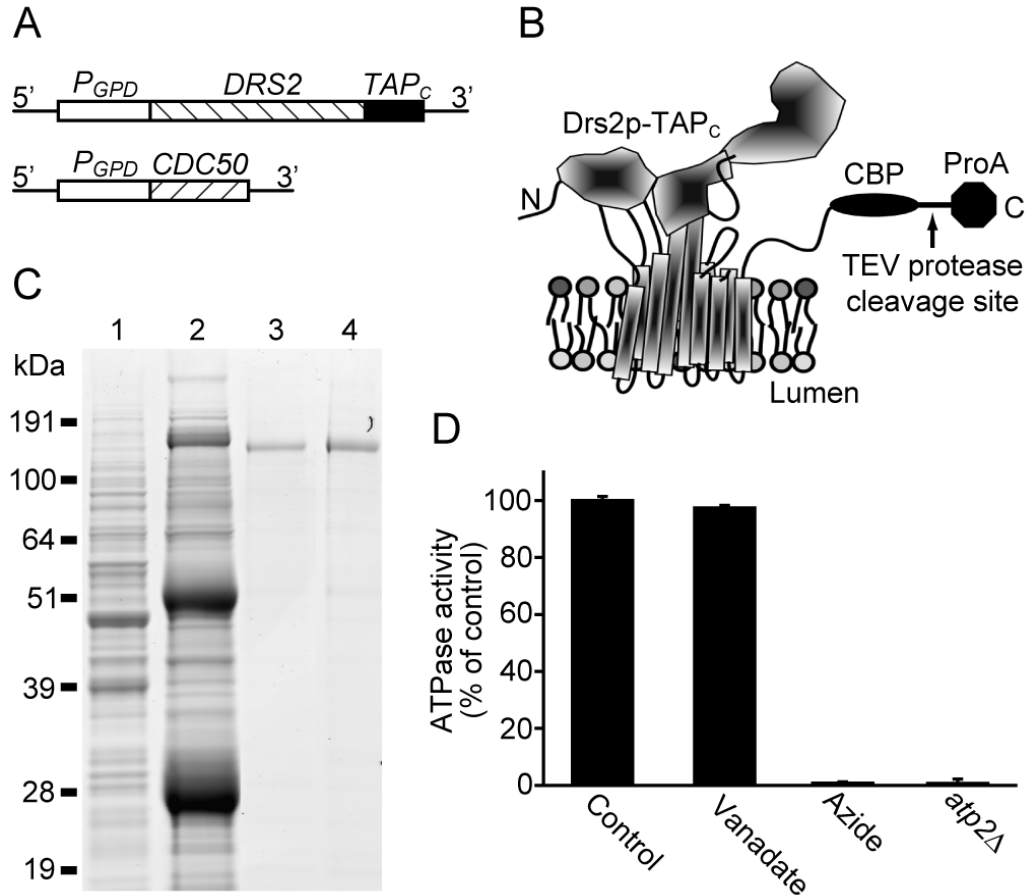


Figure 2-1. Expression and purification of Drs2p-TAP_C. (A) Chromosomal organization of *DRS2-TAP_C* and *CDC50*. (B) Schematic of Drs2p-TAP_C modeled on the crystal structure of the sarcoplasmic reticulum Ca²⁺ ATPase 1 (SERCA1) in the E1·2Ca²⁺ conformation (Toyoshima et al., 2000). CBP, calmodulin binding peptide moiety; ProA, protein A moiety; TEV, tobacco etch virus. (C) Aliquots from a Drs2p-TAP_C purification from strain XZY10b were subject to SDS-PAGE and the gel was stained with SimplyBlue. Lane 1, cell lysate; lane 2, proteins bound to the IgG beads; lane 3, proteins bound to the calmodulin beads; lane 4, final eluate. (D) ATPase activity of purified Drs2p-TAP_C preparations. The control, vanadate (100 μM) and azide (1 mM) samples were assayed using 50 ng of Drs2p-TAP_C purified from strain XZY10b (*ATP2*), and the *atp2Δ* sample was assayed using 100 ng of Drs2p-TAP_C from strain XZY38b (*atp2Δ*), deficient for the F1-ATPase.

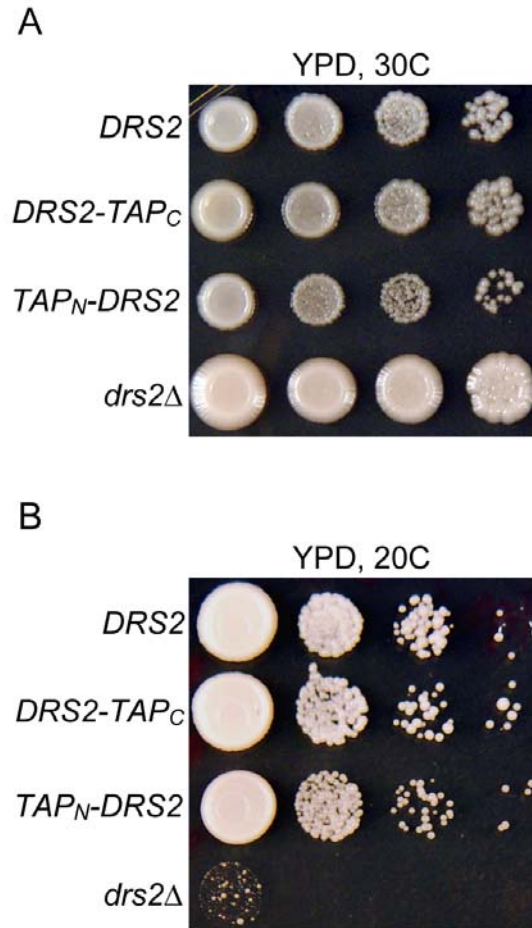


Figure 2-2. Growth phenotype of yeast strains at 30 C (A) and 20 C (B). *DRS2*, (*DRS2*; *atp2Δ*); *DRS2-TAP_C*, (*DRS2::TAP_C*; *atp2Δ*); *TAP_N-DRS2*, (*TAP_N::DRS2*; *atp2Δ*); *drs2Δ*, (*drs2Δ*; *ATP2*). Note that the *drs2Δ* strain grew better than others at 30 C due to its intact *ATP2* gene (mitochondrial F1-ATPase), but it exhibited a growth defect at 20 C.

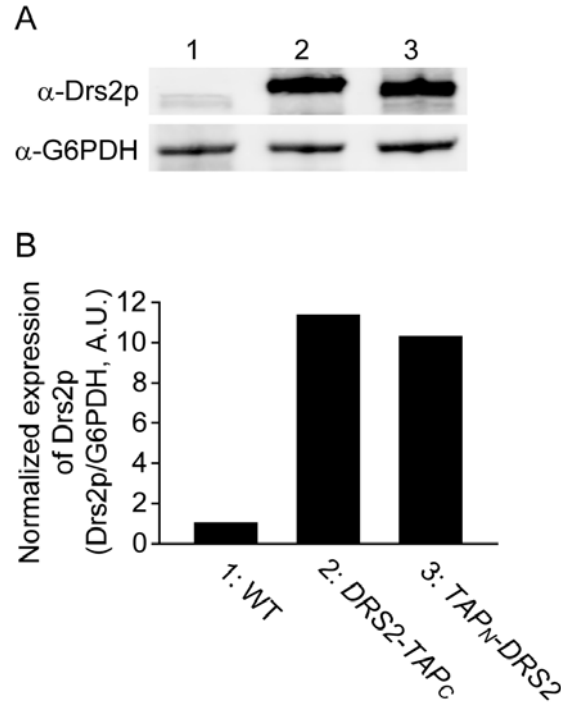


Figure 2-3. Overexpression of *DRS2-TAP_C* and *TAP_N-DRS2* in yeast. (A) Yeast BY4742 (WT, lane 1), XZY38b (*DRS2-TAP_C*, lane 2) and XZY60m (*TAP_N-DRS2*, lane 3) were grown in rich medium and harvested in mid-log phase (0.4-0.6 OD₆₀₀/mL). The cell lysates were subjected to SDS-PAGE and western blotting. Primary antibodies were used at 1:2000 (anti-Drs2p) and 1:10000 (anti-G6PDH). Blotting for G6PDH served as a loading control. (B) Quantification of Drs2p overexpression in (A). Drs2p values were corrected for the loading control and defined as (Drs2p signal) / (G6PDH signal). The WT sample was defined as 1 unit (Arbitrary Unit, A.U.).

Table 2-1. Proteins identified in purified Drs2p-TAP_C by MALDI-TOF mass spectrometry. Drs2p-TAP_C was purified from strain XZY10b (*ATP2*).

Protein name	Peptides recovered
Drs2p	177
Cdc50p	17
Vtc4p	16
Ssa1p	11
Atp1p ¹	10
Atp2p ²	7
Pma1p	7
Vtc3p	6
Rpl4ap*	5
Rtn1p	4
Tdh3p	4
Vtc2p	4
Dnf1p	3
Por1p	3
Sac1p	3
Cdc19p	2
Eno1p	2
Hsp26p	2
Kar2p	2
Rcy1p	2
Ssa2p	2
Tdh1p	2
Tub2	2
Tef1p	1

¹ α subunit of F1-ATPase; ² β subunit of F1-ATPase.

*Several additional ribosomal proteins detected by mass spectrometry are not listed.

identified by mass spectrometry (**Table 2-1**). Typically, 5% of Drs2p-TAP_C in the cell lysate was recovered in the first affinity purification step (IgG column) and 1% was recovered in the second affinity step (calmodulin column), yielding 10 µg of Drs2p per liter of culture (~10¹¹ cells).

Robust ATPase activity was detected in the purified Drs2p-TAP_C sample. However, this ATPase activity was insensitive to orthovanadate, a commonly used P-type ATPase inhibitor (Ding et al., 2000; Paterson et al., 2006), and was completely inhibited by 1 mM azide (**Figure 2-1D**). This result suggested that the ATPase activity was primarily catalyzed by contaminating mitochondrial F1-ATPase. Indeed, the α and β subunits of the F1-ATPase were detected by western blotting (**Figure 2-4**) and mass spectrometry (**Table 2-1**) as trace contaminants, but the specific activity of F1-ATPase is very high (150 µmol ATP hydrolyzed/min/mg) (Gause et al., 1981). To test if the activity was catalyzed by the F1-ATPase, the *ATP2* gene encoding the catalytic β subunit of the F1-ATPase was disrupted in the strain used for Drs2p-TAP_C purification (**Figure 2-4**). No ATPase activity could be detected in Drs2p-TAP_C preparations from the *atp2Δ* strain (**Figure 2-1D**), even though Drs2p-TAP_C was recovered with a yield and purity comparable to that shown in **Figure 2-1C**. Other ATPases were also detected at trace levels (**Table 2-1**), but their activities were below the limit of detection in these preparations. Therefore, it appeared that purified Drs2p-TAP_C was catalytically inactive *in vitro*. A variety of purification and assay conditions were tested for Drs2p-TAP_C, including the addition of potential substrate lipids such as PS, but none of the conditions used yielded an active enzyme. However, moving the affinity tag from the C-terminus to the N-terminus of Drs2p (TAP_N-Drs2p, **Figure 2-5A and B**), and modifying the TAP tag to contain a decahistidine as the second affinity module instead of the calmodulin binding peptide (**Figure 2-5B**), allowed purification of enzymatically active Drs2p.

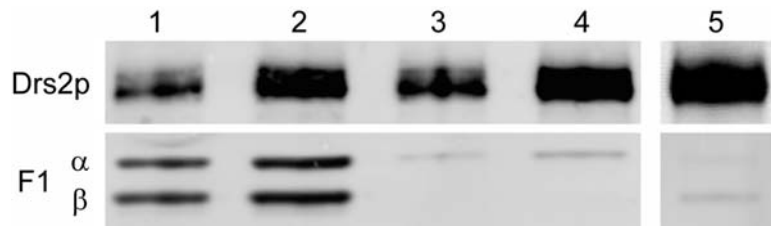


Figure 2-4. Detection and disruption of mitochondrial F1-ATPase. Cell lysates from strain XZY10b (*ATP2*) (lane 1-2, 10^5 and 2×10^5 cells), XZY38b (*atp2\Delta*) (lane3-4, 10^5 and 2×10^5 cells), and a purified Drs2p-TAP_C sample (lane 5) (10^9 cells) were subjected to SDS-PAGE and western blotting. Primary antibodies were used at 1:2000 (anti-Drs2p and anti-F1-ATPase). The antibody against the yeast F1-ATPase recognizes both α and β subunits (Puri et al., 2005), and was kindly provided by Dr. David Mueller (Rosalind Franklin University). Note that disruption of *ATP2* gene (encoding the β subunit) also reduced expression of the α subunit.

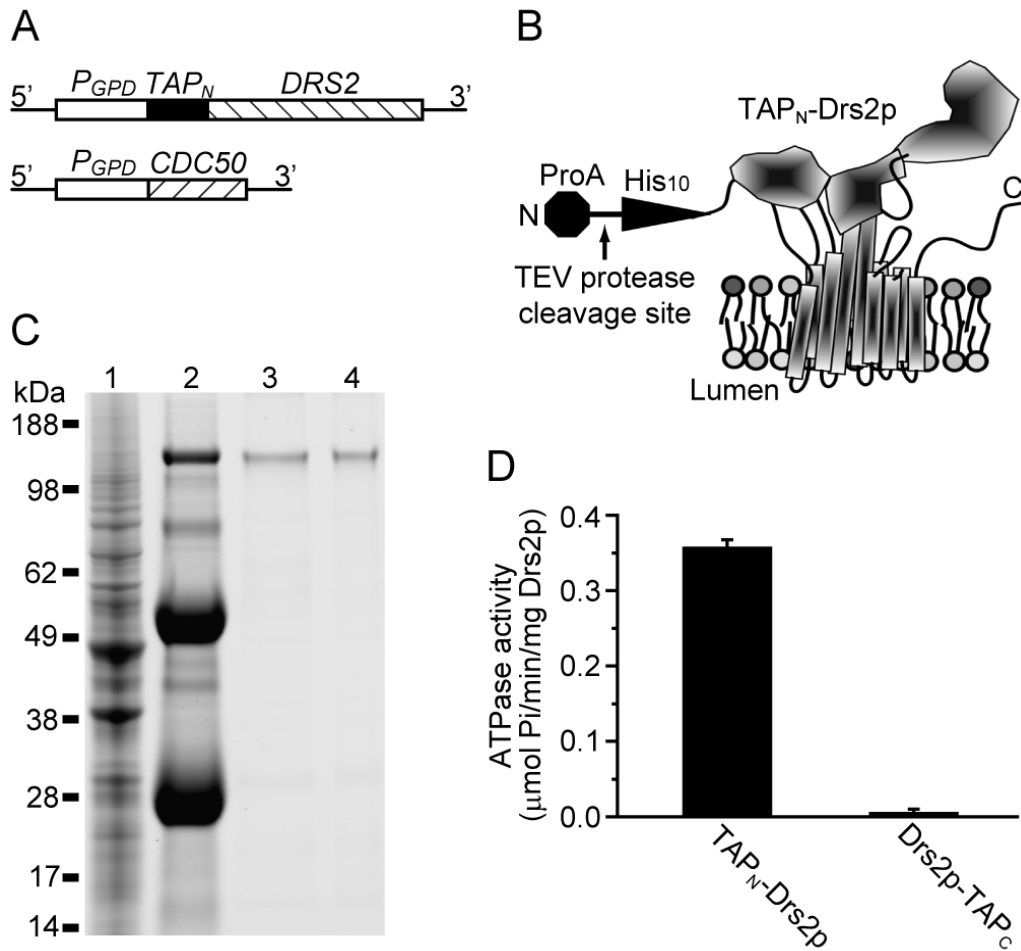


Figure 2-5. Expression and purification of TAP_N-Drs2p. (A) Chromosomal organization of TAP_N-DRS2 and CDC50. (B) Schematic of TAP_N-Drs2p. ProA, protein A moiety; His₁₀, decahistidine moiety; TEV, tobacco etch virus. (C) Aliquots from a TAP_N-Drs2p purification from strain XZY60m (*atp2Δ*) were subject to SDS-PAGE and the gel was stained with SimplyBlue. Lane 1, cell lysate; lane 2, proteins bound to the IgG beads; lane 3, proteins bound to the Ni-NTA beads; lane 4, final eluate. (D) Comparison of TAP_N-Drs2p and Drs2p-TAP_C ATPase activity purified from strain XZY60m (*atp2Δ*) and XZY38b (*atp2Δ*), respectively.

TAP_N-Drs2p was also purified from a strain that was deficient for the F1-ATPase and a comparable yield and purity was obtained (compare **Figure 2-5C** to **Figure 2-1C**). The TAP_N-Drs2p preparation now displayed robust ATPase activity relative to Drs2p-TAP_C (**Figure 2-5D**). The only significant difference between the two Drs2p preparations was the position of the tag (N-terminal versus C-terminal), indicating that the ATPase activity detected in the TAP_N-Drs2p sample was catalyzed by Drs2p and not minor contaminants in the sample. Consistent with other P-type ATPases, the ATPase activity of TAP_N-Drs2p was sensitive to orthovanadate with an IC₅₀ of 5 μM and was resistant to azide (**Figure 2-6A and B**). TAP_N-Drs2p showed an optimal pH of 7.5 (**Figure 2-6C**), a K_m of 1.5 ± 0.3 mM for ATP (**Figure 2-6D**), and a V_{max} of 0.45 ± 0.03 μmol Pi released/min/mg Drs2p (~70 ± 5 ATPs hydrolyzed/min/Drs2p, **Figure 2-6D**) under these assay conditions. The ATPase activity of TAP_N-Drs2p was also Mg²⁺-dependent (**Figure 2-6B**), as reported for purified mammalian Atp8a1 (Ding et al., 2000; Paterson et al., 2006).

To assess the oligomeric state of purified Drs2p, TAP_N-Drs2p and Drs2p-TAP_C were subjected to size exclusion chromatography. The majority of both Drs2 proteins eluted as a single peak at nearly the same volume (**Figure 2-7A**). Relative to protein standards (**Figure 2-7B**), the mass of TAP_N-Drs2p was estimated to be 181 kDa and Drs2p-TAP_C 184 kDa, very close to their predicted monomer masses of 156 kDa and 160 kDa. To probe the molecular basis of Drs2p-TAP_C inactivity, TAP_N-Drs2p and Drs2p-TAP_C were analyzed by circular dichroism (**Figure 2-8**). The spectra of the two proteins were strikingly different, suggesting possibly a difference between their tertiary structures. Importantly, the inactive Drs2p-TAP_C did not seem to be more unstructured than the active TAP_N-Drs2p, although with the caveat that the prediction for TAP_N-Drs2p may not be accurate (**Table 2-2**). Although the molecular basis for its inactivity is not fully understood, Drs2p-TAP_C served as an enzymatically-dead negative control in this study.

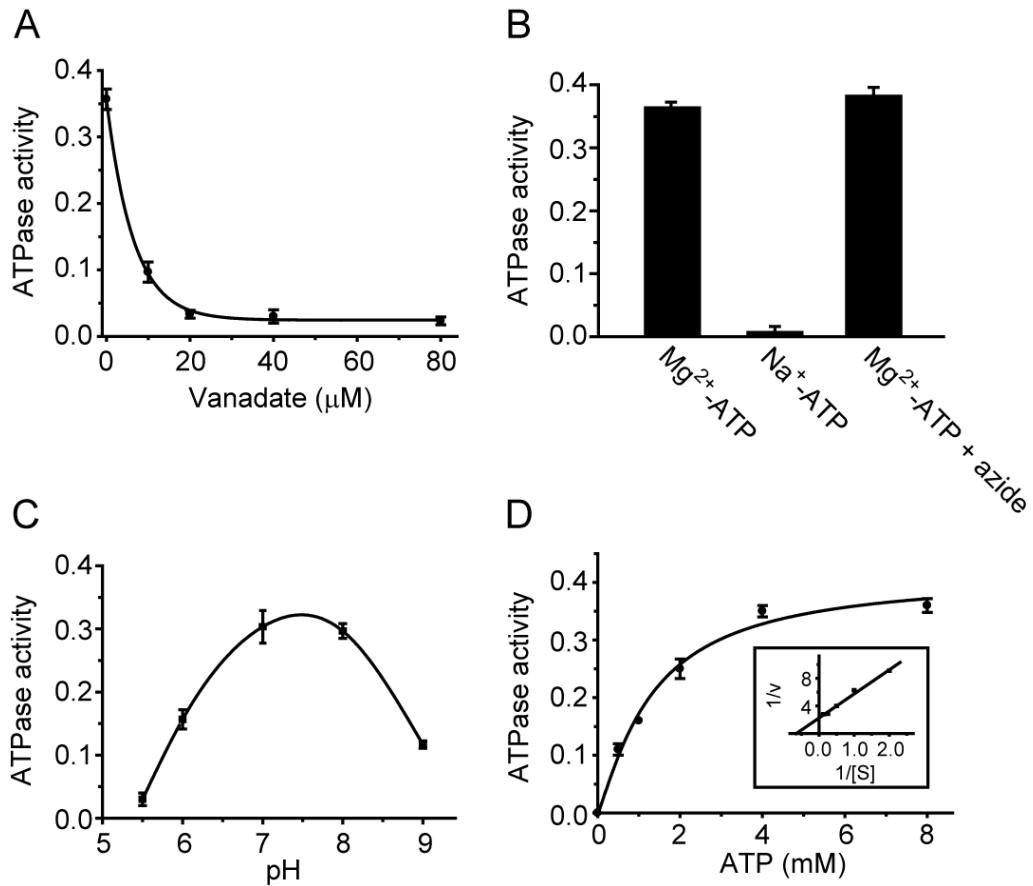


Figure 2-6. Characterization of purified Drs2p in 0.1% C_{12}E_9 . (A) Sensitivity of TAP_N -Drs2p ATPase activity to orthovanadate (VO_4^{3-}). (B) Mg^{2+} dependence of TAP_N -Drs2p ATPase activity and its resistance to azide (1 mM). (C) pH profile of TAP_N -Drs2p ATPase activity assayed as described in Materials and Methods but with varying buffers. pH 5.5 and 6, 50 mM MES; pH 7, 8 and 9, 50 mM Tris-HCl. (D) Determination of the K_m for ATP and V_{max} of ATP hydrolysis for TAP_N -Drs2p. Inset, double-reciprocal plot. Y-axis units of (A)-(D) = $\mu\text{mol Pi released}/\text{min}/\text{mg Drs2p}$.

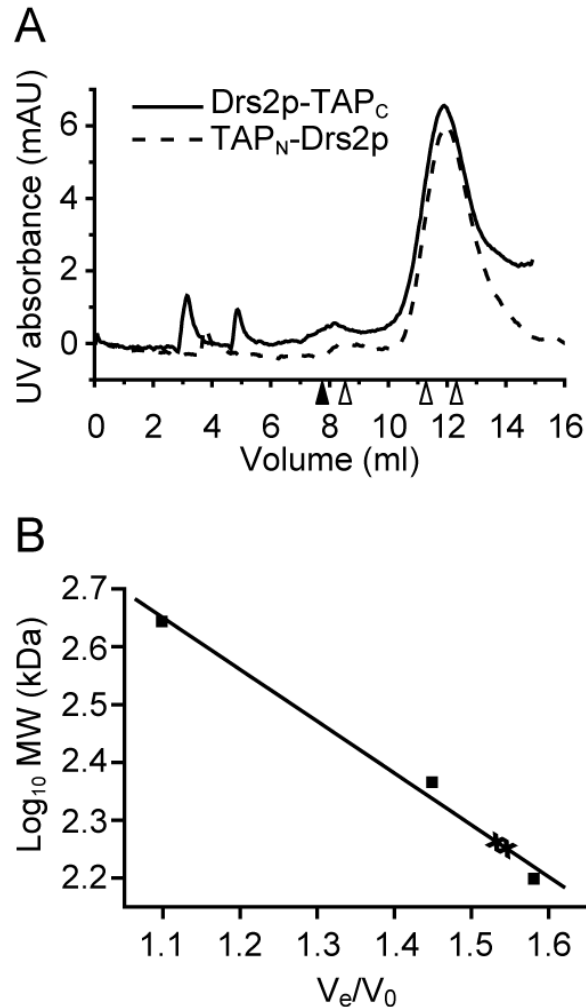


Figure 2-7. Size exclusion chromatography of purified Drs2p. (A) TAP_N-Drs2p and Drs2p-TAP_C were solubilized in 20 mM Tris-HCl (pH 7.5), 100 mM NaCl and 0.1% C₁₂E₉, and were analyzed by an ÄKTA FPLC system using a Superose 12 column from GE Healthcare. The column was pre-equilibrated with the same Drs2p buffer and samples were injected at 0 ml. The closed arrow head indicates the void volume (V₀, 7.77 ml), and the three open arrow heads (from left to right) indicate the peaks of ferritin (440 kDa), catalase (232 kDa) and aldolase (158 kDa) standards, which were dissolved in the same Drs2p buffer and analyzed individually. (B) A molecular weight (MW) standard curve was constructed using protein standards (squares) from (A). The logarithm of the hydrodynamic radius of a protein is inversely linear to the partition coefficient of the protein, which is linear to its elution volume (V_e) in a given column (Davison, 1968; Irvine, 1994; Tanford et al., 1974). Note that the logarithm of the molecular weight of proteins was approximately assumed to be linear to that of their hydrodynamic radii in this plot. The two crosses indicate the V_e/V₀ values for Drs2p-TAP_C and TAP_N-Drs2p, respectively (from left to right), and were calculated to estimate their molecular weights in the purified samples.

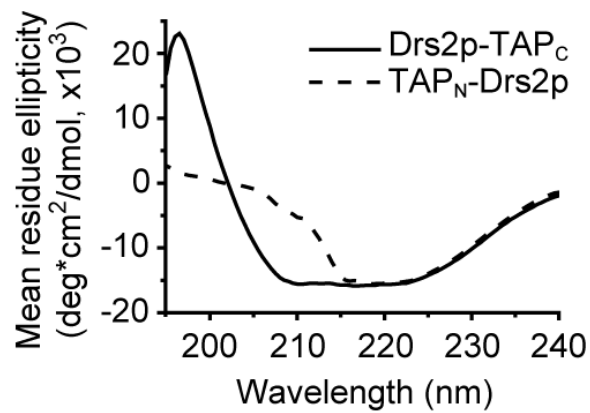


Figure 2-8. Circular dichroism spectra of purified Drs2p. TAP_N-Drs2p (40 µg/mL) and Drs2p-TAP_C (38 µg/mL) were solubilized in 20 mM Tris-HCl (pH 7.5), 100 mM NaCl and 0.1% C₁₂E₉ in a 1 mm cell, and were scanned for absorbance using a Jasco J-810 spectrometer.

Table 2-2. Secondary structure prediction from circular dichroism spectra (200-240 nm) of Drs2p by the K2D (Andrade et al., 1993) and K2D2 (Perez-Iratxeta and Andrade-Navarro, 2008) web servers.

Structure (%)	K2D Prediction		K2D2 Prediction	
	TAP _N -Drs2p	Drs2p-TAP _C	TAP _N -Drs2p	Drs2p-TAP _C
α helix	40	60	31.63	47.81
β sheet	2	6	13.51	10.21
β turn + unordered	58	34	54.86	41.98
Estimated maximum error	>0.227*	0.122	0.4	0.4

*The distance between the query and the predicted spectrum is too large. The prediction is not very reliable.

Purified TAP_N-Drs2p was incorporated into PC liposomes via detergent-mediated reconstitution (see Materials and Methods). To improve reconstitution efficiency by increasing protein to lipid ratio, single-step affinity purified TAP_N-Drs2p was used directly for reconstitution, because single-step affinity purification provided more Drs2p than the two-step purification, although with lower purity (**Figure 2-9A**, lane 0). After flotation of reconstituted samples in a glycerol step gradient, most TAP_N-Drs2p was found in the top fractions and co-fractionated with phospholipids (**Figure 2-9A**, lane 5 and 6, and **Figure 2-9B**). Importantly, most contaminating proteins from the single-step affinity purification remained at the bottom of the gradient and were well separated from the proteoliposome fractions (**Figure 2-9A**, lane 1 and 2). As determined by mass spectrometry, the proteoliposome fractions contained relatively pure TAP_N-Drs2p, comparable to that obtained from the two-step TAP procedure (**Table 2-3 and Table 2-1**). Based on negative staining and visualization by electron microscopy, the size of proteoliposomes ranged from 25 to 75 nm in diameter, with a mean diameter of 40 nm (**Figure 2-9C**). A similar result was obtained when the proteoliposomes were visualized by cryo-electron microscopy (**Figure 2-9D**). The protein to lipid ratio was 1:200 (wt/wt) in the proteoliposome samples, and we estimated that there was one Drs2p molecule per 2-3 liposomes. In our reconstituted samples, Drs2p was preferentially inserted into proteoliposomes with the ATPase domain facing outward as revealed by a protease protection assay (**Figure 2-10**). Any Drs2p reconstituted in the opposite orientation would not be stimulated by Mg²⁺-ATP present outside the proteoliposome.

To assay for flippase activity, PS (potential substrate), PC or SM (control) analogues bearing a fluorescent NBD group on a short *sn*2 acyl chain (C6) was incorporated into PC proteoliposomes during reconstitution. The TAP_N-Drs2p proteoliposomes were then assayed for flippase activity using dithionite, a membrane-impermeable quenching agent, to monitor the interleaflet distribution of NBD-phospholipid (see Materials and Methods).

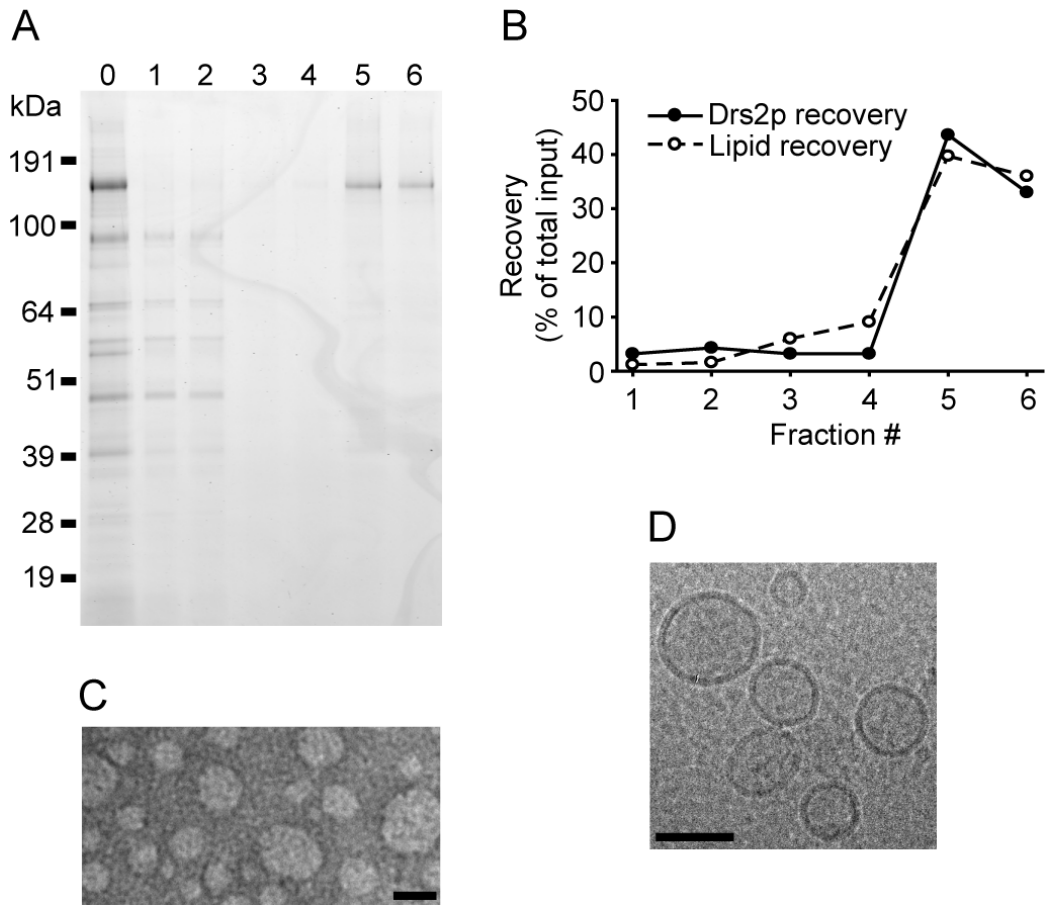


Figure 2-9. Flotation of TAP_N-Drs2p proteoliposomes in a glycerol gradient. (A) Fractions collected from the glycerol gradient were subject to SDS-PAGE and the gel was stained with SimplyBlue. Lane 0, the protein sample before reconstitution; lane 1-6, fractions (#1-6) collected from the bottom to the top of the gradient. (B) Recovery of Drs2p and phospholipid in each fraction relative to the starting material. (C) Electron micrograph of negative-stained proteoliposome sample from fraction #5. Scale bar, 50 nm. (D) Cryo-electron micrograph of proteoliposome sample from fraction #5. Scale bar, 50 nm.

Table 2-3. Proteins identified in Drs2p proteoliposomes by MALDI-TOF mass spectrometry.

Protein name	Peptides recovered	
	TAP _N -Drs2p	Drs2p-TAP _C
Drs2p	275	313
Cdc50p	20	16
Ssa1p	11	8
Ssa2p	8	6
Pma1p	7	3
Tdh3p	6	9
Psa1p	5	1
Hsp82p	4	8
Hsp26p	3	2
Por1p	3	2
Tdh2p	3	5
Rpl4ap	3	1
Rpl4bp	3	0
Eno1p	3	0
Rpl5p	2	0
Tub2p	2	0
Cdc19p	2	1
Rpp0p	1	2
Tdh1p	1	1
Sam1p	1	3
Kar2p	1	1
Yef3p	1	2
Fas1p	1	2

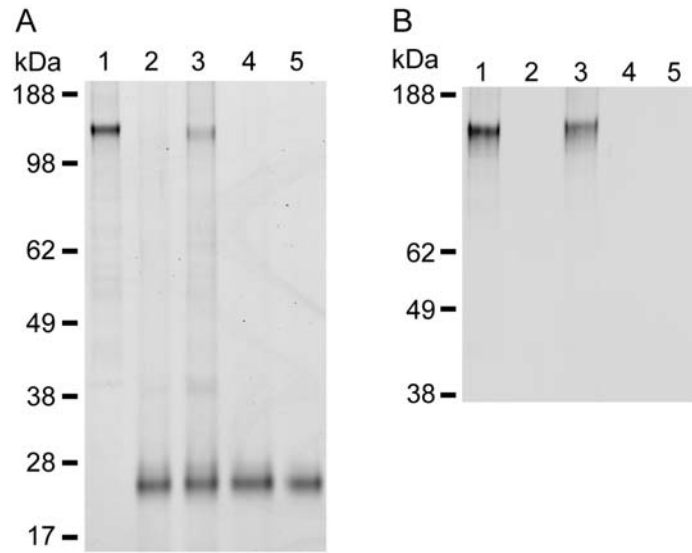


Figure 2-10. Protease protection assay of TAP_N-Drs2p proteoliposomes using trypsin. Proteoliposomes were incubated with 0.001% (wt/vol) trypsin at 37 C for 5 min, and trypsin digestion was stopped by addition of trypsin inhibitors (5 mM benzamidine hydrochloride, 2.5 μM aprotinin, 40 μM leupeptin, 10 mM PMSF) before mixing with SDS-PAGE sample buffer. (A) After SDS-PAGE, a gel was stained with SimplyBlue. Lane 1, proteoliposomes alone; lane 2, proteoliposomes incubated with trypsin before addition of trypsin inhibitors; lane 3, proteoliposomes incubated with trypsin in the presence of trypsin inhibitors; lane 4, proteoliposomes incubated with trypsin in the presence of 0.1% Triton X-100; lane 5, trypsin only. (B) After SDS-PAGE, proteins in a gel from (A) were electrotransferred onto polyvinylidene difluoride (PVDF) membrane and Drs2p was detected by western blotting using a primary antibody (1:2000) that recognizes the ATPase domain of Drs2p.

To improve the sensitivity for detecting trans-bilayer flip, the NBD-phospholipid in the outer leaflet was pre-quenched with dithionite and the proteoliposomes were re-floated in a glycerol gradient to remove the dithionite. This treatment resulted in liposomes with most fluorescent NBD-phospholipid in the inner leaflet and increased the sensitivity for detecting flip of NBD-phospholipid to the outer leaflet.

From preliminary experiments, we noticed that incubation of liposomes with ATP (Na^+ -ATP) alone caused a small non-specific increase in accessibility of NBD-phospholipid to dithionite (**Figure 2-11**). To take this effect into account, we incubated the proteoliposomes with Na^+ -ATP, which is not hydrolyzed by TAP_N -Drs2p (**Figure 2-6B**), as a background control in the flippase assay. As seen in **Figure 2-12A**, after a 30-min incubation, Na^+ -ATP caused a net ~3% increase in NBD-PS accessibility to dithionite (green trace versus black trace). While in the presence of Mg^{2+} -ATP, significantly more NBD-PS (~7%) was accessible to dithionite (blue trace versus red trace). The increased quenching of NBD-PS was not caused by Mg^{2+} alone or contaminating Ca^{2+} (**Figure 2-11**). NBD-PS was flipped across the liposome bilayer with a half-time of ~4 min (**Figure 2-12B**), and the initial velocity was about 0.02 μmol NBD-PS flipped/min/mg Drs2p (~3 NBD-PS flipped/min/Drs2p). As controls, no difference between the Mg^{2+} -ATP and Na^+ -ATP incubations was observed with TAP_N -Drs2p proteoliposomes containing NBD-PC or NBD-SM instead of NBD-PS (**Figure 2-12A and C**), indicating that PS is the moiety that was recognized and translocated. Moreover, if Drs2p activity simply caused increased leakiness of the proteoliposome to dithionite, we would have observed enhanced quenching of the NBD-PC or NBD-SM probes. In other control experiments, no increased quenching was observed with protein-free liposomes (No Drs2p) containing NBD-PS (**Figure 2-12C**), or with proteoliposomes reconstituted with the enzymatically-dead Drs2p- TAP_C and NBD-PS (**Figure 2-12C**). These data demonstrated that the increased quenching (~4%) of NBD-PS in TAP_N -Drs2p proteoliposome was mediated by

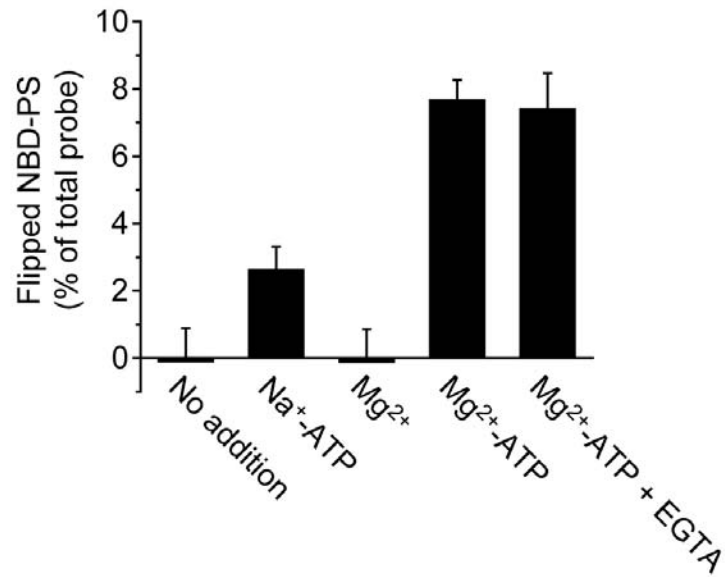


Figure 2-11. Flippase assay with TAP_N-Drs2p proteoliposomes containing NBD-PS. Proteoliposomes were incubated with no addition (proteoliposomes alone), Na⁺-ATP (5 mM), Mg²⁺ (5 mM), Mg²⁺-ATP (5 mM), or Mg²⁺-ATP (5 mM) plus EGTA (1 mM) at 37 C for 30 min, and NBD-PS flipping was measured as described in Materials and Methods. Results were averaged from 4-6 independent experiments.

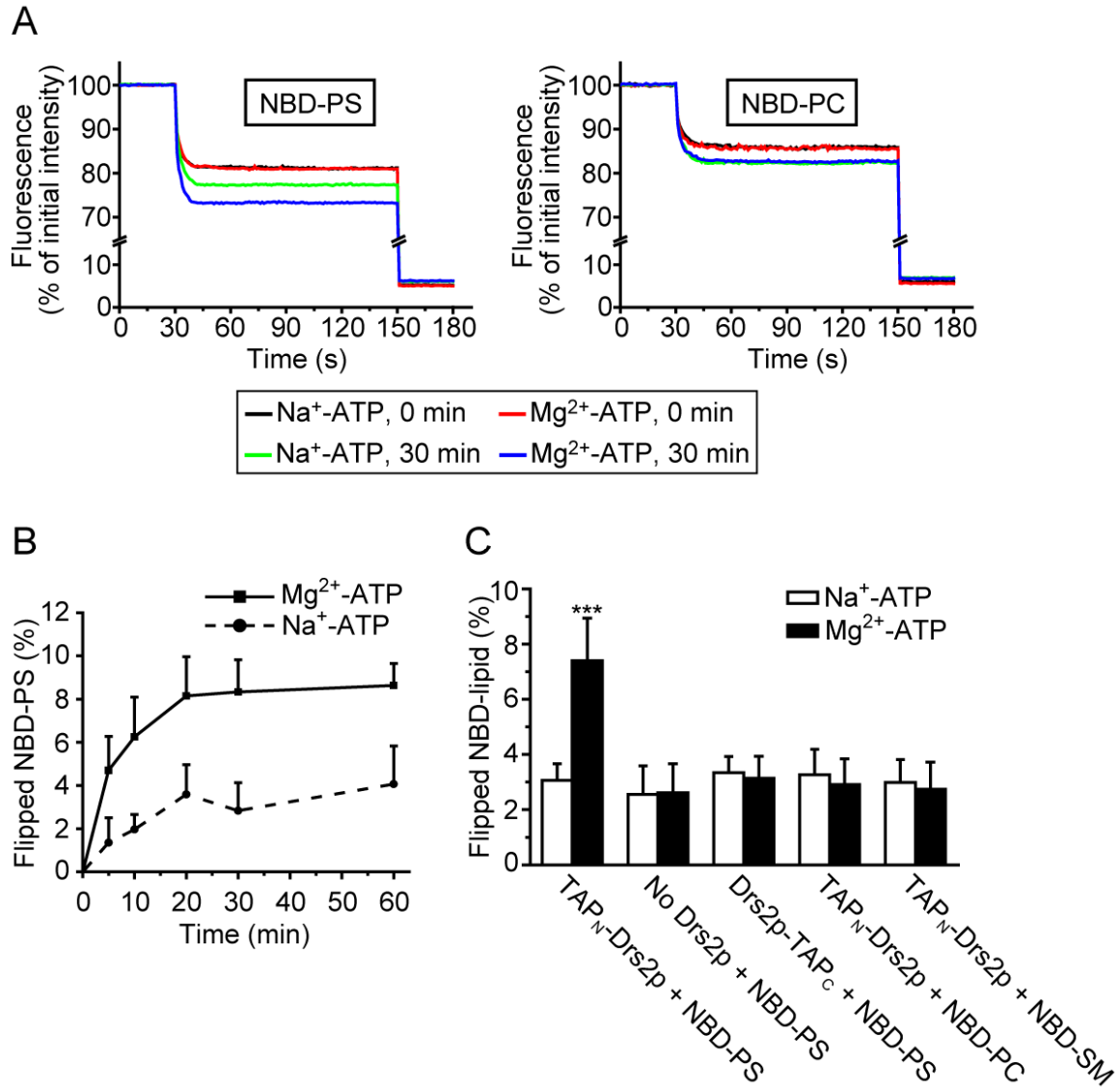


Figure 2-12. Reconstitution of NBD-PS flippase activity with TAP_N-Drs2p proteoliposomes. (A) Dithionite quenching of NBD-PS (left panel) or NBD-PC (right panel) fluorescence in TAP_N-Drs2p proteoliposomes before and after 30 min of incubation with Mg²⁺-ATP or Na⁺-ATP. Dithionite was added at 30 s to quench outer leaflet NBD-phospholipid and Triton X-100 was added at 150 s to quench remaining inner leaflet NBD-phospholipid. (B) Time course of NBD-PS translocation. Flippase assay was conducted as described in Materials and Methods, except that the incubation time varied from 0 to 60 min as indicated. Results were averaged from 4-6 independent experiments. (C) Flippase assay with liposomes containing TAP_N-Drs2p, Drs2p-TAP_C or no Drs2p and the indicated NBD-phospholipid was performed as described in Materials and Methods. The increase in outer leaflet NBD-phospholipid after a 30-min incubation with Mg²⁺-ATP or Na⁺-ATP was plotted. Results were averaged from 6-9 independent experiments. ***, *P* < 0.001.

a Mg^{2+} -, ATP- and Drs2p-dependent flippase activity specific for the PS analogue.

Furthermore, mass spectrometric studies revealed that the TAP_N-Drs2p and the Drs2p-TAP_C proteoliposomes contained a nearly identical protein composition (**Table 2-3**). In both samples, Cdc50p was recovered as the second most abundant protein based on the number of peptides recovered. However, a relatively small number of Cdc50p peptides were recovered and Cdc50p was not apparent in the gels stained by SimplyBlue (**Figure 2-1C** and **Figure 2-5C**). Thus, it appears that the majority of Drs2p was not complexed with Cdc50p in the reconstituted samples. Other proteins recovered in low quantities, such as heat shock proteins and proteins involved in metabolism and protein synthesis, are very abundant proteins in yeast and are common contaminants of affinity purifications (Gould et al., 2004). Most importantly, the two proteoliposome samples were comparable in protein composition with the major difference being the placement of the TAP tag on Drs2p, indicating that Drs2p activity is responsible for the difference in the flippase activity between the two samples.

Section 2.5: Discussion

For more than a decade it has been proposed that Drs2p and the P4-ATPase family are phospholipid translocases or flippases, and several lines of evidence indicate that Drs2p is necessary for flipping NBD-labeled PS or PE analogues in isolated Golgi membranes and post-Golgi secretory vesicles (Alder-Baerens et al., 2006; Daleke, 2003; Graham, 2004; Natarajan et al., 2004; Pomorski et al., 2004; Tang et al., 1996). However, no in vitro reconstitution of flippase activity had been achieved with a purified P4-ATPase to test whether these pumps are sufficient to directly catalyze flippase activity. Towards this goal, we purified Drs2p from yeast, reconstituted it into proteoliposomes, and demonstrated an NBD-PS flippase activity with the purified and reconstituted enzyme.

In this study, Drs2p with affinity tags at either end (TAP_N-Drs2p and Drs2p-TAP_C) was purified. Surprisingly, although the two protein preparations were very comparable in yield and purity (**Figure 2-1C** and **Figure 2-5C**; **Table 2-1** and **Table 2-3**), only TAP_N-Drs2p was catalytically active in vitro, whereas Drs2p-TAP_C was enzymatically dead (**Figure 2-5D** and **Figure 2-12C**). However, both Drs2 proteins are functional in vivo, since they supported yeast growth at low temperatures (**Figure 2-2**). By contrast, Drs2p-deficient cells exhibit a cold-sensitive growth defect (Chen et al., 1999; Hua et al., 2002; Ripmaster et al., 1993). Drs2p-TAP_C appears to be folded well enough to have exited the ER, as our purification method should remove most of the ER-localized Drs2p. Based on size exclusion chromatography, both Drs2 proteins appear to be primarily monomeric in detergent solutions and do not differ significantly from each other in oligomeric states (**Figure 2-7**). Therefore, Drs2p-TAP_C inactivity was not caused by aggregation of this protein. Moreover, no significant difference in stability and solubility was observed between TAP_N-Drs2p and Drs2p-TAP_C (**Figure 2-5C** and **Figure 2-1C**). However, the tertiary structure of TAP_N-Drs2p seems to differ from that of Drs2p-TAP_C as revealed by circular dichroism (**Figure 2-8**). Interestingly, the inactive Drs2p-TAP_C was predicted to contain more ordered structural elements than TAP_N-Drs2p (**Table 2-2**). Although the prediction for TAP_N-Drs2p may not be accurate (**Table 2-2**), which may be caused by interference from residual imidazole, these data indicate that Drs2p-TAP_C inactivity was probably not caused by denaturation of this protein. P-type ATPases undergo dramatic conformational changes during the catalytic cycle, and it is possible that Drs2p-TAP_C is inactive because it is trapped in a single conformational state. Further work will be required to determine whether the loss of Drs2p-TAP_C activity in vitro resulted from the position of the C-terminal TAP tag or from the calmodulin binding peptide versus the decahistidine module.

The ATPase activity of purified TAP_N-Drs2p was Mg²⁺-ATP-dependent and orthovanadate-sensitive (**Figure 2-6B and A**), which are consistent with the properties of purified mammalian Atp8a1 (Ding et al., 2000; Paterson et al., 2006). The specific activity of TAP_N-Drs2p was 0.45 ± 0.03 μmol Pi released/min/mg Drs2p (V_{max} , **Figure 2-6D**), and this activity is within the range of values reported for purified Atp8a1 (Ding et al., 2000; Paterson et al., 2006). However, we observed only a mild increase of ~40% in ATPase activity of the purified TAP_N-Drs2p in detergent solutions when incubated with PS, a potential phospholipid substrate for Drs2p, whereas no stimulation was observed for PC (**Figure 2-13A**). This stimulation level by PS is marginal compared to steep increases (greater than 10-fold) observed for purified mammalian Atp8a1 (Ding et al., 2000; Paterson et al., 2006). Activation of Atp8a1 ATPase activity by PS suggests that PS is a native substrate for Atp8a1. The modest PS stimulation of TAP_N-Drs2p sample may be due to co-purification of substrate phospholipid with Drs2p, such that the preparation is at near maximum activation. Another possibility is that the accessibility of the PS binding site of Drs2p to the externally added PS was poor in detergent solutions. Consistently, when purified TAP_N-Drs2p was reconstituted into proteoliposomes containing varying amounts of PS (up to 20%), the ATPase activity of TAP_N-Drs2p was stimulated up to ~400% (from 0.36 ± 0.04 to 1.28 ± 0.03 μmol Pi released/min/mg Drs2p, **Figure 2-13B**) with a K_m for PS estimated to be 5.7 mol% by fitting the data to a hyperbolic Michaelis-Menten function. However, the specific activity of TAP_N-Drs2p was relatively low compared to PS-activated bovine Atp8a1 (3-42 μmol Pi released/min/mg) (Ding et al., 2000; Moriyama and Nelson, 1988; Xie et al., 1989). Whether this difference reflects a species difference or whether only a portion of Drs2p molecules retained activity after purification remains to be determined.

Upon reconstitution, the TAP_N-Drs2p proteoliposome exhibited flippase activity that was specific for NBD-PS (**Figure 2-12**), because no activity was observed with the PC

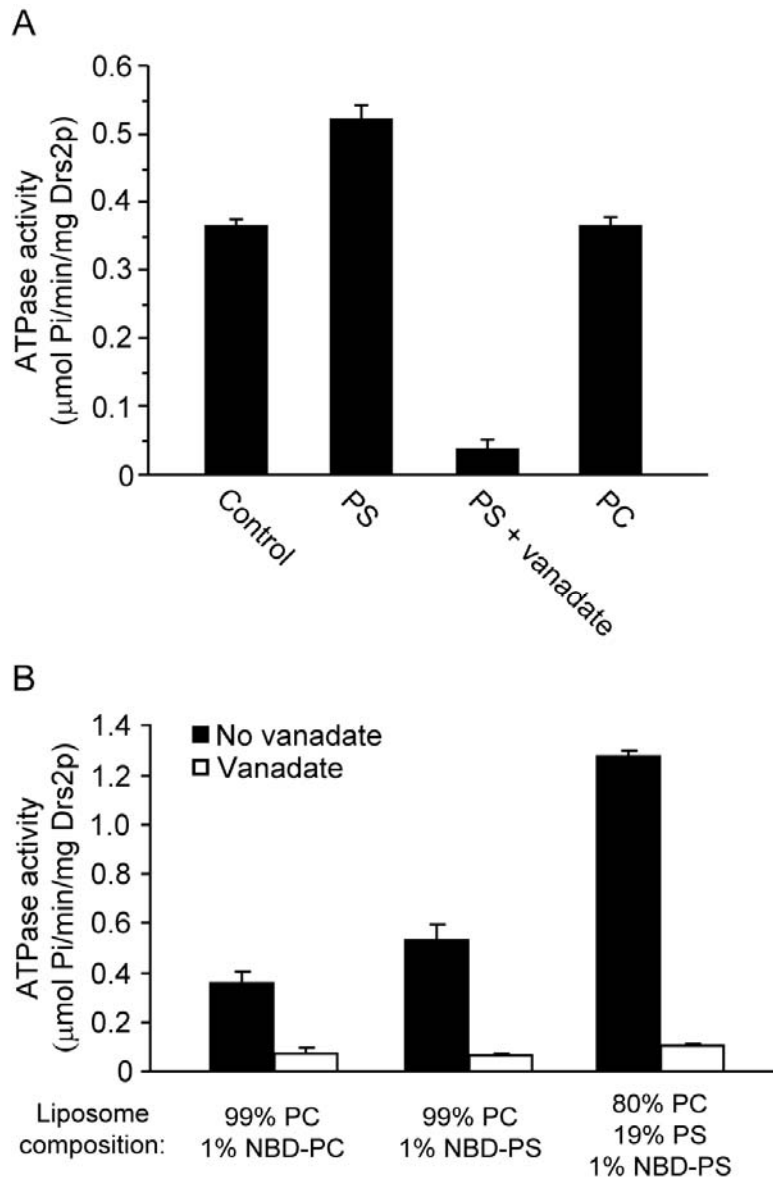


Figure 2-13. Phospholipid stimulation of TAP_N-Drs2p ATPase activity. (A) ATP activity of purified TAP_N-Drs2p in 0.1% C₁₂E₉ was assayed in the presence of PS (POPS, 400 μM), PS (POPS, 400 μM) plus orthovanadate (80 μM), or PC (POPC, 400 μM). The stock solution for each phospholipid was prepared at 4 mM by complete solubilization of dried lipids in 2% C₁₂E₉. Phospholipids were incubated with TAP_N-Drs2p for 10 min at room temperature before addition of ATP. (B) TAP_N-Drs2p was reconstituted with indicated lipids as described in Materials and Methods except that the Bio-Beads SM-2 incubation time was reduced by 50% for incomplete removal of C₁₂E₉. Reconstituted samples were floated on a glycerol gradient and proteoliposomes were recovered as described in Materials and Methods. These proteoliposomes were leaky because dithionite quenched >95% of NBD fluorescence. ATPase activity of these TAP_N-Drs2p proteoliposomes was assayed in the presence or absence of orthovanadate (80 μM).

and SM analogues (**Figure 2-12A and C**). TAP_N-Drs2p was not the only protein present in the proteoliposome, although it was the major one (**Figure 2-9A and Table 2-3**). Mass spectrometry also identified several other proteins in low abundance, including Cdc50p (**Table 2-3**). Any of these proteins could potentially be responsible for the flippase activity independently or dependently of TAP_N-Drs2p. However, the former possibility was ruled out because a control proteoliposome sample reconstituted with the enzymatically-dead Drs2p-TAP_C showed no NBD-PS flippase activity (**Figure 2-12C**) and contained a protein composition almost identical to that of the TAP_N-Drs2p proteoliposome (**Table 2-3**). These data argue strongly that Cdc50p and minor contaminants were incapable of catalyzing flippase activity without active Drs2p.

However, our data are consistent with the possibility that Cdc50p may also be required for the flippase activity of Drs2p, because Cdc50p was present in the TAP_N-Drs2p proteoliposomes (**Table 2-3**). Moreover, recent work suggests that Cdc50p facilitates the catalytic cycle of Drs2p (Lenoir et al., 2009). In the current study, we estimated that around 40% of the liposomes would contain one Drs2p molecule if an equal distribution of Drs2p in liposomes is assumed. Drs2p seemed to be inserted preferentially into the proteoliposomes with its ATPase domain facing outward (**Figure 2-10**). Therefore, at most, 40% of the liposomes would contain a Drs2p molecule that has access to externally applied Mg²⁺-ATP, and 40% would be the upper limit of NBD-PS translocation we could achieve under these conditions. We have observed a nearly saturated Mg²⁺-ATP-dependent flip of 4% NBD-PS (**Figure 2-12**), perhaps indicating that only 4% of the liposomes contain an active flippase. If the Drs2p-Cdc50p complex is essential for flippase activity, the molar concentration of Cdc50p would need to be at least 1/10 that of Drs2p to explain why we observed 1/10 the maximum expected activity. Based on mass spectrometric results, the number of Cdc50p peptides recovered in the TAP_N-Drs2p proteoliposome was about 1/10 that of Drs2p (**Table 2-3**). Thus, it is

possible that the flippase activity reported here was catalyzed by Drs2p-Cdc50p complexes and that Drs2p alone is insufficient to drive flippase activity. Alternatively, it is possible that Cdc50p is not required and the suboptimal flippase activity in the proteoliposomes resulted from the physical restraint of small liposome size (40 nm in mean diameter, **Figure 2-9C and D**), an unequal distribution of Drs2p in proteoliposomes, a high percentage of inactive Drs2p molecules in the TAP_N-Drs2p preparation, and/or the absence of other potential regulators of Drs2p activity. Further work will be required to determine the extent of Cdc50p contribution to flippase activity. Nonetheless, the studies reported here provide a critical step forward in the biochemical characterization of a phospholipid flippase and define the minimal flippase unit as a P4-ATPase, perhaps in association with its noncatalytic subunit.

Section 2.6: Chapter Acknowledgements

We thank Amy-Joan L. Ham and W. Hayes McDonald from the Mass Spectrometry Research Center at Vanderbilt University for their assistance, and Melanie D. Ohi and Melissa Chambers (Vanderbilt University) for their help with negative staining and electron microscopy. We are also grateful to Andrzej M. Krezel (Vanderbilt University) for his help with size exclusion chromatography, and Paramasivam Natarajan (Vanderbilt University) for his help with circular dichroism. The antibody against yeast mitochondrial F1-ATPase was kindly provided by David Mueller from Rosalind Franklin University. This project is supported by NIH Grant R01GM062367 to T.R.G..

CHAPTER III

EXPLORING THE BASIS OF DRS2-TAP_C PROTEIN INACTIVITY: POTENTIAL AUTO-INHIBITION BY THE C-TERMINAL TAIL

Section 3.1: Abstract

Drs2p is a yeast type-IV P-type ATPase (P4-ATPase) and flippase that couples ATP hydrolysis to phospholipid translocation. Previous studies show that ATPase activity is retained with affinity-purified Drs2p using an N-terminal tandem affinity purification (TAP) tag (TAP_N-Drs2p), but not in a comparable preparation using a C-terminal TAP tag (Drs2p-TAP_C) (Zhou and Graham, 2009). However, both TAP-tagged Drs2 proteins are functional *in vivo*. Furthermore, the purified, inactive Drs2p-TAP_C does not seem to be aggregated or denatured in detergent solutions, suggesting that there may be a biological reason for the inactivity of purified Drs2p-TAP_C. In this chapter, further experiments were conducted to address potential causes of the Drs2p-TAP_C inactivity. The N-terminal TAP_N tag does not activate Drs2p, neither does the C-terminal TAP_C tag inactivate it. Interestingly, the ATPase activity of purified Drs2p seems to be associated only with a C-terminally cleaved form of Drs2p. This proteolytic cleavage causes a partial or complete loss of the C-terminal tail in Drs2p, so the cleaved form is designated the “NoC” form. The “NoC” form was found only in the Drs2p samples purified using the TAP_N tag but not the TAP_C tag, as the “NoC” form of Drs2p also loses the TAP_C tag and does not bind to the affinity column specific for the TAP_C tag. The “NoC” form of Drs2p is estimated to be ~9 kDa smaller than Drs2p, and a potential cleavage site that generates the “NoC” form (the “NoC” cleavage site) was identified in the C-terminal tail of Drs2p by mass spectrometry. These data suggest that the intact Drs2p is auto-inhibited *in vitro* and the “NoC” form is released from this auto-inhibition, providing a molecular basis that

potentially underlies the activity difference between the purified TAP_N-Drs2p and Drs2p-TAP_C.

Section 3.2: Introduction

P-type ATPases form a large protein family of membrane pumps that uses the energy derived from ATP hydrolysis to drive movement of various substrates, such as ions, across membranes against their chemical gradient. Most P-type ATPases have three cytosolic domains (A: actuator; N: nucleotide binding; P: phosphorylation) and ten transmembrane segments comprising the membrane domain (Kuhlbrandt, 2004). The molecular basis of the P-type ATPase catalytic cycle was primarily gained from the crystal structures of one P-type ATPase, the sarcoplasmic/endoplasmic reticulum Ca²⁺ ATPase 1 (SERCA1, **Figure 3-1A**), which has been crystallized in multiple conformational states (Toyoshima and Mizutani, 2004; Toyoshima et al., 2000; Toyoshima and Nomura, 2002; Toyoshima et al., 2004). For SERCA1 (**Figure 3-1B**), the catalytic cycle starts with the E1 state, in which the ATPase binds Ca²⁺ with high affinity from the cytosolic side followed by ATP binding to the N domain. Phosphoryl transfer from ATP to a conserved aspartic acid residue in the P domain induces the transition into the E1P state. Following release of ADP, rotation of the A domain triggers the E1P to E2P transition, which destroys the Ca²⁺ binding site and opens the luminal gate for Ca²⁺ release. In the E2P state, the ATPase has a high affinity for the counter-ion substrate (H⁺), which binds from the luminal side. Hydrolysis of the aspartylphosphate in the P domain and subsequent release of the phosphate induces a conformational change to the E2 state. Release of the counter-ion substrate (H⁺) into the cytosol brings the protein back to the E1 state for next catalytic cycle. This catalytic cycle is thought to be a general model for all P-type ATPases, although some details may vary in some

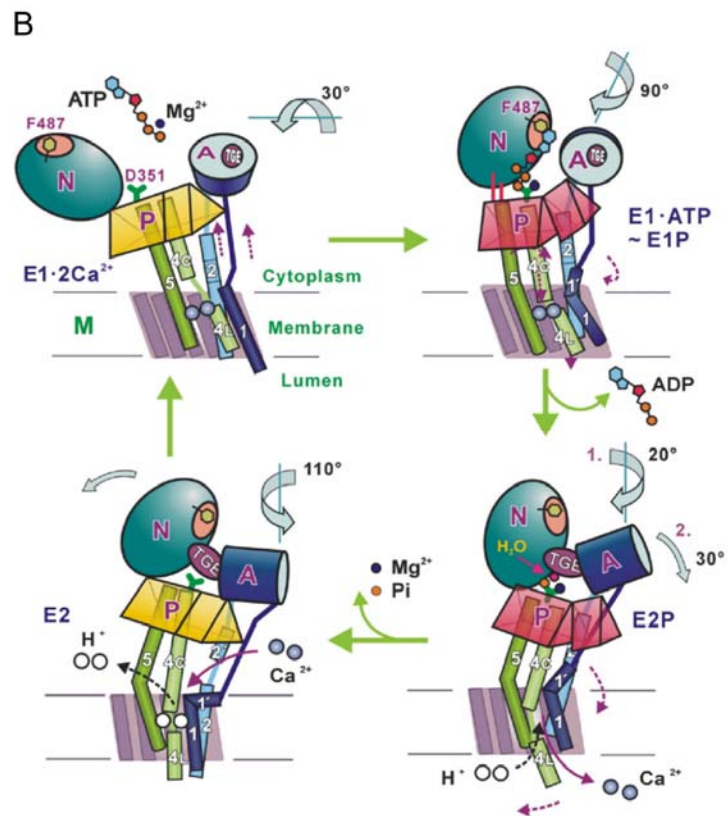
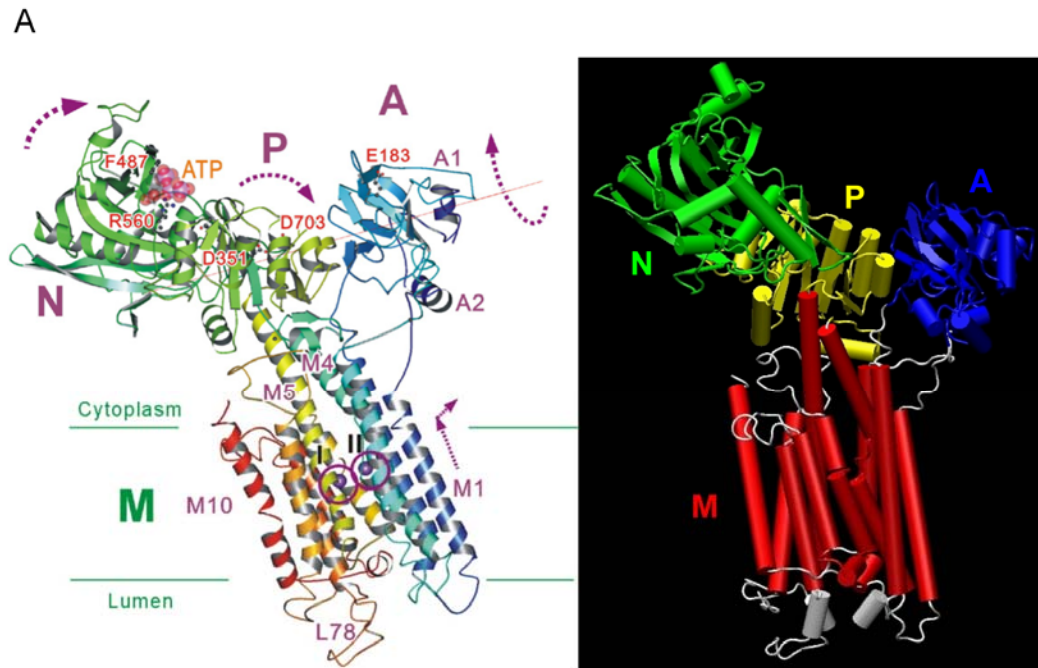


Figure 3-1. Structure and catalytic cycle of the sarcoplasmic reticulum Ca^{2+} ATPase 1.

Figure 3-1. Structure and catalytic cycle of the sarcoplasmic reticulum Ca^{2+} ATPase 1 (SERCA1). (A) Left panel: A ribbon representation of SERCA1 in the $\text{E1}\cdot 2\text{Ca}^{2+}$ conformation (PDB ID: 1SU4) (from Toyoshima, 2009). Colors change gradually from the N-terminus (blue) to the C-terminus (red). Purple circles indicate the two bound Ca^{2+} . A, actuator domain; N, nucleotide binding domain; P, phosphorylation domain; M, membrane domain. Dashed arrows indicate domain movement during the catalytic cycle. Bound ATP is shown in space-filling mode. Several α -helices such as A1 and A2 (A domain), and M1, M4, M5 and M10 (M domain) are indicated. Several key residues such as E183 (A domain, dephosphorylation), F487 and R560 (N domain, ATP binding), D351 (P domain, phosphorylation site), and D703 (P domain, coordination) are also indicated. Right panel: A cartoon representation of the left panel rendered with Swiss-PdbViewer. (B) A cartoon illustrating the structural changes and domain movement of SERCA1 during the catalytic cycle based on seven different conformational states determined by x-ray crystallography (from Toyoshima, 2009). This catalytic cycle is considered a general model for P-type ATPases (see text for details).

cases. For example, there is likely no counter-ion substrate for the plasma membrane proton pumps (Pedersen et al., 2007).

P-type ATPases are divided into five subfamilies (type-I to type-V, or P1 to P5) based on sequence homology, and are further divided into subgroups according to substrate specificity (Axelsen and Palmgren, 1998; Kuhlbrandt, 2004) (**Figure 3-2**). For example, SERCA1 belongs to the P2_A-ATPase class, and the plasma membrane proton pumps are P3_A-ATPases. In addition to the common structural features shared by all P-type ATPases (the A, P, N domains and the transmembrane segments), some subgroups were found to have an additional regulatory cytosolic domain, called R domain, within the N-terminal or C-terminal tail of the protein (Carafoli, 1994; Kuhlbrandt, 2004; Palmgren, 2001; Portillo, 2000; Sze et al., 2000). The R domain usually serves as an auto-inhibitory element that limits the activity of the ATPase and removal of the R domain by limited proteolysis or genetic engineering activates the protein. Auto-inhibition was also shown to be relieved by various regulatory activities in the R domain. For example, the P2_B-ATPase family comprising the plasma membrane Ca²⁺ pumps usually contains the R domain in the C-terminal tail (in animals) (Carafoli, 1994) or the N-terminal tail (in plants) (Sze et al., 2000) that binds and inhibits the ATPase. Binding of calmodulin to the R domain of the P2_B-ATPase displaces the auto-inhibitory tail and activates it for Ca²⁺ transport. Phosphorylation of serine or threonine residues in the R domain of P2_B-ATPases was also found to regulate ATPase activity by disrupting calmodulin binding to the R domain, resulting in protein activation (in animals) or inactivation (in plants). Another subgroup possessing an auto-inhibitory R domain is the P3_A-ATPase family, which comprises mostly plasma membrane proton pumps from plants and fungi (Palmgren, 2001; Portillo, 2000). The R domain for this family was found to be in the C-terminal tail of the protein, and phosphorylation of serine or threonine residues in the R domain of P3_A-ATPases was required for displacement of

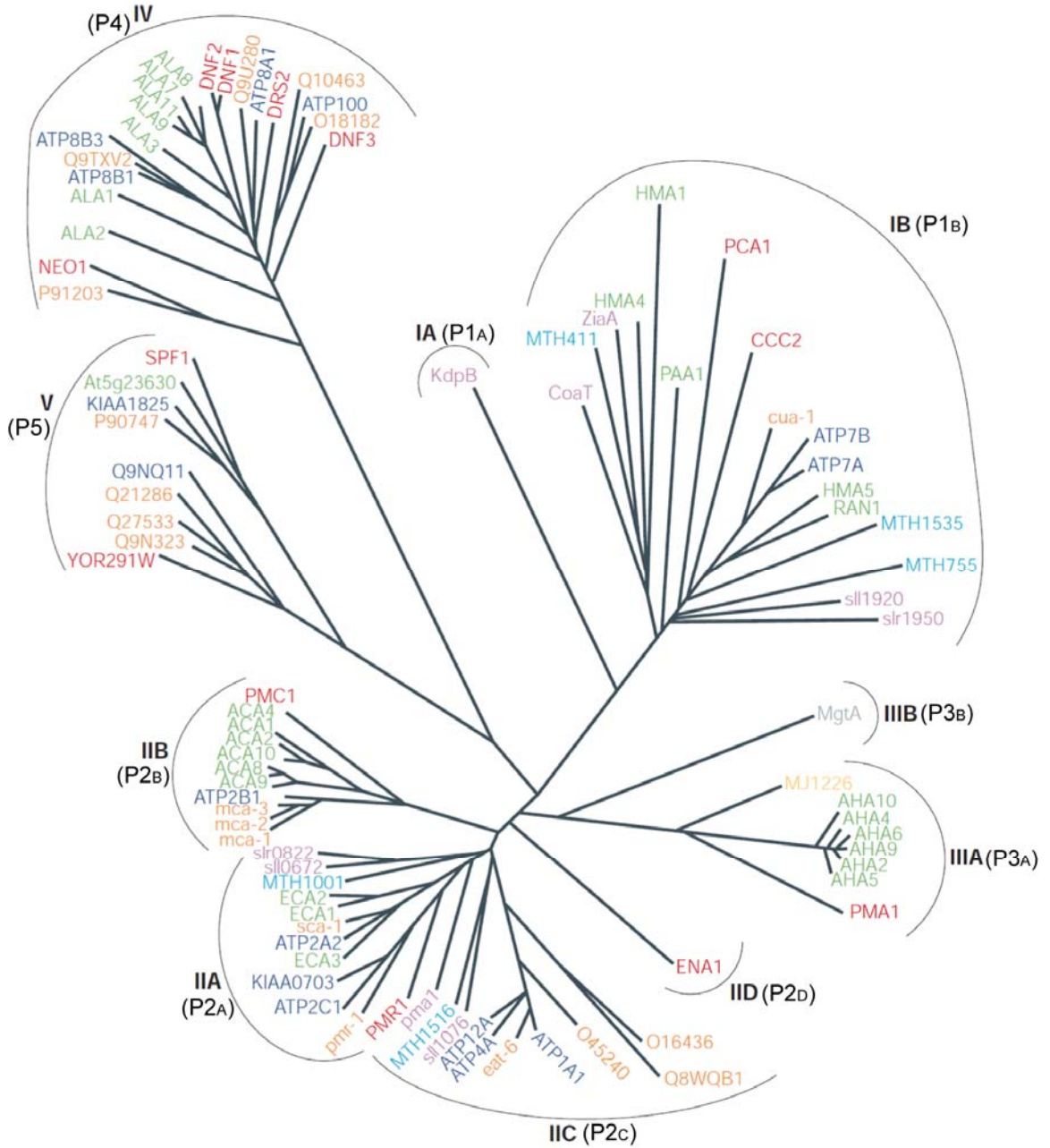


Figure 3-2. Phylogenetic tree of the P-type ATPase family.

Figure 3-2. Phylogenetic tree of the P-type ATPase family (modified from Kuhlbrandt, 2004). Subfamilies cluster according to their substrate specificity. Type IA (P1_A), bacterial Kdp-like K⁺ ATPases; type IB (P1_B), heavy metal ion transporting ATPases; type IIA (P2_A), sarcoplasmic/endoplasmic reticulum Ca²⁺ ATPases; type IIB (P2_B), plasma membrane Ca²⁺ ATPases; type IIC (P2_C), Na⁺/K⁺ ATPases and H⁺/K⁺ ATPases; type IID (P2_D), eukaryotic Na⁺ ATPases; type IIIA (P3_A), H⁺ ATPases; type IIIB (P3_B), bacterial Mg²⁺ ATPases; type IV (P4), phospholipid flippases; type V (P5), eukaryotic P-type ATPases with unknown substrate specificity. Representative genes presented in this phylogenetic analysis are color coded by species. Green, genes from *Arabidopsis thaliana*; orange, *Caenorhabditis elegans*; grey, *Escherichia coli*; dark blue, *Homo sapiens*; light blue, *Methanobacterium thermoautotrophicum*; yellow, *Methanococcus jannaschii*; purple, *Synechocystis* PCC6803; red, *Saccharomyces cerevisiae*.

the auto-inhibitory C-terminal tail. In plants, the activation of P3_A-ATPases involves binding of 14-3-3 protein to the phosphorylated R domain, but the binding protein in yeast has not yet been identified, or perhaps the yeast pump has an activation mechanism distinct from that in plants.

In addition to *cis*-regulation by the R domain, the activity of P-type ATPases can also be modulated by various *trans* regulators (Carafoli, 1994; Kuhlbrandt, 2004; Palmgren, 2001; Portillo, 2000; Sze et al., 2000). The primary mechanisms of regulation are protein interactions, such as calmodulin binding for the P2_B-ATPase Ca²⁺ pumps, 14-3-3 binding for the plant P3_A-ATPase proton pumps, as well as phosphorylation and dephosphorylation of the R domain. Some protein regulators are also membrane proteins and may have a more intimate relationship with the P-type ATPase that they regulate. In this case, the P-type ATPase and its regulatory proteins are often deemed as a multi-subunit complex, with the P-type ATPase as the catalytic subunit and others the noncatalytic subunits. For example, SERCA1 of the P2_A-ATPase family was found to associate tightly with a small integral membrane protein called phospholamban that when dephosphorylated binds and inhibits SERCA1 by stabilizing it in the E2 conformation (Carafoli, 1994; Sze et al., 2000). Phosphorylation of phospholamban dissociates it from SERCA1 and results in SERCA1 activation. The best example of the hetero-oligomeric P-type ATPase complex is the P2_C-ATPase family, comprising the Na⁺/K⁺ ATPases and the gastric H⁺/K⁺ ATPases (Geering, 2001; Kuhlbrandt, 2004). The functional unit of Na⁺/K⁺ ATPase consists of the catalytic α subunit (the P2_C-ATPase) and two additional regulatory subunits, β (a type II membrane glycoprotein) and γ (a type I membrane protein of the FXYD family). The β subunit was found to be a chaperone that is essential for assembly, membrane insertion and proper localization of the catalytic α subunit, and both β and γ subunits were shown to regulate the Na⁺/K⁺ ATPase activity. Other than proteins, lipids may also be regulators for P-type ATPases. For instance, the

P2_B-ATPase Ca²⁺ pump in erythrocytes was found to be stimulated by acidic phospholipids and unsaturated fatty acids (Carafoli, 1994).

Drs2p is a P4-ATPase from the budding yeast *Saccharomyces cerevisiae*. In steady state, Drs2p is localized primarily to the *trans* Golgi network (TGN), and is involved in multiple protein trafficking pathways between the TGN, plasma membrane and endosomes (Muthusamy et al., 2009a; Zhou et al., 2010). Drs2p was also proposed to be a phospholipid flippase, an enzyme that transports specific phospholipid substrate across membranes to the cytosolic leaflet at the expense of ATP consumption (Daleke, 2003; Graham, 2004; Pomorski et al., 2004). In recent years, Drs2p was found to be responsible for a PS flippase activity detected in isolated TGN membranes (Natarajan et al., 2004) and post-Golgi secretory vesicles (Alder-Baerens et al., 2006), as well as in proteoliposomes reconstituted with purified Drs2p (Zhou and Graham, 2009).

Interestingly, like P2_B- and P3_A-ATPases, Drs2p also possesses a C-terminal tail predicted to be 137-aa long (Chantalat et al., 2004) (**Figure 1-9**), which was shown to contain a regulatory domain (R domain). Several features of the Drs2p R domain have been identified. One is a motif that binds to Gea2p, a guanine nucleotide exchange factor for ARF GTPases (Chantalat et al., 2004). Another feature of the R domain is a region homologous to a split PH domain that binds phosphatidylinositol 4-phosphate (PI4P) (Natarajan et al., 2009), a phospholipid that is enriched in the Golgi membranes and is important for vesicle-mediated protein transport from the TGN. In recent work from our laboratory, Drs2p flippase activity was found to be virtually abolished in TGN membranes isolated from yeast cells that are deficient for Gea2p and PI4P production (Natarajan et al., 2009). Moreover, addition of Gea2p and PI4P to these TGN membranes restored flippase activity. This result suggests that Drs2p is likely auto-inhibited by its C-terminal tail in the absence of Gea2p and PI4P, both of which are positive regulators for Drs2p and stimulate its activity by binding to the Drs2p C-terminal

R domain. In addition, Kes1p, an oxysterol binding protein, was discovered to be a negative regulator of Drs2p flippase activity (Muthusamy et al., 2009b). Kes1p does not seem to bind Drs2p directly and may regulate Drs2p indirectly by modulating PI4P levels at the TGN.

Another intriguing aspect of Drs2p is that this P₄-ATPase (α subunit) requires a β subunit called Cdc50p for ER exit and proper localization (Chen et al., 2006; Saito et al., 2004), as seen in the P_{2C}-ATPase Na⁺/K⁺ pumps (Geering, 2001). However, other than being a chaperone, whether Cdc50p also plays a role in Drs2p function remains largely unknown. Recent work by Lenoir et al. brought several interesting observations to this issue (Lenoir et al., 2009). In that work, an N-terminally tagged Drs2p was affinity purified and a C-terminally tagged Cdc50p was found to be co-purified. The authors observed that a small portion of purified Drs2p molecules were capable of phosphorylation, and the percentage of Drs2p phosphorylation was higher in the Cdc50p-associated Drs2p population than in the monomeric Drs2p population. Hence, the authors suggested that Cdc50p is required for the phosphoenzyme intermediate formation of Drs2p during its catalytic cycle. Furthermore, using an in vivo split ubiquitin assay, a Drs2p mutant trapped in the E2P state was found to interact strongly with Cdc50p, whereas Drs2p mutants trapped in the E1 or E1P state did not interact with Cdc50p. Based on this observation, the authors suggested that the affinity of Cdc50p for Drs2p fluctuates during the Drs2p catalytic cycle. However, the conclusion that Cdc50p was required for the phosphoenzyme formation of Drs2p (E1 to E1P transition) but did not interact with Drs2p during this process seemed to add some complexity to this issue.

In the previous chapter, I purified TAP-tagged Drs2p using either the N-terminal tag (TAP_N-Drs2p) or the C-terminal tag (Drs2p-TAP_C), and found that only TAP_N-Drs2p retained ATPase activity after purification, despite the observation that both TAP-tagged Drs2 proteins are functional in vivo. The inactivity of purified Drs2p-TAP_C did not seem to

result from protein denaturation or aggregation. In this chapter, further studies were pursued to address the cause of purified Drs2p-TAP_C inactivity. A molecular mechanism that potentially underlies the Drs2p-TAP_C inactivity is proposed and tested. In addition, preliminary studies on the contribution of Cdc50p to the ATPase activity of purified Drs2p are presented.

Section 3.3: Materials and Methods

Section 3.3.1: Reagents

IgG Sepharose 6 Fast Flow, calmodulin Sepharose 4B, and ATP (>99% purity) were from GE Healthcare. Ni-NTA agarose was from Qiagen. AcTEV protease and SimplyBlue SafeStain (Coomassie G-250) were from Invitrogen, and Triton X-100 was from Anatrace. Antibodies used in this study were rabbit primary antibodies against Drs2p, the decahistidine (His₁₀) tag (Santa Cruz), and the calmodulin binding peptide (CBP) tag (GenScript), and an Alexa Fluor 680-labeled goat secondary antibody against rabbit IgG (Invitrogen).

Section 3.3.2: Media and strains

Yeast cells were grown in standard rich medium (1% yeast extract/2% peptone/2% dextrose) or synthetic minimal media containing required supplements (Sherman, 1991), and the nutrients were doubled in cell cultures for protein purification purposes.

Yeast strains used for protein purification were XZY38b (*MAT α his3 leu2 ura3 met15 P_{GPD}::DRS2::TAP_C P_{GPD}::CDC50 atp2 Δ ::URA3*), XZY60m (*MAT α his3 leu2 ura3 lys2 P_{GPD}::TAP_N::DRS2 P_{GPD}::CDC50 atp2 Δ ::URA3*), XZY84 (*MAT α his3 leu2 ura3 met15 P_{GPD}::CDC50::TAP_C pRS425-P_{GPD}::TAP_N::DRS2*), and XZY85 (*MAT α his3 leu2 ura3 lys2 P_{GPD}::CDC50 atp2 Δ ::URA3 pRS425-P_{GPD}::TAP_N::DRS2:TAP_C*), where TAP_C encodes the

CBP-TEV protease cleavage site-protein A tag, and TAP_N encodes the protein A-TEV protease cleavage site-His₁₀ tag.

Section 3.3.3: Protein purification

TAP-tagged Drs2p was affinity purified using a TAP procedure described previously with some modifications (Zhou and Graham, 2009). Briefly, yeast cells were cultured to near saturation (10-15 OD₆₀₀/mL in rich media and 4-6 OD₆₀₀/mL in minimal media) at 30 C, harvested and lysed by an EmulsiFlex-C3 High Pressure Homogenizer (Avestin). The cell lysate was centrifuged at 15,000 x g for 12 min, and 20% of Triton X-100 was added to the supernatant to a final concentration of 1% to solubilize Drs2p. TAP-tagged Drs2p was then purified using an IgG column plus either a Ni²⁺ column (for TAP_N) or a calmodulin column (for TAP_C). In the experiments that Drs2p was first purified using the TAP_N tag and then different Drs2p populations were separated using the TAP_C tag, the procedure was a combination of the TAP_N purification plus the second affinity step (the calmodulin column) of the TAP_C purification.

All purified Drs2p samples were centrifuged in the Microcon YM-100 filter (Millipore) at 13,000 x g for 15 min at 4 C to near dryness, and resuspended in the desired amount of storage buffer (40 mM Tris-HCl, pH 7.5/150 mM NaCl/40% glycerol/0.1% Triton X-100) to store at -20 C. Recovery of Drs2p was determined using Odyssey Infrared Imaging System (LI-COR) to quantify SimplyBlue-stained bands relative to a BSA standard curve.

Section 3.3.4: ATPase assay

Purified Drs2p was assayed for ATPase activity in ATPase buffer (50 mM Tris-HCl, pH 7.5/100 mM NaCl/50 mM KCl/1 mM NaN₃/0.1% Triton X-100/4 mM Na⁺-ATP, pH 7.5/10 mM MgCl₂) at 37 C for 2 h, and released phosphate was measured colorimetrically using a modified protocol previously described (Carter and Karl, 1982; Paterson et al., 2006;

Zimmerman and Daleke, 1993). Briefly, the volume of the sample was brought to 275 μL with deionized water, and the ATPase reaction was stopped by addition of 150 μL of molybdate solution (2 M HCl/50 mM Na_2MoO_4) and 75 μL of malachite green solution (0.042% malachite green in 1% polyvinyl alcohol solution). The sample was mixed for 2 min before addition of 500 μL of citric acid (7%) or H_2SO_4 (7.8%), and the optical density at 660 nm was read at 30 min after addition of the citric acid solution. The amount of released phosphate was determined by a phosphate standard curve constructed in the same ATPase buffer.

Section 3.3.5: Western blotting

Western blotting was performed as previously described (Chen et al., 1999). The primary antibodies used were rabbit anti-Drs2p (1:2000), anti-His₁₀ (1:200), and anti-CBP (1:500) antibody. The secondary, Alexa Fluor 680-labeled goat anti-rabbit IgG antibody was used at 1:2000. Western blots were imaged with Odyssey Infrared Imaging System (LI-COR).

Section 3.3.6: Mass spectrometry

Protein samples were subjected to SDS polyacrylamide gel electrophoresis and the protein bands of interest were excised. The protein sample was then in-gel digested with trypsin, and was loaded onto an ABI Voyager 4700 MALDI-TOF-TOF system (Applied Biosystems) and analyzed by tandem mass spectrometry (MS-MS).

Section 3.4: Results

Section 3.4.1: The content of the tag does not seem to cause the difference in ATPase activity between purified TAP_N-Drs2p and Drs2p-TAP_C.

In a previous study, both TAP_N-Drs2p and Drs2p-TAP_C were affinity purified with comparable yields and purities as determined by Coomassie staining and mass spectrometry. Although both TAP-tagged Drs2p forms appeared to be functional *in vivo*, only TAP_N-Drs2p retained ATPase activity after purification, whereas the purified Drs2p-TAP_C was inactive. The purified Drs2p-TAP_C did not seem to be aggregated or denatured compared to TAP_N-Drs2p when analyzed by size exclusion chromatography and circular dichroism spectroscopy (Zhou and Graham, 2009), suggesting that the inactivity of purified Drs2p-TAP_C may have a biologically relevant cause.

The major molecular difference between the purified TAP_N-Drs2p and Drs2p-TAP_C was that the former has a decahistidine (His₁₀, part of the TAP_N) tag appended to the N-terminus of Drs2p versus a calmodulin binding peptide (CBP, part of the TAP_C) tag appended to the C-terminus of Drs2p in the latter (**Figure 2-5B** and **Figure 2-1B**). It is possible that the content of the tag (His₁₀ vs. CBP) or the position of the tag (N- vs. C-) caused the difference in ATPase activity of purified Drs2 proteins. To address this issue, a dual-TAP-tagged Drs2p (TAP_N-Drs2p-TAP_C) was engineered in a multicopy (2 μ) plasmid and overexpressed by the glyceraldehyde-3-phosphate dehydrogenase (GPD) promoter (**Figure 3-3A and B**).

TAP_N-Drs2p-TAP_C was affinity purified using either the TAP_N tag or the TAP_C tag, and the protein yield and purity was comparable between the two preparations as judged by Coomassie staining (**Figure 3-3C**, lane 3 and 4). Theoretically, both preparations should contain Drs2p of the same molecular composition, i.e. TAP_N-Drs2p-TAP_C (more precisely, His₁₀-Drs2p-CBP). Indeed, Drs2p from both preparations appeared as a single

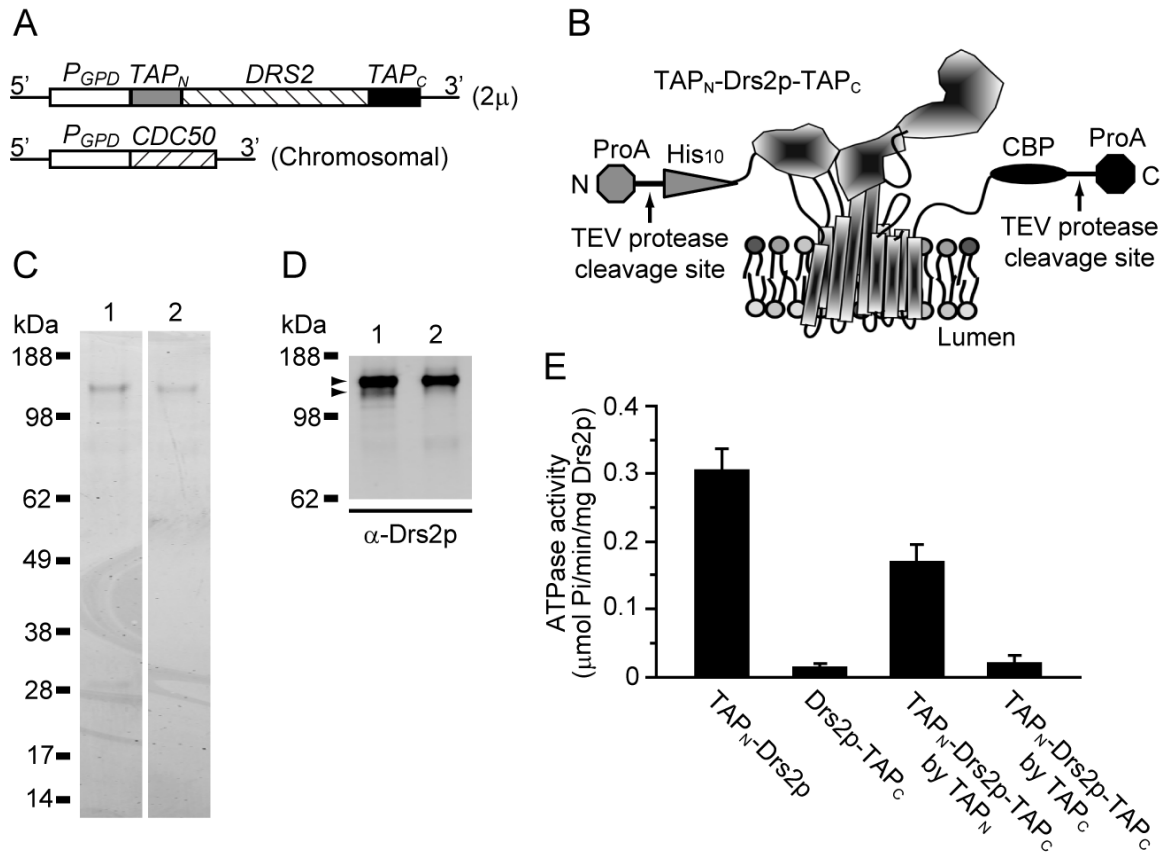


Figure 3-3. Expression and purification of TAP_N -Drs2p- TAP_C . (A) Genetic organization of TAP_N - $DRS2$ - TAP_C and $CDC50$. TAP_N - $DRS2$ - TAP_C was expressed from a 2 μ plasmid and $CDC50$ was from the chromosome. (B) Schematic of TAP_N -Drs2p- TAP_C modeled on the crystal structure of SERCA1 in the E1-2Ca²⁺ conformation (Toyoshima et al., 2000). ProA, protein A moiety; His₁₀, decahistidine moiety; CBP, calmodulin binding peptide moiety; TEV, tobacco etch virus. (C) Purified TAP_N -Drs2p- TAP_C from strain XZY85 (*atp2* Δ) using the TAP_N tag (lane 1) or TAP_C tag (lane 2) were subject to SDS-PAGE and the gel was stained with SimplyBlue. (D) Proteins in a gel from (C) were electrotransferred to polyvinylidene difluoride (PVDF) membrane for western blotting. The primary antibody against Drs2p was used at 1:2000. The upper arrow head indicates the intact TAP_N -Drs2p- TAP_C form and the lower arrow head indicates a minor band with faster mobility (the "NoC" form). Note that there was another minor band below the two arrow heads. (E) ATPase activity of purified TAP_N -Drs2p- TAP_C preparations. TAP_N -Drs2p and Drs2p- TAP_C were purified from strains XZY60m (*atp2* Δ) and XZY38b (*atp2* Δ), respectively, as previously described.

band corresponding to the size of TAP_N-Drs2p-TAP_C on a Coomassie-stained protein gel (**Figure 3-3C**, lane 3 and 4), suggesting that the bulk of purified TAP_N-Drs2p-TAP_C using either tag was in the same form as expected. However, ATPase activity was only detected in the TAP_N-Drs2p-TAP_C sample purified using the TAP_N tag, but not the TAP_C tag (**Figure 3-3E**). These data suggest that the presence of the N-terminal His₁₀ tag or the C-terminal CBP tag did not directly cause activation or inactivation of Drs2p, respectively. Rather, it is more likely the position of the tag and a reason that is inherent to the C-terminal purification method that has caused Drs2p-TAP_C to be inactive after purification.

Section 3.4.2: A cleaved form of Drs2p is present only in the TAP_N-Drs2p-TAP_C sample purified using the TAP_N tag, but not the TAP_C tag.

Although the N-terminally purified TAP_N-Drs2p-TAP_C appeared to be the same as the C-terminally purified one based on Coomassie staining, a difference between the two preparations was revealed by western blotting. Interestingly, a minor form of Drs2p with mobility faster than that of TAP_N-Drs2p-TAP_C was detected in the TAP_N-Drs2p-TAP_C sample purified using the TAP_N tag, but not the TAP_C tag (**Figure 3-3D**), suggesting that it is a C-terminally cleaved form of Drs2p. Indeed, this cleaved TAP_N-Drs2p-TAP_C remained immunoreactive with an antibody recognizing the His₁₀ tag (part of the TAP_N), but could not be detected by an antibody that recognizes the CBP tag (part of the TAP_C) (**Figure 3-4A**, lane 2 and 5). Because the cleavage resulted in a partial or complete loss of the C-terminal tail of Drs2p, this cleaved form of Drs2p was designated the “NoC” form.

The “NoC” form of TAP_N-Drs2p-TAP_C was estimated to compose ~10% of the total Drs2p molecules in the N-terminally purified TAP_N-Drs2p-TAP_C sample by measuring the intensity of bands on western blots (**Figure 3-3D**, lane 1; **Figure 3-4A**, lane 7). Based on

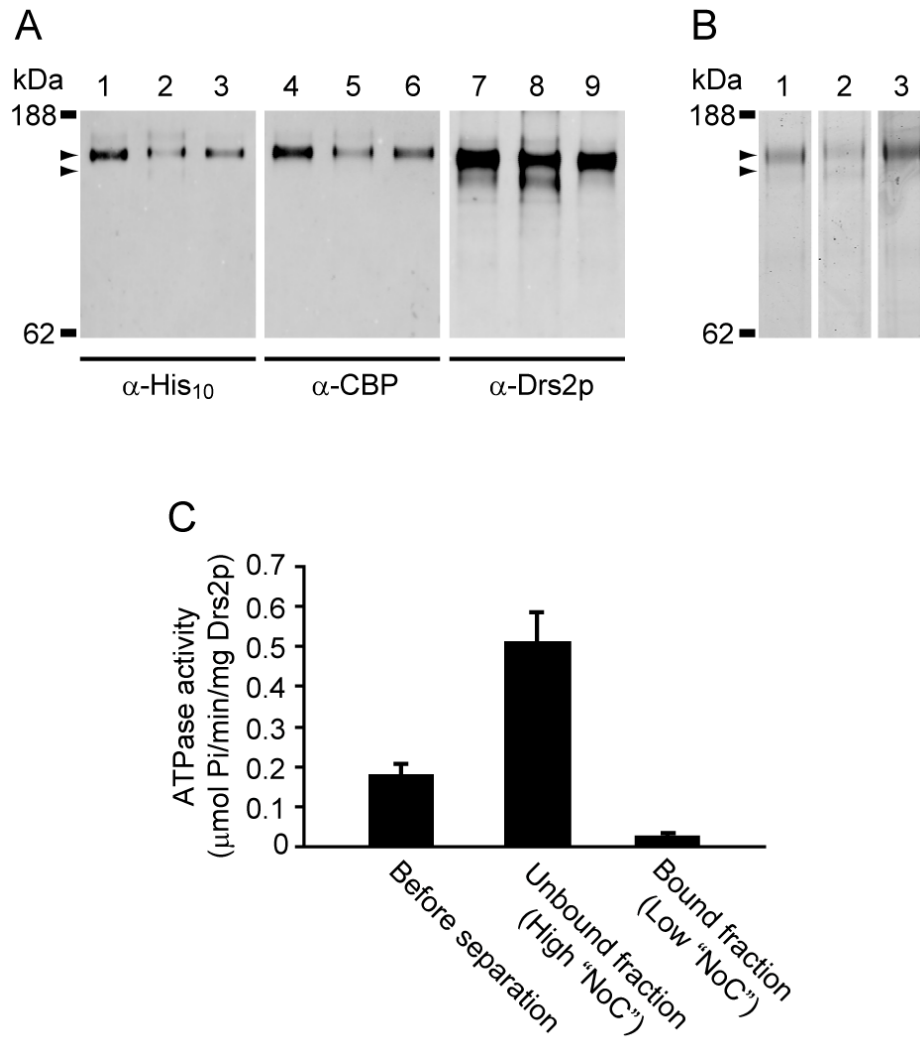


Figure 3-4. Partial separation of the "NoC" form from the intact form in purified TAP_N-Drs2p-TAP_C by calmodulin column. (A) Purified TAP_N-Drs2p-TAP_C before separation (lane 1, 4 and 7), the unbound fraction from the calmodulin column (lane 2, 5, and 8), and the bound and eluted fraction (lane 3, 6, and 9) were subjected to SDS-PAGE and western blotting. Primary antibodies were used at 1:200 (anti-His₁₀), 1:500 (anti-CBP) and 1:2000 (anti-Drs2p). The upper arrow head indicates the intact TAP_N-Drs2p-TAP_C form and the lower arrow head indicates the "NoC" form. Note that the "NoC" form is a very weak band in lane 2. (B) The three samples ordered as in (A) were analyzed by SDS-PAGE and the gel was stained with SimplyBlue. Arrow heads indicate the two forms of TAP_N-Drs2p-TAP_C as in (A). (C) ATPase activity was assayed with purified TAP_N-Drs2p-TAP_C before separation and the two fractions after separation.

mobility of proteins on western blots (**Figure 3-4A**, lane 2 and 8), the “NoC” form of TAP_N-Drs2p-TAP_C was estimated to be ~15 kDa smaller than the intact form of TAP_N-Drs2p-TAP_C, which corresponds to an ~9 kDa loss in the C-terminal tail of Drs2p.

The C-terminal tail of Drs2p has been suggested to contain an R domain that auto-inhibits Drs2p (Natarajan et al., 2009). It is possible that only the “NoC” form of Drs2p, which was recovered only in the N-terminal purifications, was active, and that it was the “NoC” form of Drs2p that conferred ATPase activity in the purified samples.

Section 3.4.3: The ATPase activity is associated with the “NoC” form of TAP_N-Drs2p-TAP_C in purified samples.

To test if the “NoC” form of Drs2p was responsible for the ATPase activity detected in the purified Drs2p samples, the “NoC” form was partially separated from the intact form in an N-terminally purified TAP_N-Drs2p-TAP_C preparation. Because the “NoC” form of TAP_N-Drs2p-TAP_C lost the C-terminal tag (the CBP tag of the TAP_C) but the intact form retained it, these two TAP_N-Drs2p-TAP_C forms were separated by binding to a calmodulin column. The unbound fraction was enriched in the “NoC” form of TAP_N-Drs2p-TAP_C (~30% of total Drs2p, **Figure 3-4A**, lane 8), whereas the bound and eluted fraction contained very little “NoC” form (<4% of total Drs2p, **Figure 3-4A**, lane 9). Consistently, the fraction enriched in the “NoC” form of TAP_N-Drs2p-TAP_C displayed a specific ATPase activity 3-4 fold higher than that of the initial preparation before the separation (**Figure 3-4C**). In contrast, the eluted fraction free of the “NoC” form was almost devoid of ATPase activity (**Figure 3-4C**). These data suggest that the ATPase activity of purified TAP_N-Drs2p-TAP_C coincided with the “NoC” form and that the intact form of Drs2p was inactive after purification, furthering supporting that the “NoC” form of TAP_N-Drs2p-TAP_C was responsible for the observed ATPase activity.

Section 3.4.4: A potential cleavage site that generates the “NoC” form of TAP_N-Drs2p-TAP_C is identified by mass spectrometry.

In the fraction enriched in the “NoC” form of TAP_N-Drs2p-TAP_C, Drs2p appeared as a doublet on Coomassie-stained gels (**Figure 3-4B**, lane 2), corresponding to the intact and the “NoC” form of TAP_N-Drs2p-TAP_C. To map the cleavage site that generates the “NoC” form (the “NoC” cleavage site) and identify the C-terminal end sequence of the “NoC” form of Drs2p (the “NoC” terminus), the band with faster mobility corresponding to the “NoC” form was excised and digested with trypsin for a mass spectrometric analysis. The eluted fraction containing little “NoC” form was also run on a gel and the protein band corresponding to the intact form of TAP_N-Drs2p-TAP_C was excised as a control for the mass spectrometric identification (**Figure 3-4B**, lane 3). If the “NoC” cleavage site was not a trypsin recognition site, that is, if the cleavage did not take place after a basic residue (R or K), the “NoC” form of Drs2p would produce a novel peptide containing the “NoC” terminus when digested with trypsin, which would not appear in the control sample containing the intact Drs2p. However, if the cleavage happened right after a basic residue, the peptide that contains the “NoC” terminus would be indistinguishable from that generated by trypsin digestion. In this case, different proteases will be needed to digest the protein samples for mass spectrometry.

The initial attempt with trypsin digestion to identify a novel peptide without a basic residue at the C-terminal end was partially successful. Because the last 57-aa region (1299-1355) of the predicted Drs2p C-terminal tail (1219-1355) lacks sufficient basic residues (**Figure 1-9A**), this region was not recovered in either the “NoC” sample or the control. Therefore, it was not known if the “NoC” cleavage site resides in this region. However, the “NoC” form was estimated to miss a sequence of ~9 kDa in size (~80-aa) of the C-terminus of Drs2p, suggesting that the “NoC” cleavage site was likely not in the C-terminal 57-aa region of Drs2p (1299-1355). The protein sequence coverage at the C-

terminus was the same for the “NoC” sample and the control, both of which were covered to residue 1298, indicating a contamination of the intact TAP_N-Drs2p-TAP_C in the “NoC” sample. However, a novel peptide ending with a glutamine residue at position 1254 (Q1254) was discovered in the “NoC” sample but not in the control sample.

It is possible that the Q1254-Q1255 sequence was the potential “NoC” cleavage site. If the “NoC” form of Drs2p ended with Q1254, the “NoC” form would lose a 101-aa long sequence from the C-terminus of Drs2p (**Figure 1-9A**), resulting in a loss of ~11 kDa in size. This value was close to that estimated by the protein mobility measurement. However, because non-traditional peptides in mass spectrometry may also arise from non-tryptic events, whether the Q1254 residue was the true C-terminal end of the “NoC” form of Drs2p will require further mass spectrometric studies with different protease digestion.

Section 3.4.5: Cdc50p preferentially binds inactive Drs2p in purified samples.

In both purified TAP_N-Drs2p and Drs2p-TAP_C samples, Cdc50p was co-purified at a substoichiometric concentration relative to Drs2p (**Table 2-3** and **Table 2-1**), suggesting that the purified Drs2p was a mixed population of Drs2p monomers and Drs2p/Cdc50p complexes. Although the role that Cdc50p plays in Drs2p activity was unclear, Cdc50p did not confer ATPase activity to the inactive, purified Drs2p-TAP_C. To further assess the contribution of Cdc50p to the ATPase activity of purified TAP_N-Drs2p, Cdc50p was fused with the TAP_C tag at the C-terminus (Cdc50p-TAP_C) and was overexpressed along with TAP_N-Drs2p by the GPD promoter (**Figure 3-5A and B**). The purified TAP_N-Drs2p sample was then loaded on a calmodulin column to separate the TAP_N-Drs2p/Cdc50p-TAP_C complex from the TAP_N-Drs2p monomer. Fractions were collected and analyzed for Drs2p and Cdc50p by western blotting to estimate relative abundance of the TAP_N-Drs2p/Cdc50p-TAP_C complex in each fraction (**Figure 3-5C and D**). Only the

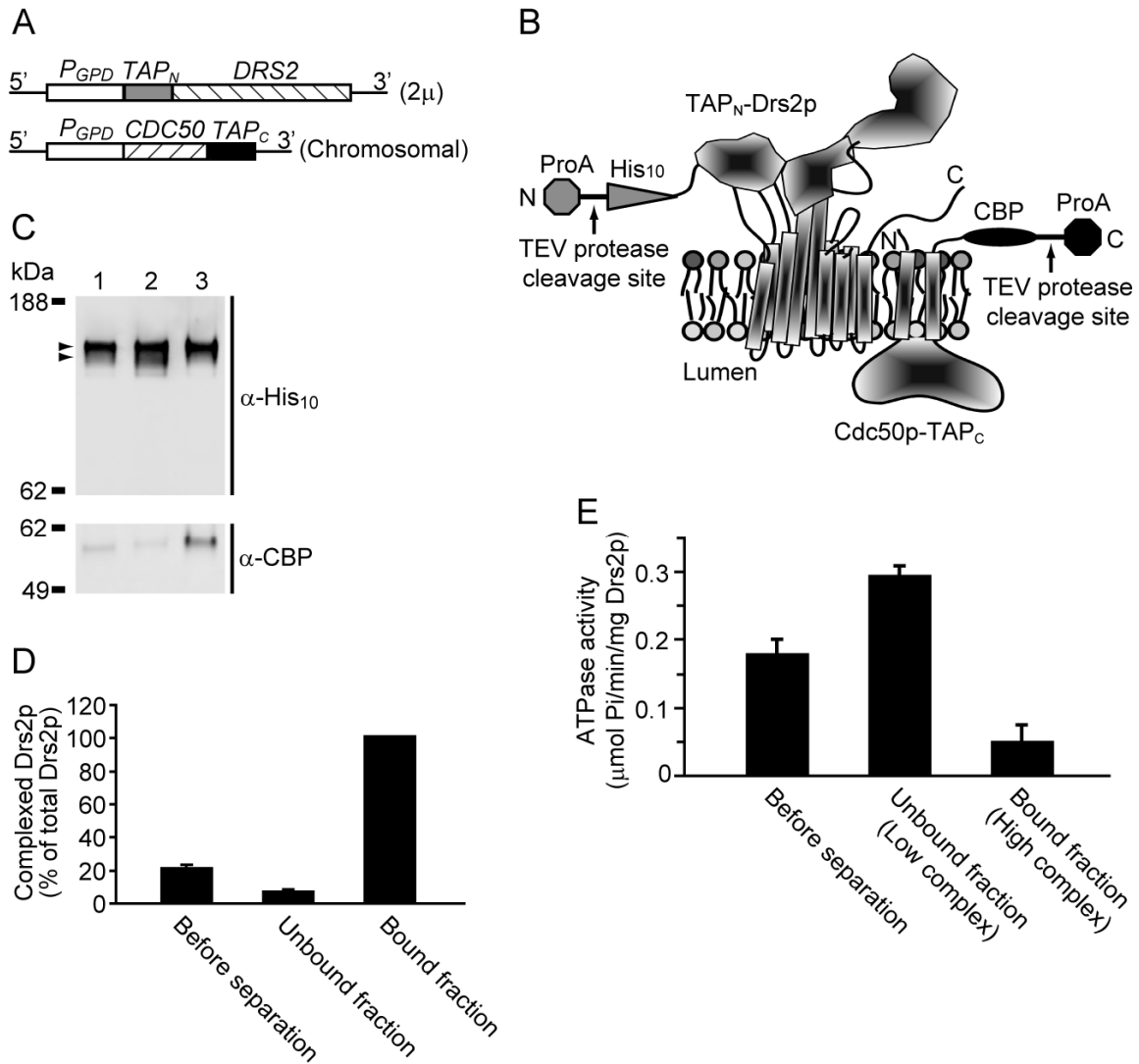


Figure 3-5. Partial separation of TAP_N-Drs2p/Cdc50p-TAP_C complex from TAP_N-Drs2p monomer in purified TAP_N-Drs2p by calmodulin column. (A) Genetic organization of TAP_N-DRS2 and CDC50-TAP_C. TAP_N-DRS2 was expressed from a 2 μ plasmid and CDC50-TAP_C was from the chromosome. (B) Schematic of TAP_N-Drs2p and Cdc50p-TAP_C. ProA, protein A moiety; His₁₀, decahistidine moiety; CBP, calmodulin binding peptide moiety; TEV, tobacco etch virus. (C) Purified TAP_N-Drs2p before separation (lane 1), the unbound fraction from the calmodulin column (lane 2), and the bound and eluted fraction (lane 3) were subjected to SDS-PAGE and western blotting. Primary antibodies were used at 1:200 (anti-His₁₀) and 1:500 (anti-CBP). The upper arrow head indicates the intact TAP_N-Drs2p form and the lower arrow head indicates the “NoC” form. (D) Estimation of the percentage of Cdc50p-complexed Drs2p according to (C). The abundance of Cdc50p relative to Drs2p was defined as Cdc50p signal (α -CBP) / Drs2p signal (α -His₁₀) in (C), and the bound fraction in (C) lane 3 was defined to be 1:1 in Cdc50p:Drs2p (mol/mol), i.e. 100% TAP_N-Drs2p/Cdc50p-TAP_C complex. Values for the other two samples were normalized. (E) ATPase activity was assayed with purified TAP_N-Drs2p before separation and the two fractions after separation.

TAP_N-Drs2p/Cdc50p-TAP_C complex would bind and be eluted from the calmodulin column because of the interaction of the TAP_C tag (the CBP module) with the column, so the eluted fraction contained purely the TAP_N-Drs2p/Cdc50p-TAP_C complex (100%). In contrast, the unbound fraction was enriched in the TAP_N-Drs2p monomer and contained fewer TAP_N-Drs2p/Cdc50p-TAP_C complexes (~6%). The original Drs2p preparation before separation contained an intermediate level of the TAP_N-Drs2p/Cdc50p-TAP_C complex (~20%).

Interestingly, we observed an inverse correlation between ATPase activity and the percentage of the TAP_N-Drs2p/Cdc50p-TAP_C complex in the samples (**Figure 3-5E**). The eluted fraction containing 100% of the TAP_N-Drs2p/Cdc50p-TAP_C complex showed ATPase activity lower than that before separation (~20%), and was lower than that of the unbound fraction (~6%). These data suggest that the Drs2p molecules that Cdc50p preferentially binds in purified samples were less active, and that the active Drs2p molecules in purified samples may not require Cdc50p for ATPase activity.

Section 3.5: Discussion

The observation that Drs2p purified using affinity tags at different termini showed different ATPase activities was intriguing. This phenomenon was originally observed between TAP_N-Drs2p and Drs2p-TAP_C, and ATPase activity was only detected in the N-terminally purified TAP_N-Drs2p (Zhou and Graham, 2009). However, Drs2p-TAP_C was functional *in vivo*, and did not seem to be unstructured or aggregated *in vitro* (Zhou and Graham, 2009). Furthermore, the tag itself was unlikely the direct cause of the different ATPase activity between the purified TAP_N-Drs2p and Drs2p-TAP_C, because a dual-TAP-tagged Drs2p (TAP_N-Drs2p-TAP_C) was also active in N-terminally purified samples, but remained dead when C-terminally purified (**Figure 3-3E**). Since high concentrations of imidazole and EDTA/EGTA seem to inhibit Drs2p ATPase activity (data not shown), to

avoid an effect of different elution buffers, the buffers for storage of TAP_N-Drs2p-TAP_C purified using either tag were exchanged to the same buffer (see Materials and Methods). Moreover, a physical binding interaction between the C-terminal tag and a column did not inactivate Drs2p, because the TAP_C tag should also bind the IgG column during the first affinity step when TAP_N-Drs2p-TAP_C was N-terminally purified. These findings suggest that there may be a mechanistic reason underlying the inactivity of the C-terminally purified Drs2p.

The C-terminal tail of Drs2p was suggested to contain an R domain that inhibits Drs2p flippase activity in isolated TGN membranes when stimulators, such as Gea2p and PI4P, are absent (Natarajan et al., 2009). One possible explanation for the inability to detect ATPase activity in purified Drs2p-TAP_C was that every Drs2p-TAP_C molecule recovered had to have an intact C-terminal tail, which inhibits Drs2p. On the other hand, the TAP_N-Drs2p sample may contain some TAP_N-Drs2p molecules that have lost the C-terminal tail and become constitutively active. In support of this possibility, the “NoC” form of Drs2p was identified only in the N-terminally, but not the C-terminally, purified Drs2p preparations (**Figure 3-3D**). Furthermore, ATPase activity was found to associate only with fractions containing the “NoC” form and became undetectable when the “NoC” form of Drs2p was depleted (**Figure 3-3E**). It would be interesting to see if addition of Gea2p and PI4P to purified Drs2p-TAP_C would activate ATPase activity, although incubation of PI4P alone with purified Drs2p-TAP_C in detergent solutions did not yield detectable ATPase activity (data not shown). It is possible that intact Drs2p requires a membrane environment for proper regulation by stimulators, and this possibility can be tested with reconstituted Drs2p-TAP_C in proteoliposomes.

A potential “NoC” terminus (Q1254) was also identified by a mass spectrometric analysis of trypsinized Drs2 proteins. The Q1254 residue resides in the Gea2p interacting region of the Drs2p R domain, which is followed by, and partially overlapped

by, the PI4P binding site (**Figure 1-9A**). In the R domain of P2_B-ATPases, the regulator (calmodulin) binding site also binds to the ATPase itself and causes auto-inhibition (Carafoli, 1994; Sze et al., 2000). Analogous to the P2_B-ATPase R domain, the regulator (Gea2p and PI4P) binding region of the Drs2p R domain may also bind to Drs2p and inhibit its activity. The Drs2p “NoC” form ending with the Q1254 residue would lose both the Gea2p interacting region and the PI4P binding site, and perhaps the auto-inhibition as well. However, there may be more than one “NoC” terminus. Supportively, at least two minors bands with faster mobility than that of intact TAP_N-Drs2p-TAP_C were observed on the western blots in **Figure 3-3D** and **Figure 3-4A**. Some “NoC” termini may not be recognized in this mass spectrometric identification using trypsin. For example, because the Gea2p interacting region and the PI4P binding site of the Drs2p R domain are extremely rich in basic residues (**Figure 1-9A**), any “NoC” terminus that ends with a basic residue would be indistinguishable from that generated by trypsin digestion and would be missed. A different protease digestion for mass spectrometry will be helpful in addressing this issue.

Affinity purified Drs2p was found to have Cdc50p co-purified at a substoichiometric concentration relative to Drs2p (Zhou and Graham, 2009), which was also observed recently by Lenoir et al. (Lenoir et al., 2009). In my purified samples, Cdc50p seemed to bind preferentially to the inactive Drs2p molecules (**Figure 3-5D and E**). Interestingly, Lenoir et al. found that Cdc50p interacted strongly with Drs2p trapped in the E2P state, but did not interact with Drs2p in its E1 or E1P state (Lenoir et al., 2009). These data suggest that the inactive, purified Drs2p (probably auto-inhibited) was likely in the E2P state, and had a higher affinity for Cdc50p than Drs2p in other conformational states such as E1 or E1P. This conformation-dependent association of Drs2p with Cdc50p may reflect a mechanism for quality control of Drs2p at the ER. Perhaps only fully functional Drs2p capable of proceeding to the E2P state and being auto-inhibited will be allowed to

associate with Cdc50p for ER exit. Upon arrival at the TGN, Drs2p is then activated by regulators, such as Gea2p and PI4P (**Figure 1-9B**). On the other hand, the Drs2p molecules that Cdc50p did not preferentially bind in the purified sample had higher ATPase activity (**Figure 3-5D and E**). Consistently, the “NoC” form of Drs2p was also detected primarily in the Drs2p monomer fraction (**Figure 3-5C**, lane 2), but much weaker in the fraction enriched in the Drs2p/Cdc50p complex form (**Figure 3-5C**, lane 3). These data suggest that the active, purified Drs2p (probably the “NoC” form) may not require Cdc50p for ATPase activity, although Cdc50p may be part of a regulatory machinery for Drs2p in vivo.

Section 3.6: Chapter Acknowledgements

We thank W. Hayes McDonald from the Mass Spectrometry Research Center from Vanderbilt University for his assistance with mass spectrometric analysis. This project is supported by National Institutes of Health Grant R01GM062367 to T.R.G..

CHAPTER IV

FORMATION AND OBSERVATION OF GIANT UNILAMELLAR VESICLES

Section 4.1: Abstract

Drs2p is a yeast flippase that translocates specific phospholipid substrates across a membrane bilayer to the cytosolic leaflet, which is proposed to be a driving force that promotes membrane deformation and vesicle budding. A direct approach to test this hypothesis is to reconstitute membrane bending and vesicle formation in chemically defined artificial membranes containing purified Drs2p. However, the Drs2p proteoliposomes generated by detergent-mediated reconstitution are too small (40 nm in diameter) to be amenable to morphological studies (Zhou and Graham, 2009). A promising means to overcome the physical restraint and technical hurdles imposed by the small size of the proteoliposomes is to convert them into giant unilamellar vesicles (GUVs). GUVs are normally 5-100 μm in diameter, and their morphological changes induced by various manipulations can be easily observed under an optical microscope in real-time (Farge and Devaux, 1992; Papadopoulos et al., 2007). This chapter describes a preliminary study on the methods of converting small, protein-free liposomes to GUVs, and observation of induced morphological changes of these GUVs. This information lays the ground for generation of Drs2p GUVs and subsequent morphological studies.

Section 4.2: Introduction

There are three major types of vesicles that mediate intracellular protein transport, namely COPI-, COPII-, and clathrin-coated vesicles (Kirchhausen, 2000b). Proteins traffic from the endoplasmic reticulum (ER) to the Golgi through COPII-coated vesicles, whereas COPI-coated vesicles mediate the retrograde transport from the Golgi back to

the ER. Clathrin-coated vesicles carry proteins between the *trans* Golgi network (TGN), the plasma membrane and endosomes. Vesicle budding of all three major types has been reconstituted from protein-free liposomes with addition of only cytosolic proteins such as coats and some accessory proteins (Matsuoka et al., 1998; Spang et al., 1998; Takei et al., 1998), indicating that these cytosolic factors alone are sufficient to drive vesicle formation. However, vesicle budding *in vivo* takes place in a tightly regulated temporal and spatial manner and cytosolic factors may not fully satisfy this layer of regulation. Furthermore, *in vitro* vesicle budding appears to be very inefficient and may occur at a rate much slower than that needed *in vivo* (Kinuta et al., 2002). Therefore, membrane factors such as phospholipids and membrane proteins likely make important contributions to this process *in vivo*. For example, Drs2p is a membrane protein that is suggested to directly facilitate the vesicle budding process (Graham, 2004; Pomorski et al., 2004).

Drs2p is a yeast flippase localized primarily at the TGN that translocates phosphatidylserine (PS) and probably phosphatidylethanolamine (PE) from the luminal leaflet to the cytosolic leaflet of TGN membranes (Natarajan et al., 2009; Natarajan et al., 2004). This directional movement of phospholipids is proposed to cause an imbalance in phospholipid number and surface area between the two leaflets and result in membrane bending toward the cytosolic leaflet (Sheetz and Singer, 1974), which is an essential step in vesicle formation. In support of this hypothesis, yeast cells deficient for Drs2p were found to be defective in forming a subset of clathrin-coated vesicles from the TGN (Chen et al., 1999; Gall et al., 2002). However, a direct test of the hypothesized role of Drs2p flippase activity on driving membrane deformation and vesicle budding in a biochemically defined membrane system remains to be pursued.

The main difficulty in reconstituting vesicle budding from the Drs2p proteoliposomes is that they are smaller, an average 40 nm in diameter (Zhou and Graham, 2009), than

vesicles formed in vivo (50-100 nm) (Kirchhausen, 2000b). Any potential morphological changes of these small liposomes induced by phospholipid movement would be restrained and difficult to observe. The best way to overcome this difficulty is to convert the small, preformed Drs2p proteoliposomes into giant unilamellar vesicles (GUVs, 5-100 μm in diameter). Because GUVs are big, vesicle budding will be more feasible. Moreover, GUVs can be observed directly under an optical microscope in real-time for morphological studies. Shape changes of GUVs have been successfully documented when the phospholipid number of the GUV bilayer was manipulated by various means. For example, pH-induced movement of phospholipids to the outer leaflet or external addition and incorporation of phospholipids to the outer leaflet were shown to induce tubulation and vesicle budding in GUVs (Farge and Devaux, 1992; Papadopoulos et al., 2007).

Several techniques are available for conversion of small vesicles to GUVs. One technique is the uncontrolled swelling method (Criado and Keller, 1987; Manley and Gordon, 2008), in which small vesicles are dehydrated followed by rehydration of the dried lipid film to form giant vesicles. An alternative to this technique is the controlled swelling method, or the electroformation method (Farge and Devaux, 1992; Girard et al., 2004; Manley and Gordon, 2008; Mathivet et al., 1996; Papadopoulos et al., 2007), in which dried lipid vesicles swell to form GUVs in an AC electric field. Each method has its own advantages and shortcomings. The uncontrolled swelling method is simple and quick, and compatible with most buffers, but the giant vesicles formed are very heterogeneous with a high percentage of multilamellar structures. In contrast, the electroformation method produces relatively homogeneous GUVs, but buffers and ions are only allowed at very low concentrations during electroformation. Another technique to convert small proteoliposomes to protein-containing GUVs involves fusion of preformed proteoliposomes either to each other or to preformed protein-free GUVs,

which usually requires special fusogenic lipids (e.g. palmitoylhomocysteine) (Connor et al., 1984), peptides (e.g. WAE, a synthetic undecameric peptide) (Kahya et al., 2001; Pecheur et al., 1997), and proteins (e.g. SNAREs) (Ohya et al., 2009; Taresté et al., 2008). Because this method adds new components and complexity to the GUV system, I focused on the first two swelling methods to generate GUVs from small vesicles. At the current stage, GUVs were formed from protein-free liposomes under conditions that should maintain native protein structures (Girard et al., 2004; Papadopoulos et al., 2007), and future studies will be expanded to generate Drs2p-containing GUVs from preformed Drs2p proteoliposomes.

Section 4.3: Materials and Methods

Section 4.3.1: Reagents

Polyoxyethylene 9-lauryl ether (C₁₂E₉) was from Sigma-Aldrich, and Bio-Beads SM-2 was from Bio-Rad. Phospholipids and fluorescent derivatives were from Avanti Polar Lipids and were DOPC (1,2-dioleoyl-*sn*-glycero-3-phosphocholine), DOPG (1,2-dioleoyl-*sn*-glycero-3-phospho-(1'-*rac*-glycerol)), DOPS (1,2-dioleoyl-*sn*-glycero-3-phospho-L-serine), and NBD-PC (1-palmitoyl-2-[6-[(7-nitro-2-1,3-benzoxadiazol-4-yl)amino]-hexanoyl]-*sn*-glycero-3-phosphocholine). Lipids were dissolved in chloroform and stored at -20 C.

Section 4.3.2: Formation of protein-free liposomes

Protein-free liposomes were formed by detergent removal method as described in chapter II with some modifications (Zhou and Graham, 2009). Briefly, 2 μmol of lipid mixture of a desired composition was dissolved in chloroform and the organic solvent was evaporated thoroughly. The dried lipid film was solubilized completely in 1 mL of

0.75% C₁₂E₉ in reconstitution buffer (40 mM Tris-HCl, pH 7.5/150 mM NaCl) and 200 mg of extensively washed Bio-Beads SM-2 was added. The mixture was incubated on an end-over-end rotator for 6 h at 4 C and another 200 mg of SM-2 beads was added for another 12 h of rotation. The solution of the mixture was then transferred to a clean tube and 400 mg of fresh SM-2 beads was added. After 6 h of rotation, the cloudy solution containing liposomes was carefully removed and stored at 4 C.

Section 4.3.3: Formation of giant vesicles by uncontrolled swelling

The uncontrolled swelling method was performed as previously described (Criado and Keller, 1987; Manley and Gordon, 2008). Briefly, 5 μ L of preformed liposomes (2 mM lipid) was deposited as an 8 mm circle on a glass slide and was dried in a desiccator for 3 h at 4 C. 20 μ L of rehydration buffer (40 mM Tris-HCl, pH 7.5/150 mM NaCl) was added gently to cover the dried lipid spot and the glass slide was placed in a sealed petri dish containing a wet paper pad for 1 h at room temperature. The newly formed giant vesicles were transferred to a glass vial using a pipette tip with a large opening and stored at room temperature.

Section 4.3.4: Formation of giant vesicles by electroformation

GUVs were generated using an electroformation method modified from a previously described protocol (Girard et al., 2004; Papadopoulos et al., 2007). Generally, 5 μ L of preformed liposomes (2 mM lipid) was carefully deposited on the conductive side of one indium tin oxide (ITO) slide, and was dried in a desiccator for 3 h at 4 C. A nitrile O-ring (12 mm diameter x 1 mm height) was then placed around the dried lipid spot to form a little chamber. After carefully filling the chamber with 100 μ L of electroformation buffer (1 mM Tris-HCl, pH 7.5/100 mM sucrose), the chamber was sealed with another ITO slide by clamping the two slides together. The two ITO slides were assembled in the way that

their conductive sides face each other and are separated by the O-ring chamber. After assembly, the conductive glasses were connected to the electrodes of a function generator. For electroformation, an AC electric field of 1 V was applied across the O-ring chamber for 4 h at room temperature at 12 Hz frequency. To detach GUVs from glass, the AC field was elevated to 2 V for 30 min at room temperature at 4 Hz frequency. GUVs were then transferred to a glass vial using a pipette tip with a large opening and stored at room temperature.

Section 4.4: Results and Discussion

Giant vesicles were formed by either the uncontrolled swelling method or the electroformation technique, and were usually 10-50 μm in diameter. As reported previously, giant vesicles generated by uncontrolled swelling were heterogeneous in size and morphology (Manley and Gordon, 2008). Most structures were multilamellar with complex shapes (**Figure 4-1A and B**). By contrast, the electroformation method generated a relatively uniform population of round-shaped vesicles that seemed to be unilamellar (**Figure 4-1C**). Therefore, the electroformation method is more efficient in generating GUVs that are suitable for morphological studies.

As a proof of principle, shape changes were induced in the protein-free GUVs and observed under an optical microscope equipped with DIC and fluorescence optics. In one experiment, the giant vesicles (90% DOPC/9% DOPG/1% NBD-PC) formed by uncontrolled swelling were transferred to a solution with the same osmolarity but a higher pH. A pH gradient was shown to induce accumulation of some lipids, such as phosphatidylglycerol (PG) and phosphatidic acid (PA), to the more basic side and cause morphology changes of GUVs such as tubulation and vesicle budding (Farge and Devaux, 1992). As shown in **Figure 4-2**, a giant vesicle was observed undergoing shape transition from a two-connected-vesicle structure to a three-connected-vesicle one. In

another example, a GUV (90% DOPC/10% DOPS) generated by electroformation was observed on a microscope slide without a cover slip. The GUV remained its original round shape for ~20 min and then started to change its shape (shrinkage) (**Figure 4-3**), which was probably due to an apparent evaporation of the solution on the slide. These preliminary observations confirm that morphology changes can be easily observed with GUVs, and the GUV is an excellent platform to study the relationship between flippase activity, membrane curvature, and vesicle budding.

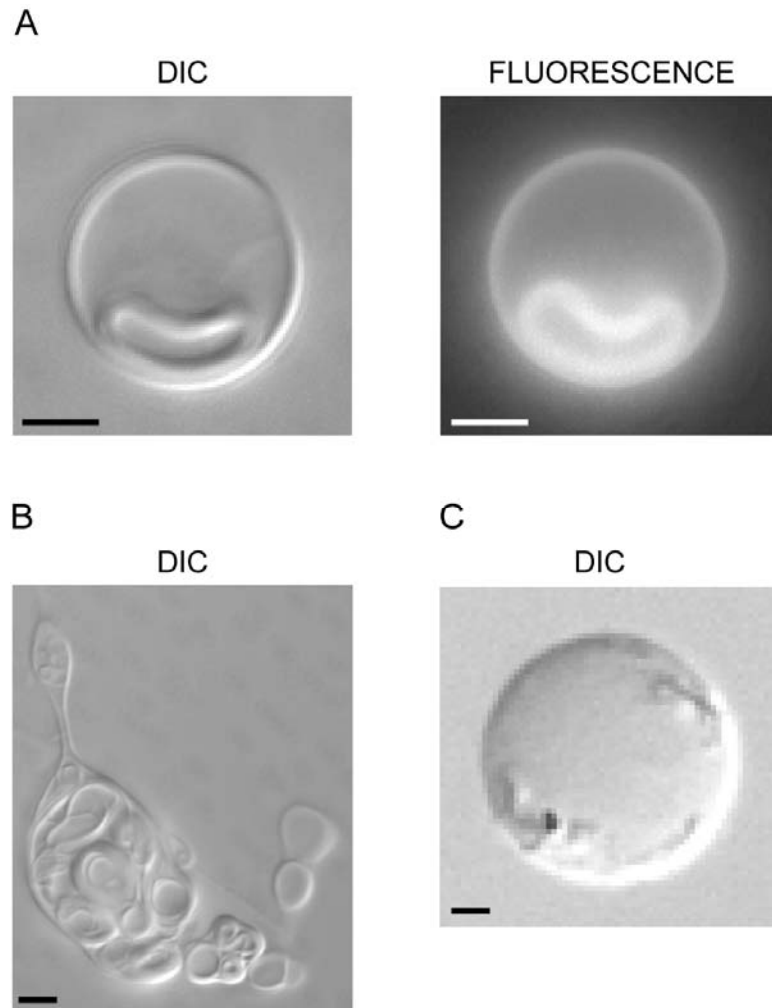


Figure 4-1. Formation of giant vesicles by swelling methods. Giant vesicles were formed by the uncontrolled swelling method (A and B, 90% DOPC/9% DOPG/1% NBD-PC) or the electroformation method (C, 90% DOPC/10% DOPS), and were observed under an optical microscope. DIC, differential interference contrast; fluorescence, green fluorescence emitted by the NBD fluorophore ($\lambda_{\text{ex}} = 460 \text{ nm}$; $\lambda_{\text{em}} = 534 \text{ nm}$). Scale bar, 5 μm .

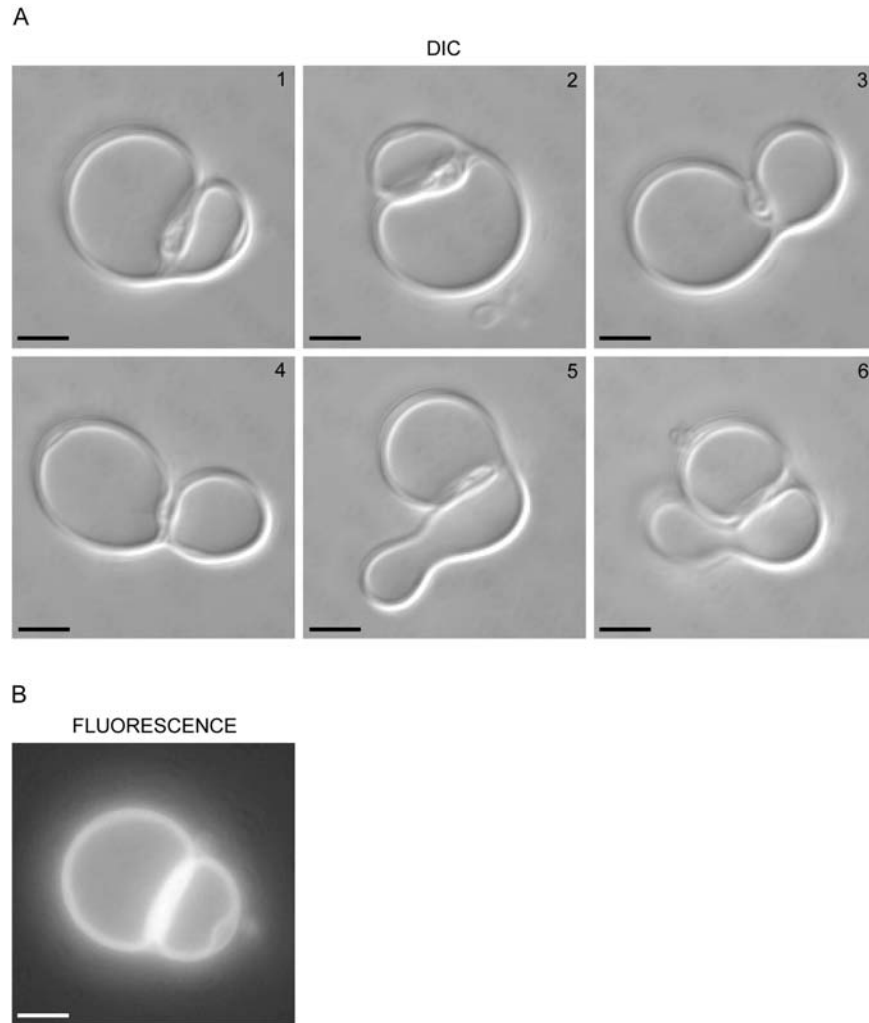


Figure 4-2. Shape change of giant vesicles induced by pH gradient. (A) A giant vesicle (90% DOPC/9% DOPG/1% NBD-PC) formed by uncontrolled swelling at pH 7.5 was transferred to a pH 10 solution without changing osmolarity. Images were taken at 1-min interval. DIC, differential interference contrast. Scale bar, 5 μm . (B) A fluorescence (NBD fluorophore) image was taken between 1 and 2 in (A). Scale bar, 5 μm .

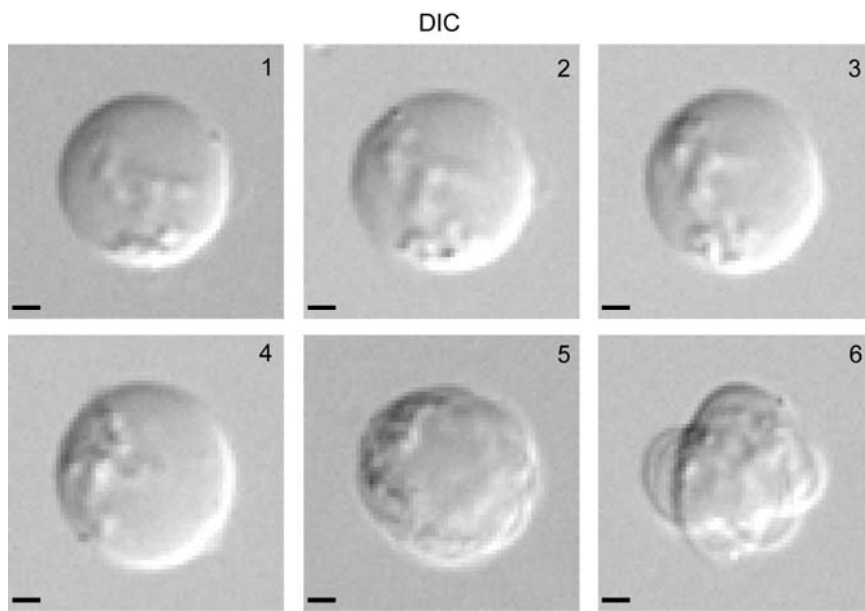


Figure 4-3. Shape change of giant unilamellar vesicles (GUVs) induced by osmolarity gradient. A GUV (90% DOPC/10% DOPS) formed by electroformation was observed using a 20x objective without using a cover slip. Images were taken at 5-min interval. At the time of taking images 5 and 6, substantial evaporation of the sample on the slide was noticed. DIC, differential interference contrast. Scale bar, 5 μ m.

CHAPTER V

SUMMARY AND FUTURE DIRECTIONS

The plasma membrane of eukaryotic cells has been known to be asymmetric in lipid composition since Bretscher described it in the early 1970s (Bretscher, 1973). Normally, the extracellular leaflet is enriched in choline-containing phospholipids such as phosphatidylcholine (PC) and sphingomyelin (SM), whereas the cytosolic leaflet is enriched in amine-containing phospholipids including phosphatidylserine (PS) and phosphatidylethanolamine (PE) (Bretscher, 1973; Daleke, 2003; Devaux, 1992; Graham, 2004; Menon, 1995; Pomorski et al., 2004). Because of their hydrophilic head groups, phospholipids diffuse very slowly across a membrane bilayer. Hence, asymmetrical biosynthesis of phospholipids at the endoplasmic reticulum (ER) could explain membrane asymmetry at the plasma membrane. However, the phospholipid distribution of the ER membrane appears to be symmetric due to the presence of ER flippases, a class of energy-independent, non-selective lipid transporters that allows bidirectional movement of newly-synthesized phospholipids to equilibrate between the two leaflets of the ER for membrane growth (Daleke, 2003; Devaux, 1992; Graham, 2004; Menon, 1995; Pomorski et al., 2004). Therefore, as Bretscher envisioned, there must be a mechanism to generate membrane asymmetry, but at a post-ER level.

Unidirectional, active translocation of phospholipids by proteins called flippases is proposed to play an important role in the generation of membrane asymmetry (Daleke, 2003; Graham, 2004; Pomorski et al., 2004). Flippases are energy-consuming, integral membrane transporters that move phospholipid substrates across membranes from the extracellular leaflet or the topologically equivalent luminal leaflet to the cytosolic leaflet. The first flippase activity documented experimentally was the aminophospholipid

translocase activity in human red blood cells (Daleke and Huestis, 1985; Seigneuret and Devaux, 1984). Since then, a goal has been to identify the flippase through purifying the protein and reconstituting its flippase activity in artificial membranes. Several lines of evidence from studies on the bovine chromaffin granule aminophospholipid translocase suggested that this enzyme belongs to a subclass of P-type ATPases, the type-IV P-type ATPases (P4-ATPases) (Moriyama and Nelson, 1988; Tang et al., 1996; Zachowski et al., 1989). A P4-ATPase, ATPase II/Atp8a1, was suggested to be responsible for the flippase activity in bovine chromaffin granules (Moriyama and Nelson, 1988; Tang et al., 1996; Zachowski et al., 1989). However, there was no report of successful reconstitution of flippase activity with any purified P4-ATPase, even with purified, active ATPase II/Atp8a1 from multiple sources (Ding et al., 2000; Moriyama and Nelson, 1988; Paterson et al., 2006; Xie et al., 1989). The closest achievement to this goal was made in 1994, when the Devaux group purified a Mg^{2+} -ATPase from human red blood cells, reconstituted this protein into liposomes and detected flippase activity toward spin-labeled PS and PE analogues (Auland et al., 1994). However, the identity of this mysterious Mg^{2+} -ATPase remains unknown today. It is possible that the reconstituted Mg^{2+} -ATPase from human red blood cells is ATPase II/Atp8a1, since ATPase II/Atp8a1 was found to be expressed in murine red blood cells (Soupene and Kuypers, 2006). Other candidates for this Mg^{2+} -ATPase include ABCB6 and Atp8a2, which were also detected in human erythrocytes and are PS-stimulatable (Daleke, 2008). Further work is required to test these possibilities.

On the other hand, studies on P4-ATPases from budding yeast provided additional evidence that these pumps are flippases. Yeast P4-ATPases, including Drs2p, Dnf1p, Dnf2p, and Dnf3p, were shown to be required for flippase activity detected in the plasma membrane (Pomorski et al., 2003; Riekhof and Voelker, 2006; Stevens et al., 2008), secretory vesicles (Alder-Baerens et al., 2006), and the *trans*-Golgi network (TGN)

(Natarajan et al., 2009; Natarajan et al., 2004). The most convincing genetic evidence came from a study on Drs2p, which is a yeast homolog of mammalian ATPase II/Atp8a1 and is localized primarily to the TGN (Chen et al., 1999; Hua et al., 2002; Tang et al., 1996). Isolated TGN membranes containing a temperature-sensitive mutant form of Drs2p as sole source of Drs2p translocated a PS analogue bearing a fluorescent 7-nitro-2-1,3-benzoxadiazol-4-yl (NBD) group on a short *sn2* acyl chain (NBD-PS), but not NBD-PC, to the cytosolic leaflet at permissive temperature (Natarajan et al., 2004). Inactivation of this mutant Drs2p at higher temperature abolished the NBD-PS flippase activity. In this experiment, altering a single protein (Drs2p) directly affected flippase activity, suggesting that Drs2p is coupled directly to this activity. Translocation of NBD-PS but not NBD-PC argues that it is the phospholipid rather than the NBD moiety that is recognized. However, there is more than one explanation for this observation. One possibility is that Drs2p pumps phospholipid substrates directly across membrane bilayer. Alternatively, Drs2p may pump an unidentified ion into the TGN to generate an ion gradient, which is then coupled by another transporter (an unidentified symporter) to phospholipid translocation.

Therefore, to seek a direct test on the candidacy of P4-ATPases as flippases, in the current study, I purified Drs2p, reconstituted it into artificial membranes, and tested if flippase activity could be detected. Reconstitution of a flippase has proven to be challenging. After many failed attempts, I succeeded finally in reconstituting the Drs2p flippase activity (Zhou and Graham, 2009). In the whole process, from the start of Drs2p expression to the end of flippase assay, optimization of every step proved to be critical to the final success.

The prerequisite of Drs2p reconstitution is to obtain pure, active Drs2p. Much useful information was obtained from purification of another P4-ATPase, ATPase II/Atp8a1. Bovine and murine ATPase II/Atp8a1 has been heterologously expressed in insect cells

and purified to apparent homogeneity with active protein in regard to ATPase activity (Ding et al., 2000; Paterson et al., 2006), but its reconstitution has not been reported. Several factors may account for the inability to reconstitute ATPase II/Atp8a1. First, perhaps a necessary β subunit was missing from the heterologous expression system. Many P4-ATPases were shown to require a noncatalytic β subunit for ER exit and proper localization (Chen et al., 2006; Furuta et al., 2007; Paulusma et al., 2008; Perez-Victoria et al., 2006; Poulsen et al., 2008; Saito et al., 2004). For example, Drs2p requires Cdc50p for function in vivo. Although the β subunit for ATPase II/Atp8a1 has not been identified, it is possible that ATPase II/Atp8a1 still requires one. Without co-expression of its β subunit, ATPase II/Atp8a1 expressed in a heterologous expression system may be folded well enough to exert ATPase activity, but insufficiently for flippase activity. Another possibility is that the β subunit is essential for the flippase activity of ATPase II/Atp8a1, but is dispensable for its ATPase activity. Second, a heterologous expression system may not be optimal for ATPase II/Atp8a1 production. Although purified ATPase II/Atp8a1 displayed ATPase activity, it is difficult to determine if this P4-ATPase remained biologically active during heterologous expression. For example, its flippase activity may be compromised when ATPase II/Atp8a1 was expressed in insect cells. Third, the purification process of ATPase II/Atp8a1 may perturb the protein folding, especially the organization of transmembrane segments, and yield protein preparations that lose flippase activity, or preparations with a high percentage of inactive protein.

To avoid these potential shortcomings, I chose to overexpress Drs2p and its β subunit, Cdc50p, in its native host, budding yeast. Because Drs2p was slightly modified with affinity tags, another advantage of using budding yeast is that the tagged Drs2p protein can be easily tested for biological activity by assessing its ability to support Drs2p-dependent growth at low temperature (Chen et al., 1999; Hua et al., 2002; Ripmaster et al., 1993).

Overexpression of Drs2p and Cdc50p was initially attempted using two multicopy 2 μ vectors harboring the *DRS2* and *CDC50* gene (data not shown). However, the expression and recovery of Drs2p was not ideal in this system, and the yield of Drs2p per liter of culture was estimated to be on the scale of 0.1 μ g, which was too low for reconstitution experiments. To improve Drs2p production, several other means were tested, and the yield of Drs2p was found to be effectively elevated by substituting the strong glyceraldehyde-3-phosphate dehydrogenase (GPD) promoter for the endogenous promoter of both *DRS2* and *CDC50* in the yeast chromosome. Although the GPD promoter is estimated to be 40+ fold stronger than the endogenous *DRS2* promoter, overexpression of Drs2p under this experimental condition was ~10 fold greater than the endogenous level, probably due to the limitation of internal membrane capacity and the ER quality control system. One advantage of using this chromosome-integrated Drs2p expression cassette over a plasmid-borne one is that cells can be cultured in rich media instead of synthetic selective media. Rich media usually allow cells to grow to a higher density, and sufficient starting material was found to be a very important factor to successful Drs2p purification.

To facilitate protein purification, I first engineered a tandem affinity purification (TAP) tag at the C-terminus of Drs2p (Drs2p-TAP_C). The TAP_C tag contains a protein A moiety (ProA) and the calmodulin binding peptide (CBP) as the first and second affinity module, respectively, separated by the tobacco etch virus (TEV) protease cleavage site (TAP_C = -CBP-TEV-ProA). Drs2p-TAP_C seemed to be active when expressed *in vivo*, because it supported cell growth at 20 C which requires functional Drs2p (Chen et al., 1999; Hua et al., 2002; Ripmaster et al., 1993). For Drs2p-TAP_C purification, a cell lysate was centrifuged at 15,000 X g for 12 min prior to detergent addition to pellet ER membranes and the supernatant containing the TGN proceeded to purification. Thus, any misfolded Drs2p-TAP_C retained in the ER by the quality control system was discarded and only

those molecules that are folded properly and have exited the ER were recovered and purified. Normally, the yield of TAP-purified Drs2p from 1 liter of culture was in the range of 1-10 μg .

Robust ATPase activity was detected in Drs2p-TAP_C preparations. However, this activity showed no sensitivity to orthovanadate, a commonly used inhibitor for P-type ATPases, which raised a concern of contamination. To test if this activity was catalyzed by Drs2p-TAP_C, I attempted to express and purify an ATPase-dead mutant of Drs2p, Drs2p(D560N), in the same C-terminally TAP-tagged form (data not shown). The original plan was to knock in the D560N mutation in the strain overexpressing Drs2p-TAP_C, but this approach unfortunately failed. Instead, I moved *DRS2-TAP_C* along with the GPD promoter to a 2 μ plasmid, and generated the D560N mutation on that plasmid. Both Drs2p-TAP_C and Drs2p(D560N)-TAP_C were purified from the 2 μ system, although the yield of Drs2p(D560N)-TAP_C was lower compared to that of Drs2p-TAP_C. ATPase activity was detected in the Drs2p-TAP_C sample, but was absent from the Drs2p(D560N)-TAP_C preparation, suggesting that this ATPase activity was catalyzed by Drs2p-TAP_C, even though it was insensitive to orthovanadate.

However, the ATPase activity in Drs2p-TAP_C preparations was found later to be sensitive to azide, an inhibitor for the mitochondrial F1-ATPase. This observation argued strongly against my previous conclusion and suggested a contamination with the F1-ATPase. To test if the ATPase activity in the Drs2p-TAP_C sample was catalyzed by the F1-ATPase, I deleted the *ATP2* gene, which encodes the catalytic subunit of the F1-ATPase, in the strain overexpressing Drs2p-TAP_C. From the *atp2 Δ* strain, Drs2p-TAP_C was purified with a yield and purity comparable to that from its isogenic mother strain. However, no ATPase activity could be detected in this Drs2p-TAP_C preparation, indicating that the ATPase activity detected previously was indeed catalyzed by the contaminating F1-ATPase and that purified Drs2p-TAP_C seems to be catalytically

inactive. These data also suggested that the contaminants present in the Drs2p-TAP_C preparation and the Drs2p(D560N)-TAP_C preparation were different, thus making purified Drs2p(D560N) an imperfect control for purified Drs2p.

Many purification and assay conditions were tested for Drs2p-TAP_C but none yielded an active enzyme. The conditions tested included purifying Drs2p-TAP_C with different detergents and assaying ATPase activity in different pH buffers, at different temperatures, in the presence of various ions, and by addition of various phospholipids including PS and PI4P (data not shown). To troubleshoot this inactive preparation of Drs2p-TAP_C, I engineered a different TAP tag at the N-terminus of Drs2p (TAP_N-Drs2p). The TAP_N tag differs from the TAP_C tag in that it contains decahistidine (His₁₀) instead of CBP as the second affinity module (TAP_N = ProA-TEV-His₁₀⁻). TAP_N-Drs2p was also overexpressed by the GPD promoter along with Cdc50p in a strain background that is deficient for the *ATP2* gene, and like Drs2p-TAP_C, TAP_N-Drs2p was functional in vivo. Purification of TAP_N-Drs2p yielded preparations with a purity and yield comparable to that of Drs2p-TAP_C, but the difference is that ATPase activity could be detected with purified TAP_N-Drs2p but not purified Drs2p-TAP_C.

To probe the difference between TAP_N-Drs2p and Drs2p-TAP_C that is responsible for their difference in ATPase activity, both Drs2 proteins were analyzed by size exclusion chromatography to determine their oligomeric states. One possibility was that different oligomeric states of Drs2p could affect its activity. However, the majority of both TAP_N-Drs2p and Drs2p-TAP_C seemed to be monomeric in detergent solutions, arguing against this possibility. Another possibility could be that the Drs2p-TAP_C structure was severely perturbed during purification. To test this possibility, both Drs2 proteins were subjected to circular dichroism analysis. Indeed, the circular dichroism spectra of the two Drs2 proteins were found to be different in the far-UV region, suggesting possibly a difference in the overall structure between TAP_N-Drs2p and Drs2p-TAP_C. However, purified Drs2p-

TAP_C did not seem to be more unstructured than TAP_N-Drs2p. Therefore, the inactivity of purified Drs2p-TAP_C was not caused simply by aggregation or denaturation of this protein, and there is probably a biologically relevant mechanism underlying this observation.

From a molecular perspective, one apparent difference between TAP_N-Drs2p and Drs2p-TAP_C is their TAP tags, in both tag position and tag content. It is possible that it was the His₁₀ of the TAP_N tag versus the CBP of the TAP_C tag, or the position of the tag that caused the difference in ATPase activity between the two Drs2 proteins. To test these possibilities, Drs2p was fused with TAP tags at both the N-terminus and the C-terminus (TAP_N-Drs2p-TAP_C), and purified using either TAP tag. To avoid any effect of different buffers, purified Drs2p samples were stored in the same buffer. Although these two Drs2p preparations should contain the same TAP_N-Drs2p-TAP_C, only the one purified using the TAP_N tag showed ATPase activity, whereas the other remained inactive. These data suggest that the His₁₀ of the TAP_N tag did not activate Drs2p, and neither did the CBP of the TAP_C tag inactivate it. Moreover, because the TAP_C tag also binds to the IgG column during the N-terminal TAP_N purification, a physical interaction of the C-terminus with a column did not cause inactivation of Drs2p. To further test the tag position influence on Drs2p activity, different affinity tags need to be engineered at either terminus of Drs2p. For example, the TAP_N tag can be fused to the C-terminus of Drs2p, or the TAP_C tag can be moved to its N-terminus. If ATPase activity would still be detected only in the Drs2p preparation using the N-terminal tag, but not the C-terminal tag, it would suggest that the position of affinity tags was the cause of the activity difference between purified TAP_N-Drs2p and Drs2p-TAP_C. Although this notion has not been fully tested, evidence described below from my data indicates that it may be true.

When TAP_N-Drs2p-TAP_C was purified, interestingly, a cleaved form (the “NoC” form) was discovered in the preparation using the TAP_N tag, but not the TAP_C tag. The

cleavage of TAP_N-Drs2p-TAP_C seems to take place in the C-terminal tail of Drs2p (thus giving the term “NoC”), because the “NoC” form of TAP_N-Drs2p-TAP_C immunoreacted with the anti-His₁₀ antibody, but not the anti-CBP antibody. The C-terminal tail of Drs2p has been suggested to be an auto-inhibitory domain, and Drs2p flippase activity was shown to be stimulated by binding of regulators, such as Gea2p and phosphatidylinositol 4-phosphate (PI4P), to its C-terminal tail (Natarajan et al., 2009). Therefore, partial or complete loss of the C-terminal tail could possibly bypass the requirement of regulators for Drs2p activity and release Drs2p from its auto-inhibition. Although the cause of Drs2p cleavage is not yet known, the “NoC” form of Drs2p may provide a molecular explanation for Drs2p-TAP_C inactivity, because this “NoC” form could be recovered only in purifications using the N-terminal, but not the C-terminal, TAP tag. Therefore, the position of affinity tags could be responsible for the activity difference between purified TAP_N-Drs2p and Drs2p-TAP_C, because these tags determine whether the “NoC” form of Drs2p was included in or excluded from the purification.

The “NoC” form of TAP_N-Drs2p-TAP_C was estimated to compose ~10% of total Drs2p molecules in purifications using the TAP_N tag. Because the intact form of TAP_N-Drs2p-TAP_C retained the TAP_C tag (the CBP module) but the “NoC” form did not, these two forms of Drs2p were separated using the CBP interaction with a calmodulin column. The unbound Drs2p fraction was enriched in the TAP_N-Drs2p-TAP_C “NoC” form, which represented ~30% of the total Drs2p molecules. In contrast, the Drs2p sample eluted from the calmodulin column contained very little “NoC” form. Consistent with our hypothesis, the Drs2p fraction enriched of the TAP_N-Drs2p-TAP_C “NoC” form showed a specific ATPase activity higher than that before separation, whereas the Drs2p sample containing no “NoC” form of TAP_N-Drs2p-TAP_C showed almost no activity. Based on mobility of proteins on western blots, the “NoC” form of TAP_N-Drs2p-TAP_C was estimated to be ~15 kDa smaller than the intact form. Meanwhile, a mass spectrometric analysis of

both intact and “NoC” form of TAP_N-Drs2p-TAP_C revealed a potential cleavage site in the C-terminal tail of Drs2p at position 1254-1255 (Q-Q), which generates a “NoC” form of TAP_N-Drs2p-TAP_C that is 17.5 kDa smaller than the intact protein, very close to the experimental value. Currently, a stop codon as well as the factor Xa protease site (IEGR|X) is being engineered at the potential cleavage site to test if the intact form of Drs2p is auto-inhibited and if only the “NoC” form of Drs2p is active in vitro. Nevertheless, although the molecular basis of Drs2p-TAP_C inactivity was not completely resolved, it served as a valuable negative control for the reconstitution experiments.

The ATPase activity of purified TAP_N-Drs2p was Mg²⁺-ATP-dependent and orthovanadate-sensitive, consistent with the properties of purified mammalian ATPase II/Atp8a1 (Ding et al., 2000; Moriyama and Nelson, 1988; Paterson et al., 2006; Xie et al., 1989). However, these properties are shared by most P-type ATPases, and we were concerned that a very abundant P-type ATPase proton pump called Pma1p may contaminate our TAP_N-Drs2p preparation. Indeed, Pma1p was detected as a trace contaminant by mass spectrometry, and was the only other P-type ATPase detected in the TAP_N-Drs2p sample. However, Pma1p has an optimal pH of 5.8 (Decottignies et al., 1994; Dufour and Goffeau, 1980), whereas the ATPase activity of purified TAP_N-Drs2p peaks at pH 7.5, indicating that it was not Pma1p that catalyzed this ATPase activity. Moreover, Pma1p and other ATPases were also found at trace levels in the inactive Drs2p-TAP_C preparation, further confirming that active TAP_N-Drs2p was responsible for ATPase activity.

The K_m of purified TAP_N-Drs2p for ATP was 1.5 ± 0.3 mM, indicating a relatively low affinity for ATP compared with many other purified P-type ATPases (Desrosiers et al., 1996; Moriyama and Nelson, 1988; Paterson et al., 2006). The nature of this low affinity could result from a suboptimal interaction between Drs2p and ATP in detergent solutions, or it could be a regulatory means for Drs2p activity. It is possible that the biological

processes that Drs2p is involved in (e.g. vesicular transport) are more actively engaged when energy is adequate, usually happening during the vegetative growth phase of cells. But when energy becomes limiting, the lower activity of Drs2p could save ATP for other cellular processes.

Purified TAP_N-Drs2p showed a V_{\max} of 0.45 ± 0.03 $\mu\text{mol Pi released/min/mg Drs2p}$ at pH 7.5 and 4 mM ATP, which is low relative to the values reported for other purified P-type ATPases, which can extend up to 75 $\mu\text{mol Pi released/min/mg}$ (Desrosiers et al., 1996). One reason could be that the substrate for Drs2p was missing in the assay. Surprisingly, I observed only a mild increase of ~40% in ATPase activity of purified TAP_N-Drs2p when incubated with PS, a phospholipid substrate for Drs2p, in detergent solutions. This stimulation was weak compared with the steep increase (greater than 10-fold) observed for purified mammalian ATPase II/Atp8a1. One possibility is co-purification of substrate phospholipid with Drs2p, so that TAP_N-Drs2p was at nearly maximum activation. Another cause may be that the delivery of PS to Drs2p was very inefficient in detergent solutions. To test these possibilities, purified TAP_N-Drs2p was incorporated into artificial membranes containing different amounts of PS (0-20%). To eliminate potential curvature restraint imposed by PS movement, these artificial membranes were made leaky by incomplete removal of detergent so that phospholipids could diffuse freely across membrane bilayer. In membranes containing no PS, TAP_N-Drs2p showed ATPase activity (0.36 ± 0.04 $\mu\text{mol Pi released/min/mg Drs2p}$) comparable to that in detergent solutions. With increasing PS concentration, the ATPase activity of TAP_N-Drs2p was stimulated up to ~400% (1.28 ± 0.03 $\mu\text{mol Pi released/min/mg Drs2p}$; 20% PS) in a dose-dependent manner. These data confirm that there was a PS-stimulatable TAP_N-Drs2p pool in purified samples. However, whether the ATPase activity without externally added PS reflected basal activity of the PS-stimulatable TAP_N-Drs2p

or full activity of a population of TAP_N-Drs2p molecules that had PS co-purified remains to be determined.

Even with PS stimulation, the ATPase activity of TAP_N-Drs2p was relatively low compared with PS-activated bovine ATPase II/Atp8a1 (3-42 μmol Pi released/min/mg) (Ding et al., 2000; Moriyama and Nelson, 1988; Xie et al., 1989). However, if the ATPase activity of purified TAP_N-Drs2p was solely conveyed by the “NoC” form of Drs2p as hypothesized above, the actual specific ATPase activity of Drs2p should be 10-fold greater (5-10 μmol Pi released/min/mg Drs2p), assuming that the “NoC” form comprises 10% of total Drs2p.

One intriguing aspect of the Drs2p ATPase activity is the contribution of Cdc50p. Drs2p requires Cdc50p association to exit the ER and proceed to the TGN (Chen et al., 2006; Saito et al., 2004), but whether the chaperone role is the sole function of Cdc50p or whether Cdc50p contributes directly to the ATPase activity of Drs2p is yet to be determined. Because Cdc50p was also recovered in the purified TAP_N-Drs2p sample, although at a substoichiometric concentration relative to Drs2p, it was possible that Drs2p requires Cdc50p for ATPase activity. To test this possibility, I took advantage of the two different TAP tags and engineered TAP_N-Drs2p and Cdc50p-TAP_C, and expressed them simultaneously. After purifying TAP_N-Drs2p, the protein preparation contained a mixed population of the TAP_N-Drs2p monomeric form and the TAP_N-Drs2p/Cdc50p-TAP_C complex form. These two populations of Drs2p were then separated by the TAP_C tag on Cdc50p, using the CBP interaction with a calmodulin column. The fraction eluted off the calmodulin column was enriched in the TAP_N-Drs2p/Cdc50p-TAP_C complex form (assuming 100%), but it had the lowest ATPase activity. Meanwhile, the unbound fraction contained few complex molecules (~6%), but showed the highest ATPase activity. The mixed population before separation displayed an intermediate level of the complex form (~20%) as well as ATPase activity. These data

suggest that purified TAP_N-Drs2p may not require Cdc50p for ATPase activity in vitro. However, there was still some Cdc50p-TAP_C in the unbound fraction that was enriched in the TAP_N-Drs2p monomeric form. Therefore, the possibility that Cdc50p contributes to the Drs2p ATPase activity cannot be ruled out completely and requires further test.

Interestingly, these data also showed that the TAP_N-Drs2p molecules that were bound preferentially by Cdc50p-TAP_C and eluted in the complex form seemed to be less active. Taking the “NoC” form of Drs2p into consideration, it is possible that Cdc50p-TAP_C has higher affinity for the intact form of TAP_N-Drs2p (auto-inhibited potentially in a single conformational state) but lower affinity for the “NoC” form of TAP_N-Drs2p (active). This hypothesis received experimental support in that the “NoC” form of TAP_N-Drs2p was readily detected by western blotting in the unbound fraction enriched in the TAP_N-Drs2p monomeric form, but much weaker in the eluted fraction containing primarily the TAP_N-Drs2p/Cdc50p-TAP_C complex form.

Furthermore, the notion that Cdc50p preferentially binds a particular conformational state of Drs2p is also consistent with a recent report by Lenoir et al. (Lenoir et al., 2009). In that work, Cdc50p was found to bind most tightly to the E2P state of Drs2p. It is very possible that the E2P state is where the intact Drs2p (such as purified Drs2p-TAP_C) is normally trapped, even in vivo. This may be part of the quality control mechanism for Drs2p at the ER that allows only properly folded Drs2p capable of phosphorylation (and trapped in the E2P state) to associate with Cdc50p for ER exit. The observation that the Drs2p(D560N) mutant form, which is incapable of phosphorylation, was found to be largely retained in the ER is consistent with this speculation. After ER exit, Drs2p may keep itself in the E2P state (auto-inhibited) until being activated by its regulators, such as Gea2p and PI4P, through binding to its C-terminal tail. Cdc50p and other molecules may also be part of this regulatory machinery for the Drs2p activity in vivo. In the case of the “NoC” form of Drs2p that lost its C-terminal tail during purification, this regulation was

lost and Drs2p was released from its auto-inhibition, at least in regard to ATPase activity. Therefore, it will be very interesting to test if the inactive Drs2p-TAP_C preparation could be activated by Gea2p and PI4P in vitro.

With the active TAP_N-Drs2p preparation, the next step toward Drs2p reconstitution was to put it back into artificial membranes. Reconstitution of membrane proteins is usually achieved through detergent-mediated proteoliposome formation (Paternostre et al., 1988; Rigaud et al., 1988). The choice of detergent, method of detergent removal, and other reconstitution conditions such as protein to lipid ratio and temperature are all important factors that determine the outcome of reconstitution.

Generally, the higher protein to lipid ratio, the more likely proteoliposomes will form successfully. The yield of TAP_N-Drs2p after two-step purification was usually in the range of 1-10 µg per liter of culture, with which I could not obtain consistent incorporation of Drs2p in liposomes during initial trials (data not shown). To increase protein to lipid ratio, single-step purified TAP_N-Drs2p was used directly for reconstitution followed by a glycerol gradient flotation to recover proteoliposomes from the top fractions. This method proved to work consistently and the proteoliposomes contained Drs2p with purity comparable to that from 2-step affinity purification. However, many more contaminating proteins, probably including some proteases, were present during reconstitution using single-step purified TAP_N-Drs2p, and Drs2p is known to be very sensitive to proteases. Therefore, the most prominent drawback of this method was that Drs2p may be degraded during reconstitution. But retrospectively, exposure of Drs2p to proteases may be a key to the success in reconstituting the Drs2p flippase activity later, because this step may help generate the “NoC” form of Drs2p that may be responsible for the observed flippase activity (see discussion later). Because of the risk of Drs2p degradation, a relatively rapid approach to efficiently remove detergent was required. After many trials on different combinations of detergent and removal method (data not

shown), I succeeded in reconstituting Drs2p in proteoliposomes with the detergent polyoxyethylene 9-lauryl ether (C₁₂E₉) removed by Bio-Beads SM-2 adsorption, a process usually completed within 24 h at 4 C.

Reconstituted Drs2p proteoliposomes were relatively small in size (~40 nm in mean diameter) as revealed by electron microscopy (EM) with negative staining and by cryo-EM. Based on the protein to lipid ratio (Drs2p:lipid ~ 1:200, wt:wt) and the assumption of an equal distribution of Drs2p in the liposomes, it was estimated that one Drs2p molecule was present per 2-3 liposomes. In other words, a maximum of 40% of the liposomes contained Drs2p, and the rest were protein-free liposomes. Reconstituted Drs2p seemed to be preferentially incorporated in the liposomes with the cytosolic ATPase domain facing outward. This preferential orientation may result from the limitation of small intravesicular space of the liposomes for placement of the bulky cytosolic domain of Drs2p. Nevertheless, the orientation of Drs2p in the proteoliposomes was in favor of measuring its flippase activity. Any Drs2p molecules that were oriented in the other direction would not be activated upon external addition of Mg²⁺-ATP.

The last but also the key step of flippase reconstitution is to measure flippase activity in reconstituted proteoliposomes. This measurement was achieved with the help of fluorescent NBD-labeled phospholipid analogues, which were also incorporated into the proteoliposomes during reconstitution and were present in both leaflets. Flippase activity was measured by monitoring the change of inter-leaflet distribution of NBD-phospholipid probes using a membrane-impermeant fluorescence quencher, dithionite, which reduces the fluorescent NBD group to the non-fluorescent ABD group (McIntyre and Sleight, 1991). When Mg²⁺-ATP was added externally, a positive flippase activity would be measured as an increase in the fraction of NBD-phospholipid probes present in the outer leaflet of the liposomes available to dithionite quenching (NBD_{outer}%).

Initial trials of flippase assay with TAP_N-Drs2p proteoliposomes seemed to show some flippase activity toward NBD-PS (0-2% increase in NBD_{outer}%), but the signals were too weak to draw a firm conclusion (data not shown). Because of the small size of the proteoliposomes, most of the NBD-phospholipid probes were initially present in the outer leaflet and did not contribute to flippase activity, but contributed to background fluorescence. Eliminating these probes from the system by prequenching the proteoliposomes with dithionite reduced background fluorescence and increased the sensitivity for detecting flippase activity. Although the prequenching conditions (a low concentration of dithionite at low temperature) I used did not result in a complete quench of the fluorescent probes in the outer leaflet (with 10-20% remaining), the improvement of the signal was adequate for detecting flippase activity. Further improvement may be achieved by optimizing the prequenching conditions.

After optimizing the assay, flippase activity was detected in the TAP_N-Drs2p proteoliposomes. The activity was specific for NBD-PS, because no activity was observed with the PC and SM analogues. The NBD-PS flippase activity was also protein-mediated, as protein-free liposomes did not show flippase activity toward NBD-PS. Furthermore, control proteoliposomes reconstituted with the inactive, purified Drs2p-TAP_C showed no NBD-PS flippase activity and still contained a protein composition almost identical to that of the TAP_N-Drs2p proteoliposome, strongly arguing that it is the active Drs2p that was responsible for the observed flippase activity, and other contaminating proteins were incapable of catalyzing this activity alone. However, since Cdc50p was also present in the TAP_N-Drs2p proteoliposome, it remains possible that Cdc50p is required for Drs2p flippase activity (see discussion below).

In reconstituted samples, a maximum of 40% of the liposomes were estimated to contain Drs2p (proteoliposomes), and so 40% would be the upper limit of detectable NBD-PS translocation. I observed a nearly saturated Mg²⁺-ATP-dependent flip of 4%

NBD-PS, indicating that only 10% of the maximum flippase activity was achieved. This observation either suggests that all proteoliposomes contained active flippase and only 10% of their probes were flipped, or that only 10% of the proteoliposomes contained active flippase and all of their probes were flipped. If the former was true, all TAP_N-Drs2p molecules would be active and catalyzing flippase activity in the proteoliposomes. Because the molar concentration of Cdc50p was estimated to be only 10-20% of the TAP_N-Drs2p concentration in the proteoliposomes, most likely TAP_N-Drs2p would not require Cdc50p for flippase activity. However, if the latter possibility was true, only 10% of the TAP_N-Drs2p molecules would be active in regard to flippase activity. Because the TAP_N-Drs2p/Cdc50p complex form may be close to 10% of the total Drs2p in the proteoliposomes, it is possible that only the complex form catalyzed flippase activity.

Alternatively, Cdc50p may not be required, and it may be the “NoC” form of TAP_N-Drs2p, which was also estimated to be 10% of the total Drs2p, that conveyed flippase activity. My current data favor this possibility, because Drs2p molecules complexed with Cdc50p seem to be less active in detergent solutions in regard to ATPase activity. Other possible reasons accounting for the suboptimal flippase activity include the physical restraint of small liposome size, an unequal distribution of Drs2p in the proteoliposomes, and/or the absence of other potential regulators of Drs2p activity, such as Gea2p and PI4P (Natarajan et al., 2009).

Further work will be required to determine the extent that Cdc50p contributed to flippase activity. For example, Drs2p preparations enriched either in the TAP_N-Drs2p monomeric form or in the TAP_N-Drs2p/Cdc50p-TAP_C complex form may be reconstituted. If the complex form is essential for flippase activity, the proteoliposomes reconstituted with the TAP_N-Drs2p/Cdc50p-TAP_C complex form would be expected to show a higher flippase activity. Similarly, to test if it is the “NoC” form of Drs2p that catalyzed flippase activity, the TAP_N-Drs2p-TAP_C “NoC” form may be enriched by separating it from the

intact form, reconstituted and assayed. Meanwhile, if the cleavage site for the “NoC” form is identified, the TAP_N-Drs2p-TAP_C “NoC” form may be directly engineered, purified and reconstituted, and a higher flippase activity will be expected if the “NoC” form is the active form. Another experiment related to the “NoC” question is to test if the current proteoliposomes reconstituted with TAP_N-Drs2p or Drs2p-TAP_C can be stimulated by addition of Drs2p regulators, such as Gea2p and PI4P.

Interestingly, reconstitution of flippase activity with another purified P4-ATPase, Atp8a2 from bovine rod outer segments, has been reported very recently by Coleman et al. (Coleman et al., 2009). With a different detergent (n-octyl-β-D-glucopyranoside) and a different removal method (dialysis), the authors reconstituted untagged Atp8a2 and successfully detected flippase activity toward NBD-PS. Furthermore, native PS was shown to compete against NBD-PS translocation in reconstituted Atp8a2 proteoliposomes, suggesting that native PS was also flipped by Atp8a2. Although PE also weakly stimulates the ATPase activity of purified Atp8a2, flippase activity toward NBD-PE was not detected, possibly due to an insufficient sensitive of the flippase assay. A mammalian Cdc50p homolog, Cdc50a, was found in the rod outer segments by mass spectrometry, but was not readily detected in purified Atp8a2 by Coomassie staining, which is not a sensitive method for detecting proteins in low abundance. Therefore, whether Atp8a2 requires a Cdc50p homolog for flippase activity remains to be determined. Both purified Drs2p and Atp8a2 are sensitive to orthovanadate, and have a similar optimal pH and a relatively high K_m for ATP. But differently, purified Atp8a2 has a very high PS-stimulated ATPase activity (~50 μmol Pi released/min/mg) in detergent solutions, ~100 fold greater than that of purified Drs2p. Whether this reflects a difference in the purification method or a difference in protein nature needs further test. Another apparent difference between purified Drs2p and Atp8a2 is that Atp8a2 seems to be fairly resistant to proteases such as trypsin. These data suggest that every flippase is unique

and so their reconstitution may be different. However, the common conclusions between Drs2p reconstitution and Atp8a2 reconstitution support strongly that P4-ATPases in general are flippases.

Summarized from my data and discussions, I propose a model for Drs2p regulation (**Figure 1-9**). In vivo, Drs2p is synthesized and folded at the ER. Properly folded Drs2p that can be phosphorylated and reach the E2P state binds Cdc50p and leaves the ER for the TGN. At the TGN, Drs2p is activated by Gea2p, PI4P and possibly other regulators through binding to the C-terminal tail of Drs2p (**Figure 1-9C**). When purified in vitro, the intact form of Drs2p remains in an inactive conformation (perhaps the E2P state) and cannot complete the catalytic cycle due to the absence of its regulators (**Figure 1-9B**). A cleaved form of Drs2p (the “NoC” form), which may result from an unknown cleavage event within the C-terminal tail during purification, becomes active because of loss of the auto-inhibitory C-terminal tail of Drs2p (**Figure 1-9D**). This “NoC” form of Drs2p can catalyze ATP hydrolysis and PS translocation in vitro even in the absence of regulators such as Gea2p and PI4P. Cdc50p may also play a role in PS flip, and is possibly an essential component of the flippase unit. So far, my data are consistent with this overall model, but more work is needed to validate it.

In addition to generating membrane asymmetry by pumping specific phospholipids to the cytosolic leaflet, some P4-ATPases, such as Drs2p, are also involved in vesicle-mediated protein transport (Graham, 2004; Muthusamy et al., 2009a; Zhou et al., 2010). Hence, a big question remaining in the flippase field today is whether flippases (e.g. Drs2p) also help to bend membranes and form vesicles through phospholipid translocation. In this hypothesis, phospholipid translocation across a membrane bilayer by flippases will cause an imbalance in phospholipid number and surface area between the two leaflets. Because the two leaflets of a bilayer are physically tightly coupled (Sheetz and Singer, 1974), this imbalance will promote deformation of the membrane

and generate curvature, which is a critical step in vesicle formation. Drs2p deficiency was found to perturb formation of a subset of clathrin-coated vesicles (Chen et al., 1999; Gall et al., 2002), supporting the notion that flippases may play an important role in vesicle budding. Moreover, it has been shown that a membrane bilayer bends toward the side with increased leaflet area when phospholipid number of the two leaflets was manipulated (Daleke and Huestis, 1985; Daleke and Huestis, 1989; Farge and Devaux, 1992; Papadopoulos et al., 2007; Seigneuret and Devaux, 1984). However, there is no direct evidence demonstrating that a flippase such as Drs2p facilitates vesicle budding by flipping phospholipid and inducing membrane curvature.

With the success of Drs2p reconstitution, it is possible now to assess the consequence of phospholipid translocation in regard to shape changes of the proteoliposomes. Predicted shape changes after moving PS from the inner leaflet to the outer leaflet include liposome elongation and tubulation, protrusion formation and crenation, or bud formation and vesicle shedding. However, the small size of the proteoliposomes (40 nm in diameter) imposes a physical restraint on shape changes as well as technical hurdles in visualization (Zhou and Graham, 2009). These problems can be overcome by converting the small proteoliposomes into giant unilamellar vesicles (GUVs, >5 μm in diameter) via an electroformation method (Girard et al., 2004; Papadopoulos et al., 2007). The biggest advantage of GUVs is that they can be observed directly under an optical microscope in real-time. Currently, I have succeeded in generating GUVs as big as 50 μm in diameter from small, protein-free liposomes and have successfully observed some expected shape changes by inducing phospholipid movement and manipulating osmolarity of the GUV system. Further work is needed to determine the proper conditions to form GUVs containing active Drs2p, which can be aided by monitoring Drs2p ATPase activity in GUVs. With this system, we will be able to study not only the relationship between phospholipid translocation and vesicle budding,

but also the substrate specificity using native phospholipids, and the influence of regulators such as Gea2p and PI4P.

By flipping phospholipid, Drs2p and other flippases help generate an asymmetrical membrane in liposomes, and probably in cells as well. In the flippase and its related fields, one problem is solved, but more questions are awaiting answers.

REFERENCES

- Aguilar RC, Watson HA, and Wendland B (2003) The yeast Epsin Ent1 is recruited to membranes through multiple independent interactions. *J Biol Chem* 278:10737-10743.
- Alder-Baerens N, Lisman Q, Luong L, Pomorski T, and Holthuis JC (2006) Loss of P4 ATPases Drs2p and Dnf3p disrupts aminophospholipid transport and asymmetry in yeast post-Golgi secretory vesicles. *Mol Biol Cell* 17:1632-1642.
- Andrade MA, Chacon P, Merelo JJ, and Moran F (1993) Evaluation of secondary structure of proteins from UV circular dichroism spectra using an unsupervised learning neural network. *Protein Eng* 6:383-390.
- Aoki Y, Uenaka T, Aoki J, Umeda M, and Inoue K (1994) A novel peptide probe for studying the transbilayer movement of phosphatidylethanolamine. *J Biochem* 116:291-297.
- Auland ME, Roufogalis BD, Devaux PF, and Zachowski A (1994) Reconstitution of ATP-dependent aminophospholipid translocation in proteoliposomes. *Proc Natl Acad Sci U S A* 91:10938-10942.
- Axelsen KB, and Palmgren MG (1998) Evolution of substrate specificities in the P-type ATPase superfamily. *J Mol Evol* 46:84-101.
- Bishop WR, and Bell RM (1985) Assembly of the endoplasmic reticulum phospholipid bilayer: the phosphatidylcholine transporter. *Cell* 42:51-60.
- Bretscher MS (1973) Membrane structure: some general principles. *Science* 181:622-629.
- Bryant NJ, and Stevens TH (1997) Two separate signals act independently to localize a yeast late Golgi membrane protein through a combination of retrieval and retention. *J Cell Biol* 136:287-297.
- Bull LN, van Eijk MJ, Pawlikowska L, DeYoung JA, Juijn JA, *et al.* (1998) A gene encoding a P-type ATPase mutated in two forms of hereditary cholestasis. *Nat Genet* 18:219-224.
- Cai SY, Gautam S, Nguyen T, Soroka CJ, Rahner C, *et al.* (2009) ATP8B1 deficiency disrupts the bile canalicular membrane bilayer structure in hepatocytes, but FXR expression and activity are maintained. *Gastroenterology* 136:1060-1069.
- Carafoli E (1994) Biogenesis: plasma membrane calcium ATPase: 15 years of work on the purified enzyme. *Faseb J* 8:993-1002.
- Carter SG, and Karl DW (1982) Inorganic phosphate assay with malachite green: an improvement and evaluation. *J Biochem Biophys Methods* 7:7-13.

- Catty P, de Kerchove d'Exaerde A, and Goffeau A (1997) The complete inventory of the yeast *Saccharomyces cerevisiae* P-type transport ATPases. *FEBS Lett* 409:325-332.
- Chantalat S, Park SK, Hua Z, Liu K, Gobin R, *et al.* (2004) The Arf activator Gea2p and the P-type ATPase Drs2p interact at the Golgi in *Saccharomyces cerevisiae*. *J Cell Sci* 117:711-722.
- Chen CY, and Graham TR (1998) An arf1Delta synthetic lethal screen identifies a new clathrin heavy chain conditional allele that perturbs vacuolar protein transport in *Saccharomyces cerevisiae*. *Genetics* 150:577-589.
- Chen CY, Ingram MF, Rosal PH, and Graham TR (1999) Role for Drs2p, a P-type ATPase and potential aminophospholipid translocase, in yeast late Golgi function. *J Cell Biol* 147:1223-1236.
- Chen S, Wang J, Muthusamy BP, Liu K, Zare S, *et al.* (2006) Roles for the Drs2p-Cdc50p complex in protein transport and phosphatidylserine asymmetry of the yeast plasma membrane. *Traffic* 7:1503-1517.
- Coleman JA, Kwok MC, and Molday RS (2009) Localization, purification, and functional reconstitution of the P4-ATPase Atp8a2, a phosphatidylserine flippase in photoreceptor disc membranes. *J Biol Chem* 284:32670-32679.
- Combet C, Blanchet C, Geourjon C, and Deleage G (2000) NPS@: network protein sequence analysis. *Trends Biochem Sci* 25:147-150.
- Connor J, Yatvin MB, and Huang L (1984) pH-sensitive liposomes: acid-induced liposome fusion. *Proc Natl Acad Sci U S A* 81:1715-1718.
- Criado M, and Keller BU (1987) A membrane fusion strategy for single-channel recordings of membranes usually non-accessible to patch-clamp pipette electrodes. *FEBS Lett* 224:172-176.
- D'Souza-Schorey C, and Chavrier P (2006) ARF proteins: roles in membrane traffic and beyond. *Nat Rev Mol Cell Biol* 7:347-358.
- Daleke DL (2003) Regulation of transbilayer plasma membrane phospholipid asymmetry. *J Lipid Res* 44:233-242.
- Daleke DL (2008) Regulation of phospholipid asymmetry in the erythrocyte membrane. *Curr Opin Hematol* 15:191-195.
- Daleke DL, and Huestis WH (1985) Incorporation and translocation of aminophospholipids in human erythrocytes. *Biochemistry* 24:5406-5416.
- Daleke DL, and Huestis WH (1989) Erythrocyte morphology reflects the transbilayer distribution of incorporated phospholipids. *J Cell Biol* 108:1375-1385.
- Davison PF (1968) Proteins in denaturing solvents: gel exclusion studies. *Science* 161:906-907.

- Decottignies A, Kolaczowski M, Balzi E, and Goffeau A (1994) Solubilization and characterization of the overexpressed PDR5 multidrug resistance nucleotide triphosphatase of yeast. *J Biol Chem* 269:12797-12803.
- Desrosiers MG, Gately LJ, Gambel AM, and Menick DR (1996) Purification and characterization of the Ca²⁺-ATPase of *Flavobacterium odoratum*. *J Biol Chem* 271:3945-3951.
- Devaux PF (1991) Static and dynamic lipid asymmetry in cell membranes. *Biochemistry* 30:1163-1173.
- Devaux PF (1992) Protein involvement in transmembrane lipid asymmetry. *Annu Rev Biophys Biomol Struct* 21:417-439.
- Devaux PF, Lopez-Montero I, and Bryde S (2006) Proteins involved in lipid translocation in eukaryotic cells. *Chem Phys Lipids* 141:119-132.
- Ding J, Wu Z, Crider BP, Ma Y, Li X, *et al.* (2000) Identification and functional expression of four isoforms of ATPase II, the putative aminophospholipid translocase. Effect of isoform variation on the ATPase activity and phospholipid specificity. *J Biol Chem* 275:23378-23386.
- Doerrler WT, Gibbons HS, and Raetz CR (2004) MsbA-dependent translocation of lipids across the inner membrane of *Escherichia coli*. *J Biol Chem* 279:45102-45109.
- Donaldson JG, and Jackson CL (2000) Regulators and effectors of the ARF GTPases. *Curr Opin Cell Biol* 12:475-482.
- Dong J, Yang G, and McHaourab HS (2005) Structural basis of energy transduction in the transport cycle of MsbA. *Science* 308:1023-1028.
- Dufour JP, and Goffeau A (1980) Molecular and kinetic properties of the purified plasma membrane ATPase of the yeast *Schizosaccharomyces pombe*. *Eur J Biochem* 105:145-154.
- Duncan MC, Cope MJ, Goode BL, Wendland B, and Drubin DG (2001) Yeast Eps15-like endocytic protein, Pan1p, activates the Arp2/3 complex. *Nat Cell Biol* 3:687-690.
- Eckford PD, and Sharom FJ (2005) The reconstituted P-glycoprotein multidrug transporter is a flippase for glucosylceramide and other simple glycosphingolipids. *Biochem J* 389:517-526.
- Enyedi A, Vorherr T, James P, McCormick DJ, Filoteo AG, *et al.* (1989) The calmodulin binding domain of the plasma membrane Ca²⁺ pump interacts both with calmodulin and with another part of the pump. *J Biol Chem* 264:12313-12321.
- Farge E, and Devaux PF (1992) Shape changes of giant liposomes induced by an asymmetric transmembrane distribution of phospholipids. *Biophys J* 61:347-357.

- Farge E, Ojcius DM, Subtil A, and Dautry-Varsat A (1999) Enhancement of endocytosis due to aminophospholipid transport across the plasma membrane of living cells. *Am J Physiol* 276:C725-733.
- Folmer DE, Elferink RP, and Paulusma CC (2009) P4 ATPases - Lipid flippases and their role in disease. *Biochim Biophys Acta* 1791:628-635.
- Ford MG, Mills IG, Peter BJ, Vallis Y, Praefcke GJ, *et al.* (2002) Curvature of clathrin-coated pits driven by epsin. *Nature* 419:361-366.
- Furuta N, Fujimura-Kamada K, Saito K, Yamamoto T, and Tanaka K (2007) Endocytic recycling in yeast is regulated by putative phospholipid translocases and the Ypt31p/32p-Rcy1p pathway. *Mol Biol Cell* 18:295-312.
- Gall WE, Geething NC, Hua Z, Ingram MF, Liu K, *et al.* (2002) Drs2p-dependent formation of exocytic clathrin-coated vesicles in vivo. *Curr Biol* 12:1623-1627.
- Gall WE, Higginbotham MA, Chen C, Ingram MF, Cyr DM, *et al.* (2000) The auxilin-like phosphoprotein Swa2p is required for clathrin function in yeast. *Curr Biol* 10:1349-1358.
- Gause EM, Buck MA, and Douglas MG (1981) Binding of citreoviridin to the beta subunit of the yeast F1-ATPase. *J Biol Chem* 256:557-559.
- Gaynor EC, Chen CY, Emr SD, and Graham TR (1998) ARF is required for maintenance of yeast Golgi and endosome structure and function. *Mol Biol Cell* 9:653-670.
- Geering K (2001) The functional role of beta subunits in oligomeric P-type ATPases. *J Bioenerg Biomembr* 33:425-438.
- Girard P, Pecreaux J, Lenoir G, Falson P, Rigaud JL, *et al.* (2004) A new method for the reconstitution of membrane proteins into giant unilamellar vesicles. *Biophys J* 87:419-429.
- Gomes E, Jakobsen MK, Axelsen KB, Geisler M, and Palmgren MG (2000) Chilling tolerance in Arabidopsis involves ALA1, a member of a new family of putative aminophospholipid translocases. *Plant Cell* 12:2441-2454.
- Gould KL, Ren L, Feoktistova AS, Jennings JL, and Link AJ (2004) Tandem affinity purification and identification of protein complex components. *Methods* 33:239-244.
- Graham TR (2004) Flippases and vesicle-mediated protein transport. *Trends Cell Biol* 14:670-677.
- Grant AM, Hanson PK, Malone L, and Nichols JW (2001) NBD-labeled phosphatidylcholine and phosphatidylethanolamine are internalized by transbilayer transport across the yeast plasma membrane. *Traffic* 2:37-50.
- Guex N, and Peitsch MC (1997) SWISS-MODEL and the Swiss-PdbViewer: an environment for comparative protein modeling. *Electrophoresis* 18:2714-2723.

Gummadi SN, Hrafnisdottir S, Walent J, Watkins WE, and Menon AK (2003) Reconstitution and assay of biogenic membrane-derived phospholipid flippase activity in proteoliposomes. *Methods Mol Biol* 228:271-279.

Hamon Y, Broccardo C, Chambenoit O, Luciani MF, Toti F, *et al.* (2000) ABC1 promotes engulfment of apoptotic cells and transbilayer redistribution of phosphatidylserine. *Nat Cell Biol* 2:399-406.

Hanson PK, Malone L, Birchmore JL, and Nichols JW (2003) Lem3p is essential for the uptake and potency of alkylphosphocholine drugs, edelfosine and miltefosine. *J Biol Chem* 278:36041-36050.

Hanson PK, and Nichols JW (2001) Energy-dependent flip of fluorescence-labeled phospholipids is regulated by nutrient starvation and transcription factors, PDR1 and PDR3. *J Biol Chem* 276:9861-9867.

Hechtberger P, Zinser E, Saf R, Hummel K, Paltauf F, *et al.* (1994) Characterization, quantification and subcellular localization of inositol-containing sphingolipids of the yeast, *Saccharomyces cerevisiae*. *Eur J Biochem* 225:641-649.

Hicke L, and Dunn R (2003) Regulation of membrane protein transport by ubiquitin and ubiquitin-binding proteins. *Annu Rev Cell Dev Biol* 19:141-172.

Hinrichsen L, Meyerholz A, Groos S, and Ungewickell EJ (2006) Bending a membrane: how clathrin affects budding. *Proc Natl Acad Sci U S A* 103:8715-8720.

Howard JP, Hutton JL, Olson JM, and Payne GS (2002) Sla1p serves as the targeting signal recognition factor for NPFX(1,2)D-mediated endocytosis. *J Cell Biol* 157:315-326.

Hua Z, Fatheddin P, and Graham TR (2002) An essential subfamily of Drs2p-related P-type ATPases is required for protein trafficking between Golgi complex and endosomal/vacuolar system. *Mol Biol Cell* 13:3162-3177.

Hua Z, and Graham TR (2003) Requirement for neo1p in retrograde transport from the Golgi complex to the endoplasmic reticulum. *Mol Biol Cell* 14:4971-4983.

Irvine GB (1994) Molecular-weight estimation for native proteins using size-exclusion high-performance liquid chromatography. *Methods Mol Biol* 32:267-274.

Itoh T, and De Camilli P (2006) BAR, F-BAR (EFC) and ENTH/ANTH domains in the regulation of membrane-cytosol interfaces and membrane curvature. *Biochim Biophys Acta* 1761:897-912.

Janke C, Magiera MM, Rathfelder N, Taxis C, Reber S, *et al.* (2004) A versatile toolbox for PCR-based tagging of yeast genes: new fluorescent proteins, more markers and promoter substitution cassettes. *Yeast* 21:947-962.

Kahya N, Pecheur EI, de Boeij WP, Wiersma DA, and Hoekstra D (2001) Reconstitution of membrane proteins into giant unilamellar vesicles via peptide-induced fusion. *Biophys J* 81:1464-1474.

- Kaksonen M, Toret CP, and Drubin DG (2006) Harnessing actin dynamics for clathrin-mediated endocytosis. *Nat Rev Mol Cell Biol* 7:404-414.
- Kato U, Emoto K, Fredriksson C, Nakamura H, Ohta A, *et al.* (2002) A novel membrane protein, Ros3p, is required for phospholipid translocation across the plasma membrane in *Saccharomyces cerevisiae*. *J Biol Chem* 277:37855-37862.
- Kean LS, Grant AM, Angeletti C, Mahe Y, Kuchler K, *et al.* (1997) Plasma membrane translocation of fluorescently-labeled phosphatidylethanolamine is controlled by transcription regulators, PDR1 and PDR3. *J Cell Biol* 138:255-270.
- Kinuta M, Yamada H, Abe T, Watanabe M, Li SA, *et al.* (2002) Phosphatidylinositol 4,5-bisphosphate stimulates vesicle formation from liposomes by brain cytosol. *Proc Natl Acad Sci U S A* 99:2842-2847.
- Kirchhausen T (2000a) Clathrin. *Annu Rev Biochem* 69:699-727.
- Kirchhausen T (2000b) Three ways to make a vesicle. *Nat Rev Mol Cell Biol* 1:187-198.
- Kopp J, and Schwede T (2004) The SWISS-MODEL Repository of annotated three-dimensional protein structure homology models. *Nucleic Acids Res* 32:D230-234.
- Kuhlbrandt W (2004) Biology, structure and mechanism of P-type ATPases. *Nat Rev Mol Cell Biol* 5:282-295.
- Lenoir G, Williamson P, Puts CF, and Holthuis JC (2009) Cdc50p plays a vital role in the ATPase reaction cycle of the putative aminophospholipid transporter Drs2p. *J Biol Chem* 284:17956-17967.
- Levy D, Bluzat A, Seigneuret M, and Rigaud JL (1990a) A systematic study of liposome and proteoliposome reconstitution involving Bio-Bead-mediated Triton X-100 removal. *Biochim Biophys Acta* 1025:179-190.
- Levy D, Gulik A, Seigneuret M, and Rigaud JL (1990b) Phospholipid vesicle solubilization and reconstitution by detergents. Symmetrical analysis of the two processes using octaethylene glycol mono-n-dodecyl ether. *Biochemistry* 29:9480-9488.
- Lewis MJ, Nichols BJ, Prescianotto-Baschong C, Riezman H, and Pelham HR (2000) Specific retrieval of the exocytic SNARE Snc1p from early yeast endosomes. *Mol Biol Cell* 11:23-38.
- Liu K, Hua Z, Nepute JA, and Graham TR (2007) Yeast P4-ATPases Drs2p and Dnf1p are essential cargos of the NPFXD/Sla1p endocytic pathway. *Mol Biol Cell* 18:487-500.
- Liu K, Surendhran K, Nothwehr SF, and Graham TR (2008) P4-ATPase requirement for AP-1/clathrin function in protein transport from the trans-Golgi network and early endosomes. *Mol Biol Cell* 19:3526-3535.
- Manley S, and Gordon VD (2008) Making giant unilamellar vesicles via hydration of a lipid film. *Curr Protoc Cell Biol* 24:3.

- Marx U, Polakowski T, Pomorski T, Lang C, Nelson H, *et al.* (1999) Rapid transbilayer movement of fluorescent phospholipid analogues in the plasma membrane of endocytosis-deficient yeast cells does not require the Drs2 protein. *Eur J Biochem* 263:254-263.
- Mathivet L, Cribier S, and Devaux PF (1996) Shape change and physical properties of giant phospholipid vesicles prepared in the presence of an AC electric field. *Biophys J* 70:1112-1121.
- Matsuoka K, Orci L, Amherdt M, Bednarek SY, Hamamoto S, *et al.* (1998) COPII-coated vesicle formation reconstituted with purified coat proteins and chemically defined liposomes. *Cell* 93:263-275.
- McIntyre JC, and Sleight RG (1991) Fluorescence assay for phospholipid membrane asymmetry. *Biochemistry* 30:11819-11827.
- Menon AK (1995) Flippases. *Trends Cell Biol* 5:355-360.
- Menon AK, Watkins WEr, and Hrafnisdottir S (2000) Specific proteins are required to translocate phosphatidylcholine bidirectionally across the endoplasmic reticulum. *Curr Biol* 10:241-252.
- Miliaras NB, Park JH, and Wendland B (2004) The function of the endocytic scaffold protein Pan1p depends on multiple domains. *Traffic* 5:963-978.
- Moriyama Y, and Nelson N (1988) Purification and properties of a vanadate- and N-ethylmaleimide-sensitive ATPase from chromaffin granule membranes. *J Biol Chem* 263:8521-8527.
- Morrot G, Herve P, Zachowski A, Fellmann P, and Devaux PF (1989) Aminophospholipid translocase of human erythrocytes: phospholipid substrate specificity and effect of cholesterol. *Biochemistry* 28:3456-3462.
- Musacchio A, Smith CJ, Roseman AM, Harrison SC, Kirchhausen T, *et al.* (1999) Functional organization of clathrin in coats: combining electron cryomicroscopy and X-ray crystallography. *Mol Cell* 3:761-770.
- Muthusamy BP, Natarajan P, Zhou X, and Graham TR (2009a) Linking phospholipid flippases to vesicle-mediated protein transport. *Biochim Biophys Acta* 1791:612-619.
- Muthusamy BP, Raychaudhuri S, Natarajan P, Abe F, Liu K, *et al.* (2009b) Control of protein and sterol trafficking by antagonistic activities of a type IV P-type ATPase and oxysterol binding protein homologue. *Mol Biol Cell* 20:2920-2931.
- Natarajan P, and Graham TR (2006) Measuring translocation of fluorescent lipid derivatives across yeast Golgi membranes. *Methods* 39:163-168.
- Natarajan P, Liu K, Patil DV, Sciorra VA, Jackson CL, *et al.* (2009) Regulation of a Golgi flippase by phosphoinositides and an ArfGEF. *Nat Cell Biol* 11:1421-1426.

- Natarajan P, Wang J, Hua Z, and Graham TR (2004) Drs2p-coupled aminophospholipid translocase activity in yeast Golgi membranes and relationship to in vivo function. *Proc Natl Acad Sci U S A* 101:10614-10619.
- Newpher TM, Smith RP, Lemmon V, and Lemmon SK (2005) In vivo dynamics of clathrin and its adaptor-dependent recruitment to the actin-based endocytic machinery in yeast. *Dev Cell* 9:87-98.
- Nossal R (2001) Energetics of clathrin basket assembly. *Traffic* 2:138-147.
- Ohya T, Miaczynska M, Coskun U, Lommer B, Runge A, *et al.* (2009) Reconstitution of Rab- and SNARE-dependent membrane fusion by synthetic endosomes. *Nature* 459:1091-1097.
- Palmgren MG (2001) PLANT PLASMA MEMBRANE H⁺-ATPases: Powerhouses for Nutrient Uptake. *Annu Rev Plant Physiol Plant Mol Biol* 52:817-845.
- Papadopoulos A, Vehring S, Lopez-Montero I, Kutschenko L, Stockl M, *et al.* (2007) Flippase activity detected with unlabeled lipids by shape changes of giant unilamellar vesicles. *J Biol Chem* 282:15559-15568.
- Parsons AB, Lopez A, Givoni IE, Williams DE, Gray CA, *et al.* (2006) Exploring the mode-of-action of bioactive compounds by chemical-genetic profiling in yeast. *Cell* 126:611-625.
- Paternostre MT, Roux M, and Rigaud JL (1988) Mechanisms of membrane protein insertion into liposomes during reconstitution procedures involving the use of detergents. 1. Solubilization of large unilamellar liposomes (prepared by reverse-phase evaporation) by triton X-100, octyl glucoside, and sodium cholate. *Biochemistry* 27:2668-2677.
- Paterson JK, Renkema K, Burden L, Halleck MS, Schlegel RA, *et al.* (2006) Lipid specific activation of the murine P4-ATPase Atp8a1 (ATPase II). *Biochemistry* 45:5367-5376.
- Paulusma CC, Folmer DE, Ho-Mok KS, de Waart DR, Hilarius PM, *et al.* (2008) ATP8B1 requires an accessory protein for endoplasmic reticulum exit and plasma membrane lipid flippase activity. *Hepatology* 47:268-278.
- Paulusma CC, Groen A, Kunne C, Ho-Mok KS, Spijkerboer AL, *et al.* (2006) Atp8b1 deficiency in mice reduces resistance of the canalicular membrane to hydrophobic bile salts and impairs bile salt transport. *Hepatology* 44:195-204.
- Pecheur EI, Hoekstra D, Sainte-Marie J, Maurin L, Bienvenue A, *et al.* (1997) Membrane anchorage brings about fusogenic properties in a short synthetic peptide. *Biochemistry* 36:3773-3781.
- Pedersen BP, Buch-Pedersen MJ, Morth JP, Palmgren MG, and Nissen P (2007) Crystal structure of the plasma membrane proton pump. *Nature* 450:1111-1114.
- Perez-Iratxeta C, and Andrade-Navarro MA (2008) K2D2: estimation of protein secondary structure from circular dichroism spectra. *BMC Struct Biol* 8:25.

- Perez-Victoria FJ, Sanchez-Canete MP, Castanys S, and Gamarro F (2006) Phospholipid translocation and miltefosine potency require both *L. donovani* miltefosine transporter and the new protein LdRos3 in Leishmania parasites. *J Biol Chem* 281:23766-23775.
- Pomorski T, Holthuis JC, Herrmann A, and van Meer G (2004) Tracking down lipid flippases and their biological functions. *J Cell Sci* 117:805-813.
- Pomorski T, Lombardi R, Riezman H, Devaux PF, van Meer G, *et al.* (2003) Drs2p-related P-type ATPases Dnf1p and Dnf2p are required for phospholipid translocation across the yeast plasma membrane and serve a role in endocytosis. *Mol Biol Cell* 14:1240-1254.
- Portillo F (2000) Regulation of plasma membrane H(+)-ATPase in fungi and plants. *Biochim Biophys Acta* 1469:31-42.
- Poulsen LR, Lopez-Marques RL, McDowell SC, Okkeri J, Licht D, *et al.* (2008) The Arabidopsis P4-ATPase ALA3 localizes to the golgi and requires a beta-subunit to function in lipid translocation and secretory vesicle formation. *Plant Cell* 20:658-676.
- Prezant TR, Chaltraw WE, Jr., and Fischel-Ghodsian N (1996) Identification of an overexpressed yeast gene which prevents aminoglycoside toxicity. *Microbiology* 142:3407-3414.
- Puri N, Lai-Zhang J, Meier S, and Mueller DM (2005) Expression of bovine F1-ATPase with functional complementation in yeast *Saccharomyces cerevisiae*. *J Biol Chem* 280:22418-22424.
- Raggers RJ, van Helvoort A, Evers R, and van Meer G (1999) The human multidrug resistance protein MRP1 translocates sphingolipid analogs across the plasma membrane. *J Cell Sci* 112 (Pt 3):415-422.
- Ren G, Vajjhala P, Lee JS, Winsor B, and Munn AL (2006) The BAR domain proteins: molding membranes in fission, fusion, and phagy. *Microbiol Mol Biol Rev* 70:37-120.
- Riekhof WR, and Voelker DR (2006) Uptake and utilization of lyso-phosphatidylethanolamine by *Saccharomyces cerevisiae*. *J Biol Chem* 281:36588-36596.
- Rigaud JL, Paternostre MT, and Bluzat A (1988) Mechanisms of membrane protein insertion into liposomes during reconstitution procedures involving the use of detergents. 2. Incorporation of the light-driven proton pump bacteriorhodopsin. *Biochemistry* 27:2677-2688.
- Rigaut G, Shevchenko A, Rutz B, Wilm M, Mann M, *et al.* (1999) A generic protein purification method for protein complex characterization and proteome exploration. *Nat Biotechnol* 17:1030-1032.
- Ripmaster TL, Vaughn GP, and Woolford JL, Jr. (1993) DRS1 to DRS7, novel genes required for ribosome assembly and function in *Saccharomyces cerevisiae*. *Mol Cell Biol* 13:7901-7912.

- Robinson M, Poon PP, Schindler C, Murray LE, Kama R, *et al.* (2006) The Gcs1 Arf-GAP mediates Snc1,2 v-SNARE retrieval to the Golgi in yeast. *Mol Biol Cell* 17:1845-1858.
- Romsicki Y, and Sharom FJ (2001) Phospholipid flippase activity of the reconstituted P-glycoprotein multidrug transporter. *Biochemistry* 40:6937-6947.
- Roth AF, Sullivan DM, and Davis NG (1998) A large PEST-like sequence directs the ubiquitination, endocytosis, and vacuolar degradation of the yeast a-factor receptor. *J Cell Biol* 142:949-961.
- Ruetz S, and Gros P (1994) Phosphatidylcholine translocase: a physiological role for the *mdr2* gene. *Cell* 77:1071-1081.
- Saito K, Fujimura-Kamada K, Furuta N, Kato U, Umeda M, *et al.* (2004) Cdc50p, a protein required for polarized growth, associates with the Drs2p P-type ATPase implicated in phospholipid translocation in *Saccharomyces cerevisiae*. *Mol Biol Cell* 15:3418-3432.
- Sakane H, Yamamoto T, and Tanaka K (2006) The functional relationship between the Cdc50p-Drs2p putative aminophospholipid translocase and the Arf GAP Gcs1p in vesicle formation in the retrieval pathway from yeast early endosomes to the TGN. *Cell Struct Funct* 31:87-108.
- Sanyal S, Frank CG, and Menon AK (2008) Distinct flippases translocate glycerophospholipids and oligosaccharide diphosphate dolichols across the endoplasmic reticulum. *Biochemistry* 47:7937-7946.
- Schmid SL (1997) Clathrin-coated vesicle formation and protein sorting: an integrated process. *Annu Rev Biochem* 66:511-548.
- Schwede T, Kopp J, Guex N, and Peitsch MC (2003) SWISS-MODEL: An automated protein homology-modeling server. *Nucleic Acids Res* 31:3381-3385.
- Seigneuret M, and Devaux PF (1984) ATP-dependent asymmetric distribution of spin-labeled phospholipids in the erythrocyte membrane: relation to shape changes. *Proc Natl Acad Sci U S A* 81:3751-3755.
- Sheetz MP, and Singer SJ (1974) Biological membranes as bilayer couples. A molecular mechanism of drug-erythrocyte interactions. *Proc Natl Acad Sci U S A* 71:4457-4461.
- Sherman F (1991) Getting started with yeast. *Methods Enzymol* 194:3-21.
- Siegmund A, Grant A, Angeletti C, Malone L, Nichols JW, *et al.* (1998) Loss of Drs2p does not abolish transfer of fluorescence-labeled phospholipids across the plasma membrane of *Saccharomyces cerevisiae*. *J Biol Chem* 273:34399-34405.
- Singer-Kruger B, Lasic M, Burger AM, Hausser A, Pipkorn R, *et al.* (2008) Yeast and human Ysl2p/hMon2 interact with Gga adaptors and mediate their subcellular distribution. *Embo J* 27:1423-1435.

Smith CJ, Grigorieff N, and Pearse BM (1998) Clathrin coats at 21 Å resolution: a cellular assembly designed to recycle multiple membrane receptors. *Embo J* 17:4943-4953.

Soupe E, and Kuypers FA (2006) Identification of an erythroid ATP-dependent aminophospholipid transporter. *Br J Haematol* 133:436-438.

Spang A, Matsuoka K, Hamamoto S, Schekman R, and Orci L (1998) Coatamer, Arf1p, and nucleotide are required to bud coat protein complex I-coated vesicles from large synthetic liposomes. *Proc Natl Acad Sci U S A* 95:11199-11204.

Stearns T, Kahn RA, Botstein D, and Hoyt MA (1990a) ADP ribosylation factor is an essential protein in *Saccharomyces cerevisiae* and is encoded by two genes. *Mol Cell Biol* 10:6690-6699.

Stearns T, Willingham MC, Botstein D, and Kahn RA (1990b) ADP-ribosylation factor is functionally and physically associated with the Golgi complex. *Proc Natl Acad Sci U S A* 87:1238-1242.

Stevens HC, Malone L, and Nichols JW (2008) The Putative Aminophospholipid Translocases, DNF1 and DNF2, Are Not Required for 7-Nitrobenz-2-oxa-1,3-diazol-4-yl-phosphatidylserine Flip across the Plasma Membrane of *Saccharomyces cerevisiae*. *J Biol Chem* 283:35060-35069.

Stevens HC, and Nichols JW (2007) The proton electrochemical gradient across the plasma membrane of yeast is necessary for phospholipid flip. *J Biol Chem* 282:17563-17567.

Sze H, Liang F, Hwang I, Curran AC, and Harper JF (2000) Diversity and regulation of plant Ca²⁺ pumps: insights from expression in yeast. *Annu Rev Plant Physiol Plant Mol Biol* 51:433-462.

Takei K, Haucke V, Slepnev V, Farsad K, Salazar M, *et al.* (1998) Generation of coated intermediates of clathrin-mediated endocytosis on protein-free liposomes. *Cell* 94:131-141.

Tanford C, Nozaki Y, Reynolds JA, and Makino S (1974) Molecular characterization of proteins in detergent solutions. *Biochemistry* 13:2369-2376.

Tang X, Halleck MS, Schlegel RA, and Williamson P (1996) A subfamily of P-type ATPases with aminophospholipid transporting activity. *Science* 272:1495-1497.

Tareste D, Shen J, Melia TJ, and Rothman JE (2008) SNAREpin/Munc18 promotes adhesion and fusion of large vesicles to giant membranes. *Proc Natl Acad Sci U S A* 105:2380-2385.

Toyoshima C (2009) How Ca²⁺-ATPase pumps ions across the sarcoplasmic reticulum membrane. *Biochim Biophys Acta* 1793:941-946.

Toyoshima C, and Mizutani T (2004) Crystal structure of the calcium pump with a bound ATP analogue. *Nature* 430:529-535.

- Toyoshima C, Nakasako M, Nomura H, and Ogawa H (2000) Crystal structure of the calcium pump of sarcoplasmic reticulum at 2.6 Å resolution. *Nature* 405:647-655.
- Toyoshima C, and Nomura H (2002) Structural changes in the calcium pump accompanying the dissociation of calcium. *Nature* 418:605-611.
- Toyoshima C, Nomura H, and Tsuda T (2004) Lumenal gating mechanism revealed in calcium pump crystal structures with phosphate analogues. *Nature* 432:361-368.
- van Helvoort A, Smith AJ, Sprong H, Fritzsche I, Schinkel AH, *et al.* (1996) MDR1 P-glycoprotein is a lipid translocase of broad specificity, while MDR3 P-glycoprotein specifically translocates phosphatidylcholine. *Cell* 87:507-517.
- Venegas V, and Zhou Z (2007) Two alternative mechanisms that regulate the presentation of apoptotic cell engulfment signal in *Caenorhabditis elegans*. *Mol Biol Cell* 18:3180-3192.
- Wang X, Wang J, Gengyo-Ando K, Gu L, Sun CL, *et al.* (2007) *C. elegans* mitochondrial factor WAH-1 promotes phosphatidylserine externalization in apoptotic cells through phospholipid scramblase SCR-1. *Nat Cell Biol* 9:541-549.
- Wendland B, and Emr SD (1998) Pan1p, yeast eps15, functions as a multivalent adaptor that coordinates protein-protein interactions essential for endocytosis. *J Cell Biol* 141:71-84.
- Wicky S, Schwarz H, and Singer-Kruger B (2004) Molecular interactions of yeast Neo1p, an essential member of the Drs2 family of aminophospholipid translocases, and its role in membrane trafficking within the endomembrane system. *Mol Cell Biol* 24:7402-7418.
- Wiederkehr A, Avaro S, Prescianotto-Baschong C, Haguenaer-Tsapir R, and Riezman H (2000) The F-box protein Rcy1p is involved in endocytic membrane traffic and recycling out of an early endosome in *Saccharomyces cerevisiae*. *J Cell Biol* 149:397-410.
- Williamson P, and Schlegel RA (2002) Transbilayer phospholipid movement and the clearance of apoptotic cells. *Biochim Biophys Acta* 1585:53-63.
- Woodward MP, and Roth TF (1978) Coated vesicles: characterization, selective dissociation, and reassembly. *Proc Natl Acad Sci U S A* 75:4394-4398.
- Wu YC, and Horvitz HR (1998) The *C. elegans* cell corpse engulfment gene *ced-7* encodes a protein similar to ABC transporters. *Cell* 93:951-960.
- Xie XS, Stone DK, and Racker E (1989) Purification of a vanadate-sensitive ATPase from clathrin-coated vesicles of bovine brain. *J Biol Chem* 264:1710-1714.
- Zachowski A, Henry JP, and Devaux PF (1989) Control of transmembrane lipid asymmetry in chromaffin granules by an ATP-dependent protein. *Nature* 340:75-76.
- Zha X, Pierini LM, Leopold PL, Skiba PJ, Tabas I, *et al.* (1998) Sphingomyelinase treatment induces ATP-independent endocytosis. *J Cell Biol* 140:39-47.

Zhou X, and Graham TR (2009) Reconstitution of phospholipid translocase activity with purified Drs2p, a type-IV P-type ATPase from budding yeast. *Proc Natl Acad Sci U S A* 106:16586-16591.

Zhou X, Liu K, Natarajan P, Muthusamy BP, and Graham TR (2010). "Coupling Drs2p to Phospholipid Translocation, Membrane Asymmetry and Vesicle Budding" In: *Membrane Asymmetry and Transmembrane Motion of Lipids*. (P. F. Devaux, ed.) John Wiley & Sons, pp. In review.

Zimmerman ML, and Daleke DL (1993) Regulation of a candidate aminophospholipid-transporting ATPase by lipid. *Biochemistry* 32:12257-12263.

Zinser E, Sperka-Gottlieb CD, Fasch EV, Kohlwein SD, Paltauf F, *et al.* (1991) Phospholipid synthesis and lipid composition of subcellular membranes in the unicellular eukaryote *Saccharomyces cerevisiae*. *J Bacteriol* 173:2026-2034.

Zullig S, Neukomm LJ, Jovanovic M, Charette SJ, Lyssenko NN, *et al.* (2007) Aminophospholipid translocase TAT-1 promotes phosphatidylserine exposure during *C. elegans* apoptosis. *Curr Biol* 17:994-999.

Zwaal RF, and Schroit AJ (1997) Pathophysiologic implications of membrane phospholipid asymmetry in blood cells. *Blood* 89:1121-1132.